Chapter 1

Basic Theory

1.1 Historical Background of Raman Spectroscopy

In 1928, when Sir Chandrasekhra Venkata Raman discovered the phenomenon that bears his name, only crude instrumentation was available. Sir Raman used sunlight as the source and a telescope as the collector; the detector was his eyes. That such a feeble phenomenon as the Raman scattering was detected was indeed remarkable.

Gradually, improvements in the various components of Raman instrumentation took place. Early research was concentrated on the development of better excitation sources. Various lamps of elements were developed (e.g., helium, bismuth, lead, zinc) (1–3). These proved to be unsatisfactory because of low light intensities. Mercury sources were also developed. An early mercury lamp which had been used for other purposes in 1914 by Kerschbaum (1) was developed. In the 1930s mercury lamps suitable for Raman use were designed (2). Hibben (3) developed a mercury burner in 1939, and Spedding and Stamm (4) experimented with a cooled version in 1942. Further progress was made by Rank and McCartney (5) in 1948, who studied mercury burners and their backgrounds. Hilger Co. developed a commercial mercury excitation source system for the Raman instrument, which consisted of four lamps surrounding the Raman tube. Welsh *et al.* (6) introduced a mercury source in 1952, which became known as the Toronto Arc. The lamp consisted of a four-turn helix of Pyrex tubing and was an improvement over the Hilger lamp. Improvements in lamps were made by

ISBN 0-12-254105-7

Ham and Walsh (7), who described the use of microwave-powered helium, mercury, sodium, rubidium and potassium lamps. Stammreich (8–12) also examined the practicality of using helium, argon, rubidium and cesium lamps for colored materials. In 1962 laser sources were developed for use with Raman spectroscopy (13). Eventually, the Ar^+ (351.1–514.5 nm) and the Kr^+ (337.4–676.4 nm) lasers became available, and more recently the Nd-YAG laser (1,064 nm) has been used for Raman spectroscopy (see Chapter 2, Section 2.2).

Progress occurred in the detection systems for Raman measurements. Whereas original measurements were made using photographic plates with the cumbersome development of photographic plates, photoelectric Raman instrumentation was developed after World War II. The first photoelectric Raman instrument was reported in 1942 by Rank and Wiegand (14), who used a cooled cascade type RCA IP21 detector. The Heigl instrument appeared in 1950 and used a cooled RCA C-7073B photomultiplier. In 1953 Stamm and Salzman (15) reported the development of photoelectric Raman instrumentation using a cooled RCA IP21 photomultiplier tube. The Hilger E612 instrument (16) was also produced at this time, which could be used as a photographic or photoelectric instrument. In the photoelectric mode a photomultiplier was used as the detector. This was followed by the introduction of the Cary Model 81 Raman spectrometer (17). The source used was the 3 kW helical Hg arc of the Toronto type. The instrument employed a twin-grating, twin-slit double monochromator.

Developments in the optical train of Raman instrumentation took place in the early 1960s. It was discovered that a double monochromator removed stray light more efficiently than a single monochromator. Later, a triple monochromator was introduced, which was even more efficient in removing stray light. Holographic gratings appeared in 1968 (17), which added to the efficiency of the collection of Raman scattering in commercial Raman instruments.

These developments in Raman instrumentation brought commercial Raman instruments to the present state of the art of Raman measurements. Now, Raman spectra can also be obtained by Fourier transform (FT) spectroscopy. FT-Raman instruments are being sold by all Fourier transform infrared (FT-IR) instrument makers, either as interfaced units to the FT-IR spectrometer or as dedicated FT-Raman instruments.

1.2 Energy Units and Molecular Spectra

Figure 1-1 illustrates a wave of polarized electromagnetic radiation traveling in the z-direction. It consists of the electric component (x-direction) and magnetic component (y-direction), which are perpendicular to each other.

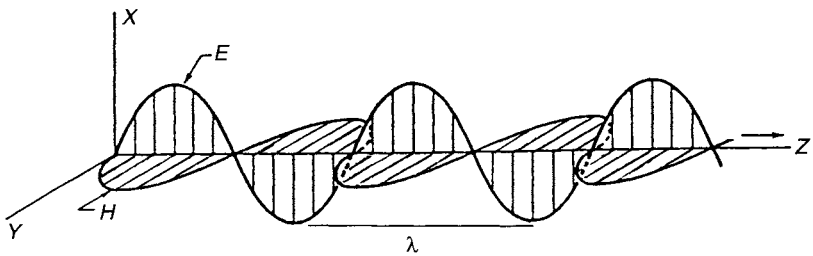

Figure 1-1 Plane-polarized electromagnetic radiation.

Hereafter, we will consider only the former since topics discussed in this book do not involve magnetic phenomena. The electric field strength (E) at a given time (t) is expressed by

$$E = E_0 \cos 2\pi\nu t, \tag{1-1}$$

where E_0 is the amplitude and ν is the frequency of radiation as defined later.

The distance between two points of the same phase in successive waves is called the "wavelength," λ, which is measured in units such as Å (angstrom), nm (nanometer), mμ (millimicron), and cm (centimeter). The relationships between these units are:

$$1\ \text{Å} = 10^{-8}\ \text{cm} = 10^{-1}\ \text{nm} = 10^{-1}\text{m}\mu. \tag{1-2}$$

Thus, for example, 4,000 Å = 400 nm = 400 mμ.

The frequency, ν, is the number of waves in the distance light travels in one second. Thus,

$$\nu = \frac{c}{\lambda}, \tag{1-3}$$

where c is the velocity of light (3×10^{10} cm/s). If λ is in the unit of centimeters, its dimension is (cm/s)/(cm) = 1/s. This "reciprocal second" unit is also called the "hertz" (Hz).

The third parameter, which is most common to vibrational spectroscopy, is the "wavenumber," $\tilde{\nu}$, defined by

$$\tilde{\nu} = \frac{\nu}{c}. \tag{1-4}$$

The difference between ν and $\tilde{\nu}$ is obvious. It has the dimension of (1/s)/(cm/s) = 1/cm. By combining (1–3) and (1–4) we have

$$\tilde{\nu} = \frac{\nu}{c} = \frac{1}{\lambda}\ (\text{cm}^{-1}). \tag{1-5}$$

Table 1-1 Units Used in Spectroscopy*

10^{12}	tera	T
10^{9}	giga	G
10^{6}	mega	M
10^{3}	kilo	k
10^{2}	hecto	h
10^{1}	deca	da
10^{-1}	deci	d
10^{-2}	centi	c
10^{-3}	milli	m
10^{-6}	micro	μ
10^{-9}	nano	n
10^{-12}	pico	p
10^{-15}	femto	f
10^{-18}	atto	a

*Notations: T, G, M, k, h, da, μ, n—Greek; d, c, m—Latin; p—Spanish; f—Swedish; a—Danish.

Thus, 4,000 Å corresponds to $25 \times 10^3\,\mathrm{cm}^{-1}$, since

$$\tilde{\nu} = \frac{1}{\lambda(\mathrm{cm})} = \frac{1}{4 \times 10^3 \times 10^{-8}} = 25 \times 10^3\ (\mathrm{cm}^{-1}).$$

Table 1-1 lists units frequently used in spectroscopy. By combining (1-3) and (1-4), we obtain

$$\nu = \frac{c}{\lambda} = c\tilde{\nu}. \tag{1-6}$$

As shown earlier, the wavenumber ($\tilde{\nu}$) and frequency (ν) are different parameters, yet these two terms are often used interchangeably. Thus, an expression such as "frequency shift of $30\,\mathrm{cm}^{-1}$" is used conventionally by IR and Raman spectroscopists and we will follow this convention through this book.

If a molecule interacts with an electromagnetic field, a transfer of energy from the field to the molecule can occur only when Bohr's frequency condition is satisfied. Namely,

$$\Delta E = h\nu = h\frac{c}{\lambda} = hc\tilde{\nu}. \tag{1-7}$$

Here ΔE is the difference in energy between two quantized states, h is Planck's constant (6.62×10^{-27} erg s) and c is the velocity of light. Thus, $\tilde{\nu}$ is directly proportional to the energy of transition.

Suppose that

$$\Delta E = E_2 - E_1, \tag{1-8}$$

where E_2 and E_1 are the energies of the excited and ground states, respectively. Then, the molecule "absorbs" ΔE when it is excited from E_1 to E_2, and "emits" ΔE when it reverts from E_2 to E_1*.

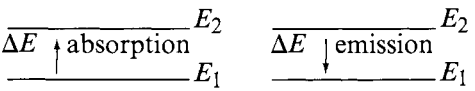

Using the relationship given by Eq. (1-7), Eq. (1-8) is written as

$$\Delta E = E_2 - E_1 = hc\tilde{\nu}. \tag{1-9}$$

Since h and c are known constants, ΔE can be expressed in terms of various energy units. Thus, 1 cm^{-1} is equivalent to

$$\begin{aligned}\Delta E &= [6.62 \times 10^{-27}\ (\text{erg s})][3 \times 10^{10}(\text{cm/s})][1(1/\text{cm})] \\ &= 1.99 \times 10^{-16}\ (\text{erg/molecule}) \\ &= 1.99 \times 10^{-23}\ (\text{joule/molecule}) \\ &= 2.86\ (\text{cal/mole}) \\ &= 1.24 \times 10^{-4}\ (\text{eV/molecule})\end{aligned}$$

In the preceding conversions, the following factors were used:

$$\begin{aligned}1\ (\text{erg/molecule}) &= 2.39 \times 10^{-8}\ (\text{cal/molecule}) \\ &= 1 \times 10^{-7}\ (\text{joule/molecule}) \\ &= 6.2422 \times 10^{11}\ (\text{eV/molecule}) \\ \text{Avogadro number}, N_o &= 6.025 \times 10^{23}\ (1/\text{mole}) \\ 1\ (\text{cal}) &= 4.184\ (\text{joule})\end{aligned}$$

Figure 1-2 compares the order of energy expressed in terms of $\tilde{\nu}$ (cm^{-1}), λ (cm) and ν (Hz).

As indicated in Fig. 1-2 and Table 1-2, the magnitude of ΔE is different depending upon the origin of the transition. In this book, we are mainly concerned with vibrational transitions which are observed in infrared (IR) or Raman spectra**. These transitions appear in the $10^4 \sim 10^2$ cm^{-1} region and

*If a molecule loses ΔE via molecular collision, it is called a "radiationless transition."

**Pure rotational and rotational–vibrational transitions are also observed in IR and Raman spectra. Many excellent textbooks are available on these and other subjects (see general references given at the end of this chapter).

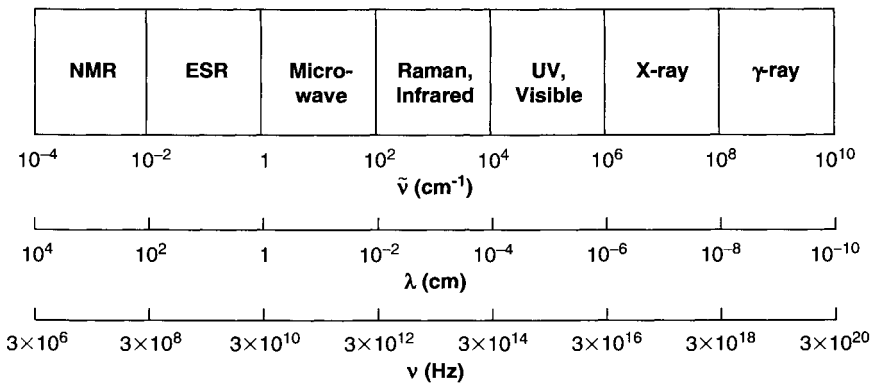

Figure 1-2 Energy units for various portions of electromagnetic spectrum.

Table 1-2 Spectral Regions and Their Origins

Spectroscopy	Range ($\tilde{\nu}$, cm^{-1})	Origin
γ-ray	$10^{10}-10^{8}$	Rearrangement of elementary particles in the nucleus
X-ray (ESCA, PES)	$10^{8}-10^{6}$	Transitions between energy levels of inner electrons of atoms and molecules
UV-Visible	$10^{6}-10^{4}$	Transitions between energy levels of valence electrons of atoms and molecules
Raman and infrared	$10^{4}-10^{2}$	Transitions between vibrational levels (change of configuration)
Microwave	$10^{2}-1$	Transitions between rotational levels (change of orientation)
Electron spin resonance (ESR)	$1-10^{-2}$	Transitions between electron spin levels in magnetic field
Nuclear magnetic resonance (NMR)	$10^{-2}-10^{-4}$	Transitions between nuclear spin levels in magnetic fields

originate from vibrations of nuclei constituting the molecule. As will be shown later, Raman spectra are intimately related to electronic transitions. Thus, it is important to know the relationship between electronic and vibrational states. On the other hand, vibrational spectra of small molecules in the gaseous state exhibit rotational fine structures.* Thus, it is also important to

*In solution, rotational fine structures are not observed because molecular collisions (10^{-13}s) occur before one rotation is completed (10^{-11}s) and the levels of individual molecules are perturbed differently. In the solid state, molecular rotation does not occur because of intermolecular interactions.

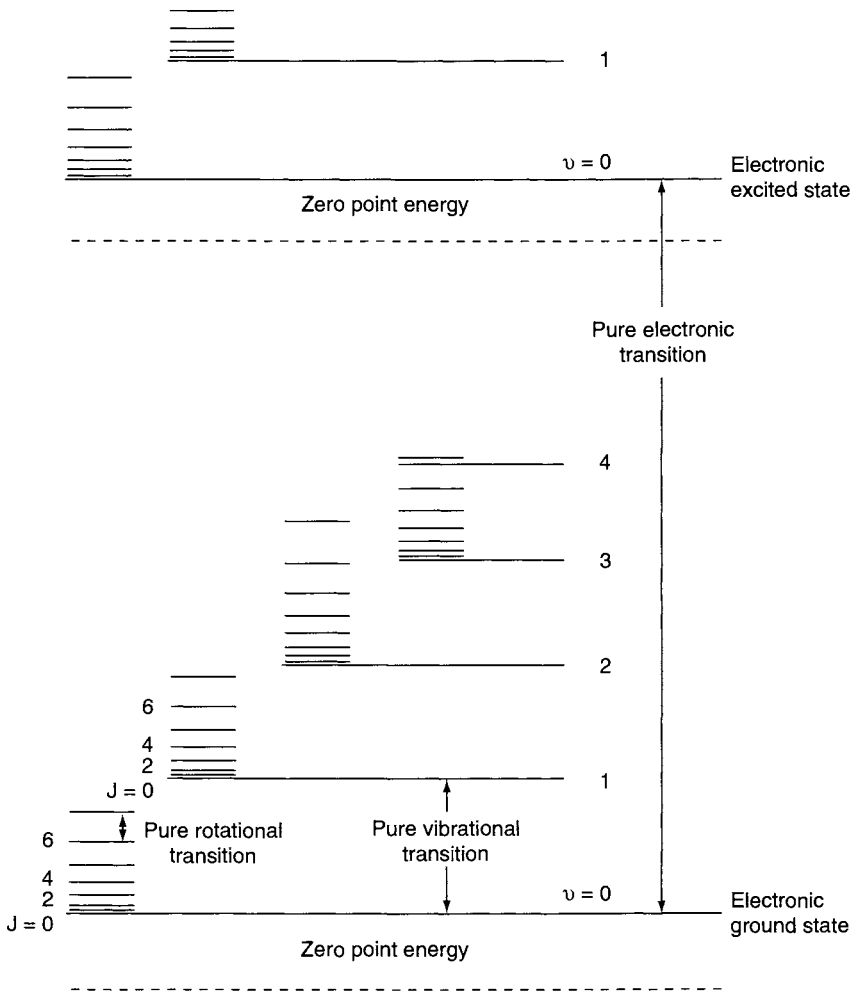

Figure 1-3 Energy levels of a diatomic molecule. (The actual spacings of electronic levels are much larger, and those of rotational levels much smaller, than those shown in the figure.)

know the relationship between vibrational and rotational states. Figure 1-3 illustrates the three types of transitions for a diatomic molecule.

1.3 Vibration of a Diatomic Molecule

Consider the vibration of a diatomic molecule in which two atoms are connected by a chemical bond.

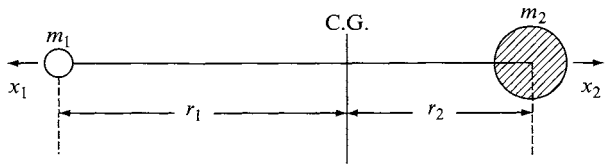

Here, m_1 and m_2 are the masses of atom 1 and 2, respectively, and r_1 and r_2 are the distances from the center of gravity (C.G.) to the atoms designated. Thus, $r_1 + r_2$ is the equilibrium distance, and x_1 and x_2 are the displacements of atoms 1 and 2, respectively, from their equilibrium positions. Then, the conservation of the center of gravity requires the relationships:

$$m_1 r_1 = m_2 r_2, \tag{1-10}$$

$$m_1(r_1 + x_1) = m_2(r_2 + x_2). \tag{1-11}$$

Combining these two equations, we obtain

$$x_1 = \left(\frac{m_2}{m_1}\right) x_2 \quad \text{or} \quad x_2 = \left(\frac{m_1}{m_2}\right) x_1. \tag{1-12}$$

In the classical treatment, the chemical bond is regarded as a spring that obeys Hooke's law, where the restoring force, f, is expressed as

$$f = -K(x_1 + x_2). \tag{1-13}$$

Here K is the force constant, and the minus sign indicates that the directions of the force and the displacement are opposite to each other. From (1-12) and (1-13), we obtain

$$f = -K\left(\frac{m_1 + m_2}{m_1}\right) x_2 = -K\left(\frac{m_1 + m_2}{m_2}\right) x_1. \tag{1-14}$$

Newton's equation of motion ($f = ma$; m = mass; a = acceleration) is written for each atom as

$$m_1 \frac{d^2 x_1}{dt^2} = -K\left(\frac{m_1 + m_2}{m_2}\right) x_1, \tag{1-15}$$

$$m_2 \frac{d^2 x_2}{dt^2} = -K\left(\frac{m_1 + m_2}{m_1}\right) x_2. \tag{1-16}$$

By adding

$$(1\text{-}15) \times \left(\frac{m_2}{m_1 + m_2}\right) \quad \text{and} \quad (1\text{-}16) \times \left(\frac{m_1}{m_1 + m_2}\right),$$

we obtain

$$\frac{m_1 m_2}{m_1 + m_2}\left(\frac{d^2x_1}{dt^2} + \frac{d^2x_2}{dt^2}\right) = -K(x_1 + x_2). \tag{1-17}$$

Introducing the reduced mass (μ) and the displacement (q), (1-17) is written as

$$\mu \frac{d^2q}{dt^2} = -Kq. \tag{1-18}$$

The solution of this differential equation is

$$q = q_0 \sin(2\pi\nu_0 t + \varphi), \tag{1-19}$$

where q_0 is the maximum displacement and φ is the phase constant, which depends on the initial conditions. ν_0 is the classical vibrational frequency given by

$$\nu_0 = \frac{1}{2\pi}\sqrt{\frac{K}{\mu}}. \tag{1-20}$$

The potential energy (V) is defined by

$$dV = -f\,dq = Kq\,dq.$$

Thus, it is given by

$$\begin{aligned} V &= \frac{1}{2}Kq^2 \\ &= \frac{1}{2}Kq_0^2 \sin^2(2\pi\nu_0 t + \varphi) \\ &= 2\pi^2\nu_0^2\mu q_0^2 \sin^2(2\pi\nu_0 t + \varphi). \end{aligned} \tag{1-21}$$

The kinetic energy (T) is

$$\begin{aligned} T &= \frac{1}{2}m_1\left(\frac{dx_1}{dt}\right)^2 + \frac{1}{2}m_2\left(\frac{dx_2}{dt}\right)^2 \\ &= \frac{1}{2}\mu\left(\frac{dq}{dt}\right)^2 \\ &= 2\pi^2\nu_0^2\mu q_0^2 \cos^2(2\pi\nu_0 t + \varphi). \end{aligned} \tag{1-22}$$

Thus, the total energy (E) is

$$\begin{aligned} E &= T + V \\ &= 2\pi^2\nu_0^2\mu q_0^2 = \text{constant} \end{aligned} \tag{1-23}$$

Figure 1-4 shows the plot of V as a function of q. This is a parabolic potential, $V = \frac{1}{2}Kq^2$, with $E = T$ at $q = 0$ and $E = V$ at $q = \pm q_0$. Such a vibrator is called a *harmonic oscillator*.

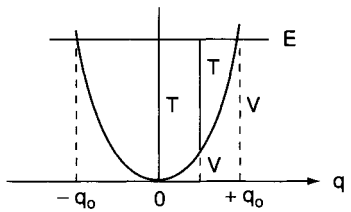

Figure 1-4 Potential energy diagram for a harmonic oscillator.

In quantum mechanics (18,19) the vibration of a diatomic molecule can be treated as a motion of a single particle having mass μ whose potential energy is expressed by (1-21). The Schrödinger equation for such a system is written as

$$\frac{d^2\psi}{dq^2} + \frac{8\pi^2\mu}{h^2}\left(E - \frac{1}{2}Kq^2\right)\psi = 0. \tag{1-24}$$

If (1-24) is solved with the condition that ψ must be single-valued, finite and continuous, the eigenvalues are

$$E_v = h\nu\left(v + \frac{1}{2}\right) = hc\tilde{\nu}\left(v + \frac{1}{2}\right), \tag{1-25}$$

with the frequency of vibration

$$\nu = \frac{1}{2\pi}\sqrt{\frac{K}{\mu}} \quad \text{or} \quad \tilde{\nu} = \frac{1}{2\pi c}\sqrt{\frac{K}{\mu}}. \tag{1-26}$$

Here, v is the vibrational quantum number, and it can have the values 0, 1, 2, 3, ... The corresponding eigenfunctions are

$$\psi_v = \frac{(\alpha/\pi)^{1/4}}{\sqrt{2^v v!}} e^{-\alpha q^2/2} H_v(\sqrt{\alpha}q), \tag{1-27}$$

where

$$\alpha = 2\pi\sqrt{\mu K/h} = 4\pi^2\mu\nu/h \quad \text{and} \quad H_v(\sqrt{\alpha}q)$$

is a Hermite polynomial of the vth degree. Thus, the eigenvalues and the corresponding eigenfunctions are

$$\begin{array}{lll} v = 0, & E_0 = \frac{1}{2}h\nu, & \psi_0 = (\alpha/\pi)^{1/4} e^{-\alpha q^2/2} \\ v = 1, & E_1 = \frac{3}{2}h\nu, & \psi_1 = (\alpha/\pi)^{1/4} 2^{1/2} q e^{-\alpha q^2/2}. \\ \vdots & \vdots & \vdots \end{array} \tag{1-28}$$

One should note that the quantum-mechanical frequency (1-26) is exactly the same as the classical frequency (1-20). However, several marked differences must be noted between the two treatments. First, classically, E is zero when q is zero. Quantum-mechanically, the lowest energy state ($\upsilon = 0$) has the energy of $\frac{1}{2}h\nu$ (zero point energy) (see Fig. 1-3) which results from Heisenberg's uncertainty principle. Secondly, the energy of a such a vibrator can change continuously in classical mechanics. In quantum mechanics, the energy can change only in units of $h\nu$. Thirdly, the vibration is confined within the parabola in classical mechanics since T becomes negative if $|q| > |q_0|$ (see Fig. 1-4). In quantum mechanics, the probability of finding q outside the parabola is not zero (tunnel effect) (Fig. 1-5).

In the case of a harmonic oscillator, the separation between the two successive vibrational levels is always the same ($h\nu$). This is not the case of an actual molecule whose potential is approximated by the Morse potential function shown by the solid curve in Fig. 1-6.

$$V = D_e\left(1 - e^{-\beta q}\right)^2. \tag{1-29}$$

Here, D_e is the dissociation energy and β is a measure of the curvature at the bottom of the potential well. If the Schrödinger equation is solved with this potential, the eigenvalues are (18,19)

$$E_\upsilon = hc\omega_e\left(\upsilon + \frac{1}{2}\right) - hc\chi_e\omega_e\left(\upsilon + \frac{1}{2}\right)^2 + \cdots, \tag{1-30}$$

where ω_e is the wavenumber corrected for anharmonicity, and $\chi_e\omega_e$ indicates the magnitude of anharmonicity. Equation (1-30) shows that the energy levels of the anharmonic oscillator are no longer equidistant, and the separation decreases with increasing ν as shown in Fig. 1-6. Thus far, anharmonicity

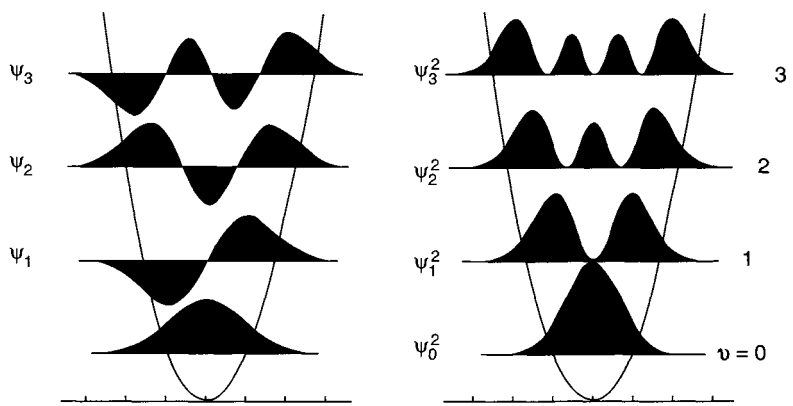

Figure 1-5 Wave functions (left) and probability distributions (right) of the harmonic oscillator.

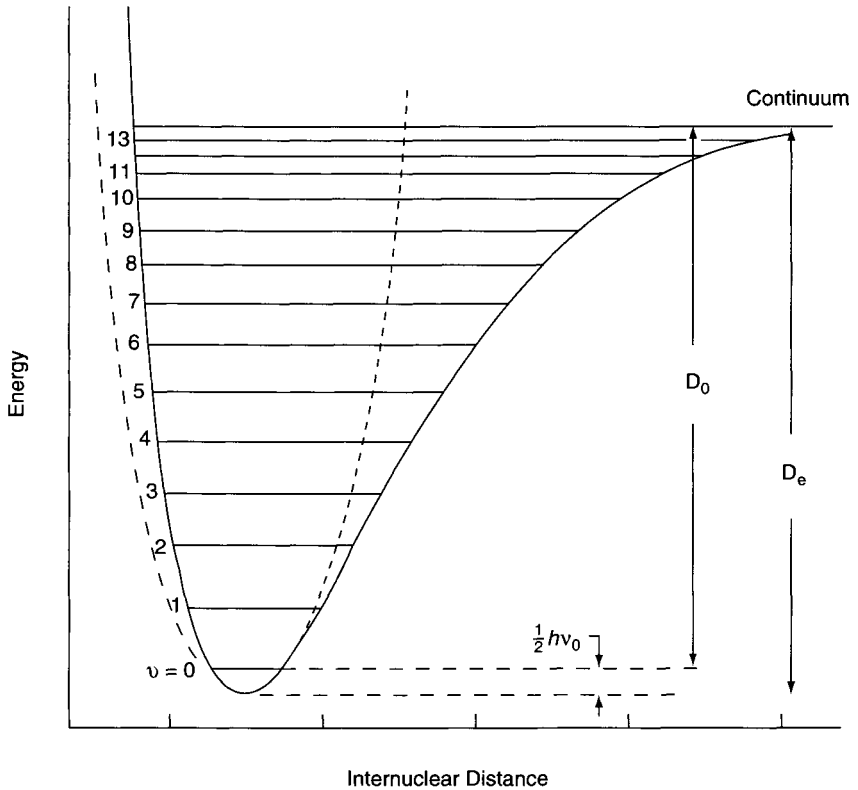

Figure 1-6 Potential energy curve for a diatomic molecule. Solid line indicates a Morse potential that approximates the actual potential. Broken line is a parabolic potential for a harmonic oscillator. D_e and D_0 are the theoretical and spectroscopic dissociation energies, respectively.

corrections have been made mostly on diatomic molecules (see Table 1-3), because of the complexity of calculations for large molecules.

According to quantum mechanics, only those transitions involving $\Delta\upsilon = \pm 1$ are allowed for a harmonic oscillator. If the vibration is anharmonic, however, transitions involving $\Delta\upsilon = \pm 2, \pm 3, \ldots$ (overtones) are also weakly allowed by selection rules. Among many $\Delta\upsilon = \pm 1$ transitions, that of $\upsilon = 0 \leftrightarrow 1$ (fundamental) appears most strongly both in IR and Raman spectra. This is expected from the Maxwell–Boltzmann distribution law, which states that the population ratio of the $\upsilon = 1$ and $\upsilon = 0$ states is given by

$$\frac{P_{\upsilon=1}}{P_{\upsilon=0}} = e^{-\Delta E/kT}, \tag{1-31}$$

Table 1-3 Relationships among Vibrational Frequency, Reduced Mass and Force Constant

Molecule	Obs. $\tilde{\nu}$ (cm^{-1})	ω_e (cm^{-1})	μ (awu)	K (mdyn/Å)
H_2	4,160	4,395	0.5041	5.73
HD	3,632	3,817	0.6719	5.77
D_2	2,994	3,118	1.0074	5.77
HF	3,962	4,139	0.9573	9.65
HCl	2,886	2,989	0.9799	5.16
HBr	2,558	2,650	0.9956	4.12
HI	2,233	2,310	1.002	3.12
F_2	892	—	9.5023	4.45
Cl_2	546	565	17.4814	3.19
Br_2	319	323	39.958	2.46
I_2	213	215	63.466	1.76
N_2	2,331	2,360	7.004	22.9
CO	2,145	2,170	6.8584	19.0
NO	1,877	1,904	7.4688	15.8
O_2	1,555	1,580	8.000	11.8

where ΔE is the energy difference between the two states, k is Boltzmann's constant (1.3807×10^{-16} erg/degree), and T is the absolute temperature. Since $\Delta E = hc\tilde{\nu}$, the ratio becomes smaller as $\tilde{\nu}$ becomes larger. At room temperature,

$$\begin{aligned} kT &= 1.38 \times 10^{-6} \text{ (erg/degree) } 300 \text{ (degree)} \\ &= 4.14 \times 10^{-14} \text{ (erg)} \\ &= \left[4.14 \times 10^{-14} \text{ (erg)}\right] / \left[1.99 \times 10^{-16} \text{ (erg/cm}^{-1}\text{)}\right] \\ &= 208 \text{ (cm}^{-1}\text{)}. \end{aligned}$$

Thus, if $\bar{\nu} = 4,160\,\text{cm}^{-1}$ (H_2 molecule), $P(\upsilon = 1)/P(\upsilon = 0) = 2.19 \times 10^{-9}$. Therefore, almost all of the molecules are at $\upsilon = 0$. On the other hand, if $\tilde{\nu} = 213\,\text{cm}^{-1}$ (I_2 molecule), this ratio becomes 0.36. Thus, about 27% of the I_2 molecules are at $\upsilon = 1$ state. In this case, the transition $\upsilon = 1 \rightarrow 2$ should be observed on the low-frequency side of the fundamental with much less intensity. Such a transition is called a "hot band" since it tends to appear at higher temperatures.

1.4 Origin of Raman Spectra

As stated in Section 1.1, vibrational transitions can be observed in either IR or Raman spectra. In the former, we measure the absorption of infrared light by the sample as a function of frequency. The molecule absorbs $\Delta E = h\nu$ from

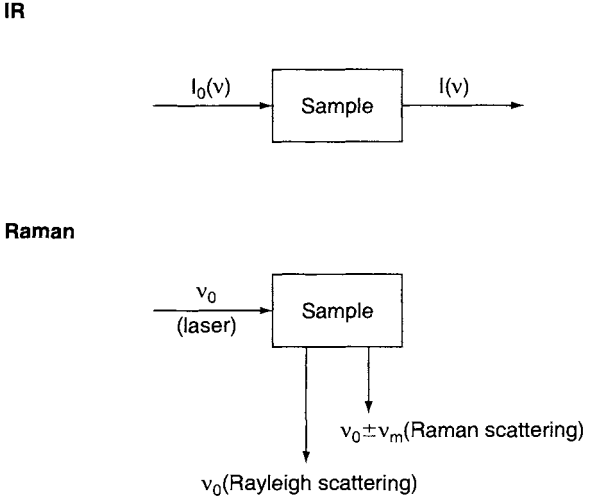

Figure 1-7 Differences in mechanism of Raman vs IR.

the IR source at each vibrational transition. The intensity of IR absorption is governed by the Beer–Lambert law:

$$I = I_0 e^{-\varepsilon cd}. \tag{1-32}$$

Here, I_0 and I denote the intensities of the incident and transmitted beams, respectively, ε is the molecular absorption coefficient,* and c and d are the concentration of the sample and the cell length, respectively (Fig. 1-7). In IR spectroscopy, it is customary to plot the percentage transmission (T) versus wave number ($\tilde{\nu}$):

$$T(\%) = \frac{I}{I_0} \times 100. \tag{1-33}$$

It should be noted that T (%) is not proportional to c. For quantitative analysis, the absorbance (A) defined here should be used:

$$A = \log \frac{I_0}{I} = \varepsilon cd. \tag{1-34}$$

The origin of Raman spectra is markedly different from that of IR spectra. In Raman spectroscopy, the sample is irradiated by intense laser beams in the UV-visible region (ν_0), and the scattered light is usually observed in the direction perpendicular to the incident beam (Fig. 1-7; see also Chapter 2,

*ε has the dimension of l/moles cm when c and d are expressed in units of moles/liter and centimeters, respectively.

Section 2.3). The scattered light consists of two types: one, called *Rayleigh scattering*, is strong and has the same frequency as the incident beam (ν_0), and the other, called *Raman scattering*, is very weak ($\sim 10^{-5}$ of the incident beam) and has frequencies $\nu_0 \pm \nu_m$, where ν_m is a vibrational frequency of a molecule. The $\nu_0 - \nu_m$ and $\nu_0 + \nu_m$ lines are called the *Stokes* and *anti-Stokes* lines, respectively. Thus, in Raman spectroscopy, we measure the vibrational frequency (ν_m) as a shift from the incident beam frequency (ν_0).* In contrast to IR spectra, Raman spectra are measured in the UV-visible region where the excitation as well as Raman lines appear.

According to classical theory, Raman scattering can be explained as follows: The electric field strength (E). of the electromagnetic wave (laser beam) fluctuates with time (t) as shown by Eq. (1-1):

$$E = E_0 \cos 2\pi\nu_0 t, \tag{1-35}$$

where E_0 is the vibrational amplitude and ν_0 is the frequency of the laser. If a diatomic molecule is irradiated by this light, an electric dipole moment P is induced:

$$P = \alpha E = \alpha E_0 \cos 2\pi\nu_0 t. \tag{1-36}$$

Here, α is a proportionality constant and is called *polarizability*. If the molecule is vibrating with a frequency ν_m, the nuclear displacement q is written

$$q = q_0 \cos 2\pi\nu_m t, \tag{1-37}$$

where q_0 is the vibrational amplitude. For a small amplitude of vibration, α is a linear function of q. Thus, we can write

$$\alpha = \alpha_0 + \left(\frac{\partial\alpha}{\partial q}\right)_0 q_0 + \ldots \tag{1-38}$$

Here, α_0 is the polarizability at the equilibrium position, and $(\partial\alpha/\partial q)_0$ is the rate of change of α with respect to the change in q, evaluated at the equilibrium position.

Combining (1-36) with (1-37) and (1-38), we obtain

$$\begin{aligned} P &= \alpha E_0 \cos 2\pi\nu_0 t \\ &= \alpha_0 E_0 \cos 2\pi\nu_0 t + \left(\frac{\partial\alpha}{\partial q}\right)_0 q E_0 \cos 2\pi\nu_0 t \\ &= \alpha_0 E_0 \cos 2\pi\nu_0 t + \left(\frac{\partial\alpha}{\partial q}\right)_0 q_0 E_0 \cos 2\pi\nu_0 t \cos 2\pi\nu_m t \end{aligned}$$

*Although Raman spectra are normally observed for vibrational and rotational transitions, it is possible to observe Raman spectra of electronic transitions between ground states and low-energy excited states.

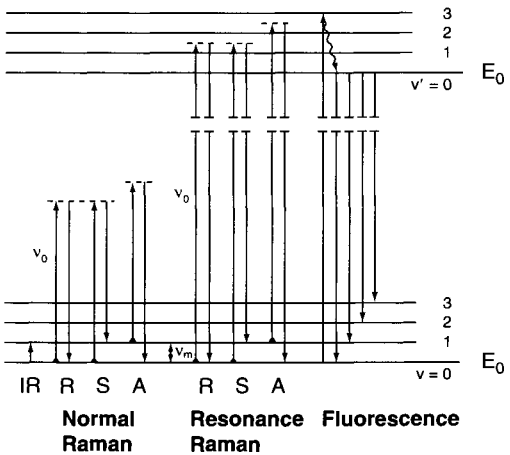

Figure 1-8 Comparison of energy levels for the normal Raman, resonance Raman, and fluorescence spectra.

$$= \alpha_0 E_0 \cos 2\pi\nu_0 t + \frac{1}{2}\left(\frac{\partial\alpha}{\partial q}\right)_0 q_0 E_0[\cos\{2\pi(\nu_0 + \nu_m)t\} + \cos\{2\pi(\nu_0 - \nu_m)t\}]. \quad (1\text{-}39)$$

According to classical theory, the first term represents an oscillating dipole that radiates light of frequency ν_0 (Rayleigh scattering), while the second term corresponds to the Raman scattering of frequency $\nu_0 + \nu_m$ (anti-Stokes) and $\nu_0 - \nu_m$ (Stokes). If $(\partial\alpha/\partial q)_0$ is zero, the vibration is not Raman-active. Namely, to be Raman-active, the rate of change of polarizability (α) with the vibration must not be zero.

Figure 1-8 illustrates Raman scattering in terms of a simple diatomic energy level. In IR spectroscopy, we observe that $\upsilon = 0 \rightarrow 1$ transition at the electronic ground state. In normal Raman spectroscopy, the exciting line (ν_0) is chosen so that its energy is far below the first electronic excited state. The dotted line indicates a "virtual state" to distinguish it from the real excited state. As stated in Section 1.2, the population of molecules at $\upsilon = 0$ is much larger than that at $\upsilon = 1$ (Maxwell–Boltzmann distribution law). Thus, the Stokes (S) lines are stronger than the anti-Stokes (A) lines under normal conditions. Since both give the same information, it is customary to measure only the Stokes side of the spectrum. Figure 1-9 shows the Raman spectrum of CCl_4*.

*A Raman spectrum is expressed as a plot, intensity vs. Raman shift ($\Delta\tilde{\nu} = \tilde{\nu}_0 \pm \tilde{\nu}$). However, $\Delta\tilde{\nu}$ is often written as $\tilde{\nu}$ for brevity.

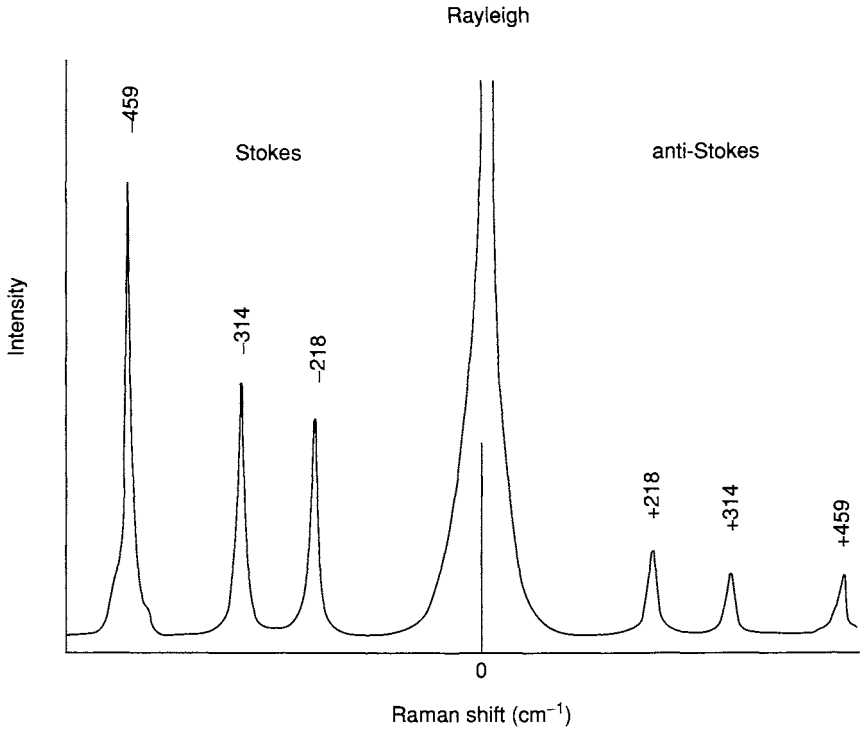

Figure 1-9 Raman spectrum of CCl_4 (488.0 nm excitation).

Resonance Raman (RR) scattering occurs when the exciting line is chosen so that its energy intercepts the manifold of an electronic excited state. In the liquid and solid states, vibrational levels are broadened to produce a continuum. In the gaseous state, a continuum exists above a series of discrete levels. Excitation of these continua produces RR spectra that show extremely strong enhancement of Raman bands originating in this particular electronic transition. Because of its importance, RR spectroscopy will be discussed in detail in Section 1.15. The term "pre-resonance" is used when the exciting line is close in energy to the electronic excited state. Resonance fluorescence (RF) occurs when the molecule is excited to a discrete level of the electronic excited state (20). This has been observed for gaseous molecules such as I_2, Br_2. Finally, fluorescence spectra are observed when the excited state molecule decays to the lowest vibrational level via radiationless transitions and then emits radiation, as shown in Fig. 1-8. The lifetime of the excited state in RR is very short ($\sim 10^{-14}$ s), while those in RF and fluorescence are much longer ($\sim 10^{-8}$ to 10^{-5} s).

1.5 Factors Determining Vibrational Frequencies

According to Eq. (1-26), the vibrational frequency of a diatomic molecule is given by

$$\tilde{\nu} = \frac{1}{2\pi c}\sqrt{\frac{K}{\mu}} \tag{1-40}$$

where K is the force constant and μ is the reduced mass. This equation shows that $\tilde{\nu}$ is proportional to $\sqrt{K}$ (force constant effect), but inversely proportional to $\sqrt{\mu}$ (mass effect). To calculate the force constant, it is convenient to rewrite the preceding equations as

$$K = 4\pi^2 c^2 \omega_e^2 \mu. \tag{1-41}$$

Here, the vibrational frequency (observed) has been replaced by ω_e (Eq. (1-30)) in order to obtain a more accurate force constant. Using the unit of millidynes/Å (mdyn/Å) or 10^5 (dynes/cm) for K, and the atomic weight unit (awu) for μ, Eq. (1-41) can be written as

$$\begin{aligned} K &= 4(3.14)^2(3 \times 10^{10})^2 \left[\frac{\mu}{6{,}025 \times 10^{23}}\right] \omega_e^2 \\ &= (5.8883 \times 10^{-2}) \mu \omega_e^2. \end{aligned} \tag{1-42}$$

For $H^{35}Cl$, $\omega_e = 2{,}989\,\text{cm}^{-1}$ and μ is 0.9799. Then, its K is 5.16×10^5 (dynes/cm) or 5.16 (mdyn/Å). If such a calculation is made for a number of diatomic molecules, we obtain the results shown in Table 1-3. In all four series of compounds, the frequency decreases in going downward in the table. However, the origin of this downward shift is different in each case. In the $H_2 > HD > D_2$ series, it is due to the mass effect since the force constant is not affected by isotopic substitution. In the HF > HCl > HBr > HI series, it is due to the force constant effect (the bond becomes weaker in the same order) since the reduced mass is almost constant. In the $F_2 > Cl_2 > Br_2 > I_2$ series, however, both effects are operative; the molecule becomes heavier and the bond becomes weaker in the same order. Finally, in the $N_2 > CO > NO > O_2$, series, the decreasing frequency is due to the force constant effect that is expected from chemical formulas, such as N≡N, and O=O, with CO and NO between them.

It should be noted, however, that a large force constant does not necessarily mean a stronger bond, since the force constant is the curvature of the potential well near the equilibrium position,

$$K = \left(\frac{d^2 V}{dq^2}\right)_{q \to 0} \tag{1-43}$$

whereas the bond strength (dissociation energy) is measured by the depth of the potential well (Fig. 1-6). Thus, a large K means a sharp curvature near the bottom of the potential well, and does not directly imply a deep potential well. For example,

	HF		HCl		HBr		HI
K (mdyn/Å)	9.65	>	5.16	>	4.12	>	3.12
D_e (kcal/mole)	134.6	>	103.2	>	87.5	>	71.4

However,

	F_2		Cl_2		Br_2		I_2
K (mdyn/Å)	4.45	>	3.19	>	2.46	>	1.76
D_e (kcal/mole)	37.8	<	58.0	>	46.1	>	36.1

A rough parallel relationship is observed between the force constant and the dissociation energy when we plot these quantities for a large number of compounds.

1.6 Vibrations of Polyatomic Molecules

In diatomic molecules, the vibration occurs only along the chemical bond connecting the nuclei. In polyatomic molecules, the situation is complicated because all the nuclei perform their own harmonic oscillations. However, we can show that any of these complicated vibrations of a molecule can be expressed as a superposition of a number of "normal vibrations" that are completely independent of each other.

In order to visualize normal vibrations, let us consider a mechanical model of the CO_2 molecule shown in Fig. 1-10. Here, the C and O atoms are represented by three balls, weighing in proportion to their atomic weights, that are connected by springs of a proper strength in proportion to their force constants. Suppose that the C—O bonds are stretched and released

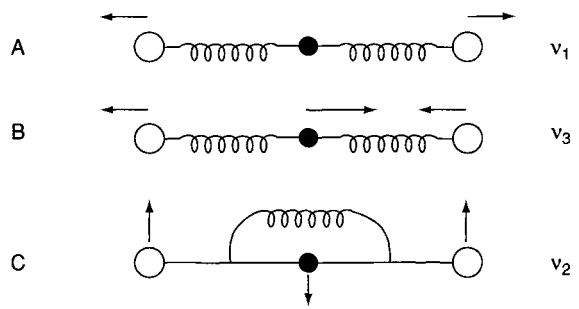

Figure 1-10 Atomic motions in normal modes of vibrations in CO_2.

simultaneously as shown in Fig. 1-10A. Then, the balls move back and forth along the bond direction. This is one of the normal vibrations of this model and is called the symmetric (in-phase) stretching vibration. In the real CO_2 molecule, its frequency (ν_1) is ca. 1,340 cm^{-1}. Next, we stretch one C—O bond and shrink the other, and release all the balls simultaneously (Fig. 1-10B). This is another normal vibration and is called the antisymmetric (out-of-phase) stretching vibration. In the CO_2 molecule, its frequency (ν_3) is ca. 2,350 cm^{-1}. Finally, we consider the case where the three balls are moved in the perpendicular direction and released simultaneously (Fig. 1-10C). This is the third type of normal vibration called the (symmetric) bending vibration. In the CO_2 molecule, its frequency (ν_2) is ca. 667 cm^{-1}.

Suppose that we strike this mechanical model with a hammer. Then, this model would perform an extremely complicated motion that has no similarity to the normal vibrations just mentioned. However, if this complicated motion is photographed with a stroboscopic camera with its frequency adjusted to that of the normal vibration, we would see that each normal vibration shown in Fig. 1-10 is performed faithfully. In real cases, the stroboscopic camera is replaced by an IR or Raman instrument that detects only the normal vibrations.

Since each atom can move in three directions (x,y,z), an N-atom molecule has $3N$ degrees of freedom of motion. However, the $3N$ includes six degrees of freedom originating from translational motions of the whole molecule in the three directions and rotational motions of the whole molecule about the three principal axes of rotation, which go through the center of gravity. Thus, the net vibrational degrees of freedom (number of normal vibrations) is $3N - 6$. In the case of linear molecules, it becomes $3N - 5$ since the rotation about the molecular axis does not exist. In the case of the CO_2 molecule, we have $3 \times 3 - 5 = 4$ normal vibrations shown in Fig. 1-11. It should be noted that ν_{2a} and ν_{2b} have the same frequency and are different only in the direction of vibration by 90°. Such a pair is called a set of doubly degenerate vibrations. Only two such vibrations are regarded as unique since similar vibrations in any other directions can be expressed as a linear combination of ν_{2a} and ν_{2b}. Figure 1-12 illustrates the three normal vibrations ($3 \times 3 - 6 = 3$) of the H_2O molecule.

Theoretical treatments of normal vibrations will be described in Section 1.20. Here, it is sufficient to say that we designate "normal coordinates" Q_1, Q_2 and Q_3 for the normal vibrations such as the ν_1, ν_2 and ν_3, respectively, of Fig. 1-12, and that the relationship between a set of normal coordinates and a set of Cartesian coordinates ($q_1, q_2, \ldots$) is given by

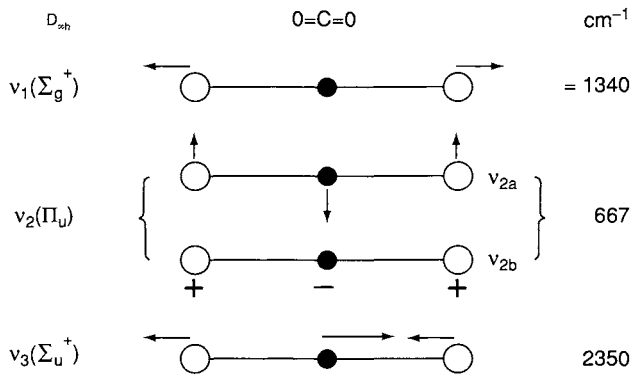

Figure 1-11 Normal modes of vibration in CO_2 (+ and − denote vibrations going upward and downward, respectively, in direction perpendicular to the paper plane).

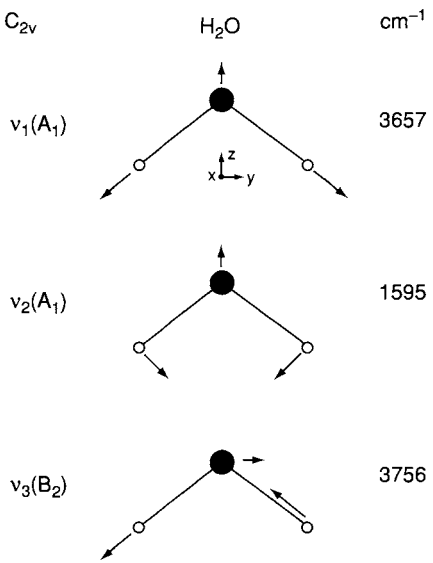

Figure 1-12 Normal modes of vibrations in H_2O.

$$
\begin{aligned}
q_1 &= B_{11}Q_1 + B_{12}Q_2 + \ldots, \\
q_2 &= B_{21}Q_1 + B_{22}Q_2 + \ldots, \\
&\ldots,
\end{aligned}
\tag{1-44}
$$

so that the modes of normal vibrations can be expressed in terms of Cartesian coordinates if the B_{ij} terms are calculated.

1.7 Selection Rules for Infrared and Raman Spectra

To determine whether the vibration is active in the IR and Raman spectra, the selection rules must be applied to each normal vibration. Since the origins of IR and Raman spectra are markedly different (Section 1.4), their selection rules are also distinctively different. According to quantum mechanics (18,19) a vibration is IR-active if the dipole moment is changed during the vibration and is Raman-active if the polarizability is changed during the vibration.

The IR activity of small molecules can be determined by inspection of the mode of a normal vibration (normal mode). Obviously, the vibration of a homopolar diatomic molecule is not IR-active, whereas that of a heteropolar diatomic molecule is IR-active. As shown in Fig. 1-13, the dipole moment of the H_2O molecule is changed during each normal vibration. Thus, all these vibrations are IR-active. From inspection of Fig. 1-11, one can readily see that ν_2 and ν_3 of the CO_2 molecule are IR-active, whereas ν_1 is not IR-active.

To discuss Raman activity, let us consider the nature of the polarizability (α) introduced in Section 1.4. When a molecule is placed in an electric field (laser beam), it suffers distortion since the positively charged nuclei are attracted toward the negative pole, and electrons toward the positive pole (Fig. 1-14). This charge separation produces an induced dipole moment (P) given by

$$P = \alpha E. \tag{1-45}*$$

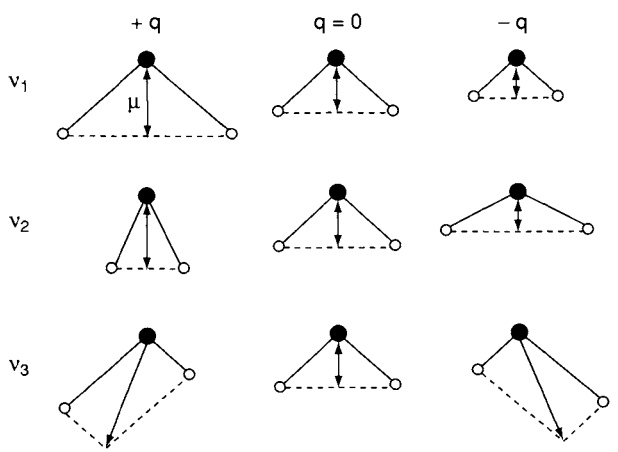

Figure 1-13 Change in dipole moment for H_2O molecule during each normal vibration.

*A more accurate expression is given by Eq. 3-1 in Chapter 3.

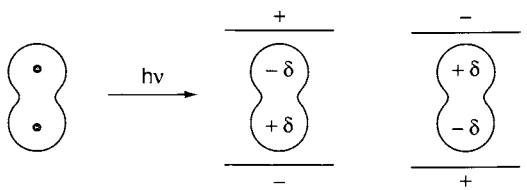

Figure 1-14 Polarization of a diatomic molecule in an electric field.

In actual molecules, such a simple relationship does not hold since both P and E are vectors consisting of three components in the x, y and z directions. Thus, Eq. (1-45) must be written as

$$\begin{aligned} P_x &= \alpha_{xx}E_x + \alpha_{xy}E_y + \alpha_{xz}E_z, \\ P_y &= \alpha_{yx}E_x + \alpha_{yy}E_y + \alpha_{yz}E_z, \\ P_z &= \alpha_{zx}E_x + \alpha_{zy}E_y + \alpha_{zz}E_z. \end{aligned} \tag{1-46}$$

In matrix form, this is written as

$$\begin{bmatrix} P_x \\ P_y \\ P_z \end{bmatrix} = \begin{bmatrix} \alpha_{xx} & \alpha_{xy} & \alpha_{xz} \\ \alpha_{yx} & \alpha_{yy} & \alpha_{yz} \\ \alpha_{zx} & \alpha_{zy} & \alpha_{zz} \end{bmatrix} \begin{bmatrix} E_x \\ E_y \\ E_z \end{bmatrix} \tag{1-47}$$

The first matrix on the right-hand side is called the *polarizability tensor*. In normal Raman scattering, this tensor is symmetric; $\alpha_{xy} = \alpha_{yz}$, $\alpha_{xz} = \alpha_{zx}$ and $\alpha_{yz} = \alpha_{zy}$. According to quantum mechanics, the vibration is Raman-active if one of these components of the polarizability tensor is changed during the vibration.

In the case of small molecules, it is easy to see whether or not the polarizability changes during the vibration. Consider diatomic molecules such as H_2 or linear molecules such as CO_2. Their electron clouds have an elongated water melon like shape with circular cross-sections. In these molecules, the electrons are more polarizable (a larger α) along the chemical bond than in the direction perpendicular to it. If we plot α_i (α in the i-direction) from the center of gravity in all directions, we end up with a three-dimensional surface. Conventionally, we plot $1/\sqrt{\alpha_i}$ rather than α_i itself and call the resulting three-dimensional body a *polarizability ellipsoid.* Figure 1-15 shows the changes of such an ellipsoid during the vibrations of the CO_2 molecule.

In terms of the polarizability ellipsoid, the vibration is Raman-active if the *size, shape* or *orientation* changes during the normal vibration. In the ν_1 vibration, the size of the ellipsoid is changing; the diagonal elements (α_{xx}, α_{yy} and α_{zz}) are changing simultaneously. Thus, it is Raman-active. Although the size of the ellipsoid is changing during the ν_3 vibration, the ellipsoids at

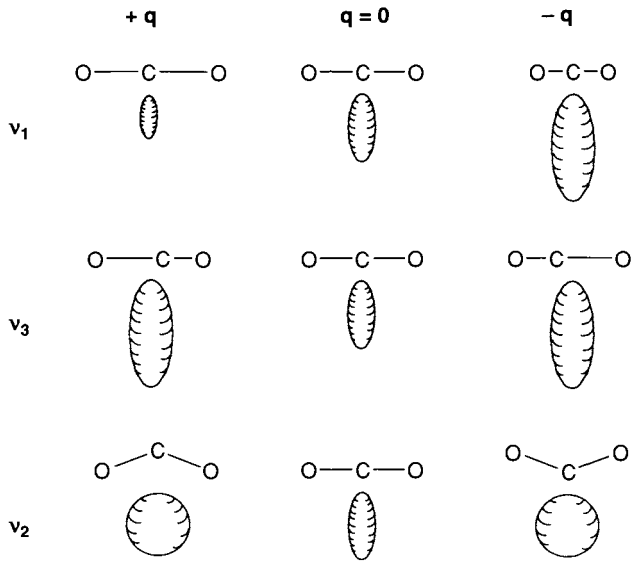

Figure 1-15 Changes in polarizability ellipsoids during vibration of CO_2 molecule.

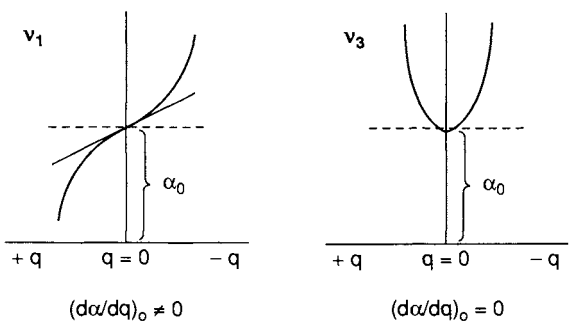

Figure 1-16 Difference between ν_1 and ν_3 vibrations in CO_2 molecule.

two extreme displacements ($+q$ and $-q$) are exactly the same in this case. Thus, this vibration is not Raman-active if we consider a small displacement. The difference between the ν_1 and ν_3 is shown in Fig. 1-16. Note that the Raman activity is determined by $(d\alpha/dq)_0$ (slope near the equilibrium position). During the ν_2 vibration, the shape of the ellipsoid is sphere-like at two extreme configurations. However, the size and shape of the ellipsoid are exactly the same at $+q$ and $-q$. Thus, it is not Raman-active for the same reason as that of ν_3. As these examples show, it is not necessary to figure out the exact size, shape or orientation of the ellipsoid to determine Raman activity.

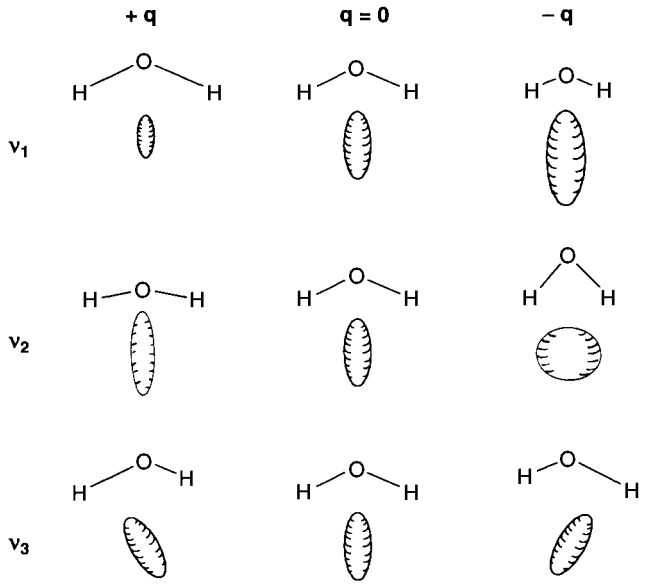

Figure 1-17 Changes in polarizability ellipsoid during normal vibrations of H_2O molecule.

Figure 1-17 illustrates the changes in the polarizability ellipsoid during the normal vibrations of the H_2O molecule. Its ν_1 vibration is Raman-active, as is the ν_1 vibration of CO_2. The ν_2 vibration is also Raman-active because the *shape* of the ellipsoid is different at $+q$ and $-q$. In terms of the polarizability tensor, α_{xx}, α_{yy} and α_{zz} are all changing with different rates. Finally, the ν_3 vibration is Raman-active because the *orientation* of the ellipsoid is changing during the vibration. This activity occurs because an off-diagonal element (α_{yz} in this case) is changing.

One should note that, in CO_2, the vibration that is symmetric with respect to the center of symmetry (ν_1) is Raman-active but not IR-active, whereas those that are antisymmetric with respect to the center of symmetry (ν_2 and ν_3) are IR-active but not Raman-active. This condition is called the *mutual exclusion principle* and holds for any molecules having a center of symmetry.*

The preceding examples demonstrate that IR and Raman activities can be determined by inspection of the normal mode. Clearly, such a simple approach is not applicable to large and complex molecules. As will be shown in Section 1.14, group theory provides elegant methods to determine IR and Raman activities of normal vibrations of such molecules.

*This principle holds even if a molecule has no atom at the center of symmetry (e.g., benzene).

1.8 Raman versus Infrared Spectroscopy

Although IR and Raman spectroscopies are similar in that both techniques provide information on vibrational frequencies, there are many advantages and disadvantages unique to each spectroscopy. Some of these are listed here.

1. As stated in Section 1.7, selection rules are markedly different between IR and Raman spectroscopies. Thus, some vibrations are only Raman-active while others are only IR-active. Typical examples are found in molecules having a center of symmetry for which the mutual exclusion rule holds. In general, a vibration is IR-active, Raman-active, or active in both; however, totally symmetric vibrations are always Raman-active.

2. Some vibrations are inherently weak in IR and strong in Raman spectra. Examples are the stretching vibrations of the C≡C, C=C, P=S, S—S and C—S bonds. In general, vibrations are strong in Raman if the bond is covalent, and strong in IR if the bond is ionic (O—H, N—H). For covalent bonds, the ratio of relative intensities of the C≡C, C=C and C—C bond stretching vibrations in Raman spectra is about 3:2:1.* Bending vibrations are generally weaker than stretching vibrations in Raman spectra.

3. Measurements of depolarization ratios provide reliable information about the symmetry of a normal vibration in solution (Section 1.9). Such information can not be obtained from IR spectra of solutions where molecules are randomly orientated.

4. Using the resonance Raman effect (Section 1.15), it is possible to selectively enhance vibrations of a particular chromophoric group in the molecule. This is particularly advantageous in vibrational studies of large biological molecules containing chromophoric groups (Sections 4.1 and 6.1.)

5. Since the diameter of the laser beam is normally 1–2 mm, only a small sample area is needed to obtain Raman spectra. This is a great advantage over conventional IR spectroscopy when only a small quantity of the sample (such as isotopic chemicals) is available.

6. Since water is a weak Raman scatterer, Raman spectra of samples in aqueous solution can be obtained without major interference from water vibrations. Thus, Raman spectroscopy is ideal for the studies of biological compounds in aqueous solution. In contrast, IR spectroscopy suffers from the strong absorption of water.

*In general, the intensity of Raman scattering increases as the $(d\alpha/dq)_0$ becomes larger.

7. Raman spectra of hygroscopic and/or air-sensitive compounds can be obtained by placing the sample in sealed glass tubing. In IR spectroscopy, this is not possible since glass tubing absorbs IR radiation.

8. In Raman spectroscopy, the region from 4,000 to 50 cm^{-1} can be covered by a single recording. In contrast, gratings, beam splitters, filters and detectors must be changed to cover the same region by IR spectroscopy.

Some disadvantages of Raman spectroscopy are the following:

1. A laser source is needed to observe weak Raman scattering. This may cause local heating and/or photodecomposition, especially in resonance Raman studies (Section 1.15) where the laser frequency is deliberately tuned in the absorption band of the molecule.

2. Some compounds fluoresce when irradiated by the laser beam.

3. It is more difficult to obtain rotational and rotation–vibration spectra with high resolution in Raman than in IR spectroscopy. This is because Raman spectra are observed in the UV-visible region where high resolving power is difficult to obtain.

4. The state of the art Raman system costs much more than a conventional FT-IR spectrophotometer although less expensive versions have appeared which are smaller and portable and suitable for process applications (Section 2-10).

Finally, it should be noted that vibrational (both IR and Raman) spectroscopy is unique in that it is applicable to the solid state as well as to the gaseous state and solution. In contrast, X-ray diffraction is applicable only to the crystalline state, whereas NMR spectroscopy is applicable largely to the sample in solution.

1.9 Depolarization Ratios

As stated in the preceding section, depolarization ratios of Raman bands provide valuable information about the symmetry of a vibration that is indispensable in making band assignments. Figure 1-18 shows a coordinate system which is used for measurements of depolarization ratios. A molecule situated at the origin is irradiated from the y-direction with plane polarized light whose electric vector oscillates on the yz-plane (E_z). If one observes scattered radiation from the x-direction, and measures the intensities in the

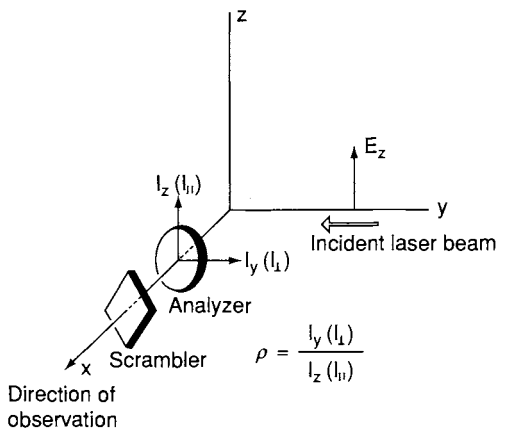

Figure 1-18 Irradiation of sample from the y-direction with plane polarized light, with the electronic vector in the z-direction.

$y(I_y)$ and $z(I_z)$-directions using an analyzer, the depolarization ratio (ρ_p) measured by polarized light (p) is defined by

$$\rho_p = \frac{I_\perp(I_y)}{I_\parallel(I_z)}. \tag{1-48}$$

Figure 2-1 of Chapter 2 shows an experimental configuration for depolarization measurements in 90° scattering geometry. In this case, the polarizer is not used because the incident laser beam is almost completely polarized in the z direction. If a premonochromator is placed in front of the laser, a polarizer must be inserted to ensure complete polarization. The scrambler (crystal quartz wedge) must always be placed after the analyzer since the monochromator gratings show different efficiencies for $\perp$ and $\parallel$ polarized light. For information on precise measurements of depolarization ratios, see Refs. 21–24.

Suppose that a tetrahedral molecule such as CCl_4 is irradiated by plane polarized light (E_z). Then, the induced dipole (Section 1.7) also oscillates in the same yz-plane. If the molecule is performing the totally symmetric vibration, the polarizability ellipsoid is always sphere-like; namely, the molecule is polarized equally in every direction. Under such a circumstance, $I_\perp(I_y) = 0$ since the oscillating dipole emitting the radiation is confined to the xz-plane. Thus, $\rho_p = 0$. Such a vibration is called *polarized* (abbreviated as p). In liquids and solutions, molecules take random orientations. Yet this conclusion holds since the polarizability ellipsoid is spherical throughout the totally symmetric vibration.

If the molecule is performing a non-totally symmetric vibration, the polarizability ellipsoid changes its shape from a sphere to an ellipsoid during the

vibration. Then, the induced dipole would be largest along the direction of largest polarizability, namely along one of the minor axes of the ellipsoid. Since these axes would be randomly oriented in liquids and solutions, the induced dipole moments would also be randomly oriented. In this case, the ρ_p is nonzero, and the vibration is called *depolarized* (abbreviated as *dp*). Theoretically, we can show (25) that

$$\rho_p = \frac{3g^s + 5g^a}{10g^0 + 4g^s} \tag{1-49}$$

where

$$g^0 = \frac{1}{3}(\alpha_{xx} + \alpha_{yy} + \alpha_{zz})^2,$$

$$g^s = \frac{1}{3}\left[(\alpha_{xx} - \alpha_{yy})^2 + (\alpha_{yy} - \alpha_{zz})^2 + (\alpha_{zz} - \alpha_{xx})^2\right] + \frac{1}{2}\left[(\alpha_{xy} + \alpha_{yx})^2 + (\alpha_{yz} + \alpha_{zy})^2 + (\alpha_{xz} + \alpha_{zx})^2\right],$$

$$g^a = \frac{1}{2}\left[(\alpha_{xy} - \alpha_{yx})^2 + (\alpha_{xz} - \alpha_{zx})^2 + (\alpha_{yz} - \alpha_{zy})^2\right].$$

In normal Raman scattering, $g^a = 0$ since the polarizability tensor is symmetric. Then, (1-49) becomes

$$\rho_p = \frac{3g^s}{10g^0 + 4g^s} \tag{1-50}$$

For totally symmetric vibrations, $g^0 > 0$ and $g^s \geq 0$. Thus, $0 \leq \rho_p < \frac{3}{4}$ (polarized). For non-totally symmetric vibrations, $g^0 = 0$ and $g^s > 0$. Then, $\rho_p = \frac{3}{4}$ (depolarized).

In resonance Raman scattering ($g^a \neq 0$), it is possible to have $\rho_p > \frac{3}{4}$. For example, if $\alpha_{xy} = -\alpha_{yx}$ and the remaining off-diagonal elements are zero, $g^0 = g^s = 0$ and $g^a \neq 0$. Then, (1-49) gives $\rho_p \to \infty$. This is called *anomalous* (or *inverse*) *polarization* (abbreviated as ap or ip). As will be shown in Section 1.15, resonance Raman spectra of metallopophyrins exhibit polarized (A_{1g}) and depolarized (B_{1g} and B_{2g}) vibrations as well as those of anomalous (or inverse) polarization (A_{2g}).

Figure 1-19 shows the Raman spectra of CCl_4 obtained with 90° scattering geometry. In this case, the ρ_p values obtained were 0.02 for the totally symmetric (459 cm^{-1}) and 0.75 for the non-totally symmetric modes (314 and 218 cm^{-1}). For ρ_p values in other scattering geometry, see Ref. 26.

Although polarization data are normally obtained for liquids and single crystals,* it is possible to measure depolarization ratios of Raman lines from solids by suspending them in a material with similar index of refraction (27).

*For an example of the use of polarized Raman spectra of calcite single crystal, see Section 1.19.

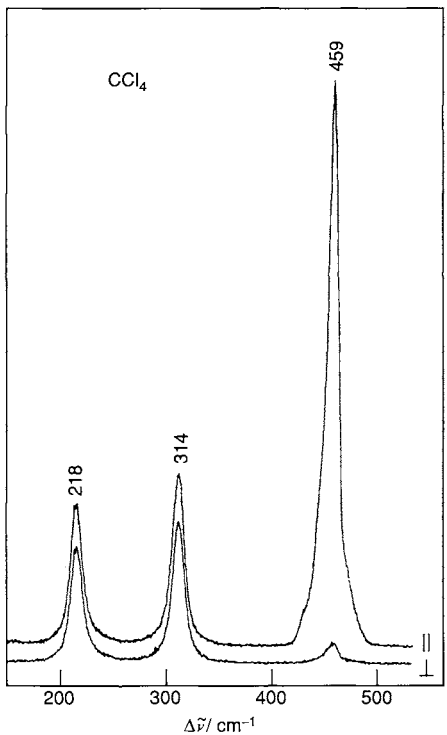

Figure 1-19 Raman spectrum of CCl_4 (500–200 cm^{-1}) in parallel and perpendicular polarization (488 nm excitation).

The use of suspensions can be circumvented by adding carbon black or CuO (28). The function of dark (black) additives appears to be related to a reduction of the penetration depth of the laser beam, causing an attenuation of reflected or refractive radiation, which is scrambled relative to polarization.

1.10 The Concept of Symmetry

The various experimental tools that are utilized today to solve structural problems in chemistry, such as Raman, infrared, NMR, magnetic measurements and the diffraction methods (electron, X-ray, and neutron), are based on symmetry considerations. Consequently, the symmetry concept as applied to molecules is thus very important.

Symmetry may be defined in a nonmathematical sense, where it is associated with beauty—with pleasing proportions or regularity in form, harmonious arrangement, or a regular repetition of certain characteristics (e.g.,

periodicity). In the mathematical or geometrical definition, symmetry refers to the correspondence of elements on opposite sides of a point, line, or plane, which we call the center, axis, or plane of symmetry (symmetry elements). It is the mathematical concept that is pursued in the following sections. The discussion in this section will define the symmetry elements in an isolated molecule (the point symmetry)—of which there are five. The number of ways by which symmetry elements can combine constitute a group, and these include the 32 crystallographic point groups when one considers a crystal. Theoretically, an infinite number of point groups can exist, since there are no restrictions on the order of rotational axes of an isolated molecule. However, in a practical sense, few molecules possess rotational axes C_n where $n > 6$. Each point group has a character table (see Appendix 1), and the features of these tables are discussed. The derivation of the selection rules for an isolated molecule is made with these considerations. If symmetry elements are combined with translations, one obtains operations or elements of symmetry that can define the symmetry of space as in a crystal. Two symmetry elements, the screw axis (rotation followed by a translation) and the glide plane (reflection followed by a translation), when added to the five point group symmetry elements, constitute the seven space symmetry elements. This final set of symmetry elements allows one to determine selection rules for the solid state.

Derivation of selection rules for a particular molecule illustrates the complementary nature of infrared and Raman spectra and the application of group theory to the determination of molecular structure.

1.11 Point Symmetry Elements

The spatial arrangement of the atoms in a molecule is called its equilibrium configuration or structure. This configuration is invariant under a certain set of geometric operations called a group. The molecule is oriented in a coordinate system (a right-hand *xyz* coordinate system is used throughout the discussion in this section). If by carrying out a certain geometric operation on the original configuration, the molecule is transformed into another configuration that is superimposable on the original (i.e., indistinguishable from it, although its orientation may be changed), the molecule is said to contain a symmetry element. The following symmetry elements can be cited.

1.11.1 Identity (E)

The symmetry element that transforms the original equilibrium configuration into another one superimposable on the original without change in

orientation, in such a manner that each atom goes into itself, is called the identity and is denoted by E or I (E from the German *Einheit* meaning "unit" or, loosely, "identical"). In practice, this operation means to leave the molecule unchanged.

1.11.2 Rotation Axes (C_n)

If a molecule is rotated about an axis to a new configuration that is indistinguishable from the original one, the molecule is said to possess a rotational axis of symmetry. The rotation can be clockwise or counterclockwise, depending on the molecule. For example, the same configuration is obtained for the water molecule whether one rotates the molecule clockwise or counterclockwise. However, for the ammonia molecule, different configurations are obtained, depending on the direction around which the rotation is performed. The angle of rotation may be $2\pi/n$, or $360°/n$, where n can be 1, 2, 3, 4, 5, $6, \ldots, \infty$. The order of the rotational axis is called n (sometimes p), and the notation C_n is used, where C (cyclic) denotes rotation. In cases where several axes of rotation exist, the highest order of rotation is chosen as the principal (z) axis. Linear molecules have an infinitefold axes of symmetry (C_∞).

The selection of the axes in a coordinate system can be confusing. To avoid this, the following rules are used for the selection of the z axis of a molecule:

(1) In molecules with only one rotational axis, this axis is taken as the z axis.
(2) In molecules where several rotational axes exist, the highest-order axis is selected as the z axis.
(3) If a molecule possesses several axes of the highest order, the axis passing through the greatest number of atoms is taken as the z axis.

For the selection of the x axis the following rules can be cited:

(1) For a planar molecule where the z axis lies in this plane, the x axis can be selected to be normal to this plane.
(2) In a planar molecule where the z axis is chosen to be perpendicular to the plane, the x axis must lie in the plane and is chosen to pass through the largest number of atoms in the molecule.
(3) In nonplanar molecules the plane going through the largest number of atoms is located as if it were in the plane of the molecule and rule (1) or (2) is used. For complex molecules where a selection is difficult, one chooses the x and y axes arbitrarily.

1.11.3 Planes of Symmetry (σ)

If a plane divides the equilibrium configuration of a molecule into two parts that are mirror images of each other, then the plane is called a symmetry

plane. If a molecule has two such planes, which intersect in a line, this line is an axis of rotation (see the previous section); the molecule is said to have a vertical rotation axis C; and the two planes are referred to as vertical planes of symmetry, denoted by σ_v. Another case involving two planes of symmetry and their intersection arises when a molecule has more than one axis of symmetry. For example, planes intersecting in an n-fold axis perpendicular to n twofold axes, with each of the planes bisecting the angle between two successive twofold axes, are called diagonal and are denoted by the symbol σ_d. Figure 1-20a–c illustrates the symmetry elements of

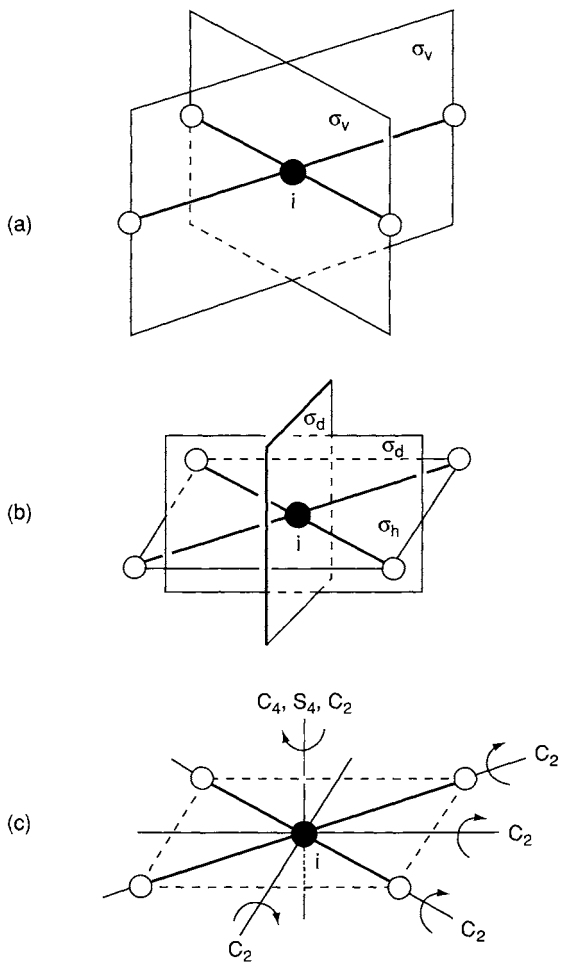

Figure 1-20 Symmetry elements for a planar AB_4 molecule (e.g., $PtCl_4^{2-}$ ion).

the planar AB_4 molecule (e.g., $PtCl_4^{2-}$ ion). If a plane of symmetry is perpendicular to the principal rotational axis, it is called horizontal and is denoted by σ_h.

1.11.4 Center of Symmetry (i)

If a straight line drawn from each atom of a molecule through a certain point meets an equivalent atom equidistant from the point, we call the point the center of symmetry of the molecule. The center of symmetry may or may not coincide with the position of an atom. The designation for the center of symmetry, or center of inversion, is i. If the center of symmetry is situated on an atom, the total number of atoms in the molecule is odd. If the center of symmetry is not on an atom, the number of atoms in the molecule is even. Figure 1-20C illustrates a center of symmetry and rotational axes for the planar AB_4 molecule.

1.11.5 Rotation Reflection Axes (S_n)

If a molecule is rotated $360°/n$ about an axis and then reflected in a plane perpendicular to the axis, and if the operation produces a configuration indistinguishable from the original one, the molecule has the symmetry element of rotation–reflection, which is designated by S_n.

Table 1-4 lists the point symmetry elements and the corresponding symmetry operations. The notation used by spectroscopists and chemists, and used here, is the so-called Schoenflies system, which deals only with point groups. Crystallographers generally use the Hermann–Mauguin system, which applies to both point and space groups.

Table 1-4 Point Symmetry Elements and Symmetry Operations

	Symmetry Element	Symmetry Operation
1.	Identity (E or I)	Molecule unchanged
2.	Axis of rotation (C_n)	Rotation about axis by $2\pi/n, n = 1, 2, 3, 4, 5, 6, \ldots, \infty$ for an isolated molecule and $n = 1, 2, 3, 4$ and 6 for a crystal.
3.	Center of symmetry or center of inversion (i)	Inversion of all atoms through center.
4.	Plane of symmetry (σ)	Reflection in the plane.
5.	Rotation reflection axis (S_n)	Rotation about axis by $2\pi/n$ followed by reflection in a plane perpendicular to the axis

(*a*) *Point Groups*

It can be shown that a group consists of mathematical elements (symmetry elements or operations), and if the operation is taken to be performing one symmetry operation after another in succession, and the result of these operations is equivalent to a single symmetry operation in the set, then the set will be a mathematical group. The postulates for a complete set of elements $A, B, C, \ldots$ are as follows:

(1) For every pair of elements A and B, there exists a binary operation that yields the product AB belonging to the set.
(2) This binary product is associative, which implies that $A(BC) = (AB)C$.
(3) There exists an identity element E such that for every A, $AE = EA = A$.
(4) There is an inverse A^{-1} for each element A such that $AA^{-1} = A^{-1}A = E$.

For molecules it would seem that the point symmetry elements can combine in an unlimited way. However, only certain combinations occur. In the mathematical sense, the sets of all its symmetry elements for a molecule that adhere to the preceding postulates constitute a point group. If one considers an isolated molecule, rotation axes having $n = 1, 2, 3, 4, 5, 6$ to ∞ are possible. In crystals n is limited to $n = 1, 2, 3, 4$, and 6 because of the *space-filling requirement*. Table 1-5 lists the symmetry elements of the 32 point groups.

(*b*) *Rules for Classifying Molecules into their Proper Point Group*

The method for the classification of molecules into different point groups suggested by Zeldin (29) is outlined in Table 1-6. The method can be described as follows:

(1) Determine whether the molecule belongs to a special group such as $D_{\infty h}$, $C_{\infty v}$, T_d, O_h or I_h. If the molecule is linear, it will be either $D_{\infty h}$ or $C_{\infty v}$. If the molecule has an infinite number of twofold axes perpendicular to the C_∞ axis, it will fall into point group $D_{\infty h}$. If not, it is $C_{\infty v}$.
(2) If the molecule is not linear, it may belong to a point group of extremely high symmetry such as T_d, O_h, or I_h.
(3) If (1) or (2) is not found to be the case, look for a proper axis of rotation of the highest order in the molecule. If none is found, the molecule is of low symmetry, falling into point group C_3, C_i, or C_1. The presence in the molecule of a plane of symmetry or an inversion center will distinguish among these point groups.
(4) If C_n axes exist, select the one of highest order. If the molecule also has an S_{2n} axis, with or without an inversion center, the point group is S_n.

Table 1-5 The 32 Crystallographic Point Groups[a]

Symbol	Plane	Axes of Symmetry				Center	Example
	σ	$6(C_6)$	$4(C_4)$	$3(C_3)$	$2(C_2)$	i	
C_1	—	—	—	—	—	—	CH_3CHO
C_2	—	—	—	—	1	—	H_2O_2
C_3	—	—	—	1	—	—	$B(OH)_3$
C_4	—	—	1	—	—	—	$H_2S(s)$
C_6	—	1	—	—	—	—	—
C_s	1	—	—	—	—	—	HCOCl
C_{2h}	1	—	—	—	1	1	*trans*-CHCl═CHCl
C_{3h}	1	—	—	1	—	—	$C^+(NH_2)_3$
C_{4h}	1	—	1	—	—	1	$C_4H_4Cl_4$
C_{6h}	1	1	—	—	—	1	—
D_2	—	—	—	—	3	—	—
D_3	—	—	—	1	3	—	$Co(H_2NCH_2CH_2NH_2)_3^{3+}$
D_4	—	—	1	—	4	—	cyclobutane
D_6	—	1	—	—	6	—	—
D_{2h}	3	—	—	—	3	1	C_2H_4
D_{3h}	4	—	—	1	3	—	BCl_3

D_{4h}	5	—	1	—	4	1	$PtCl_4^{2-}$
D_{6h}	7	1	—	—	6	1	C_6H_6
$S_2(C_i)$	—	—	—	—	—	1	FClHC-CHClF
S_4	—	—	—	—	1	—	$C_{10}H_4F_4$
$S_6(C_{3i})$	—	—	—	1	—	1	—
D_{2d}	2	—	—	—	3	—	$CH_2{=}C{=}CH_2$
D_{3d}	3	—	—	1	3	1	Cyclohexane
C_{2v}	2	—	—	—	1	—	$H_2O(g)$
C_{3v}	3	—	—	1	—	—	$NH_3(g)$
C_{4v}	4	—	1	—	—	—	IF_5
C_{6v}	6	1	—	—	—	—	—
T	—	—	—	4	3	—	$NH_3(s)$
O	—	—	3	4	6	—	—
T_h	3	—	—	4	3	1	$CO_2(s)$
O_h	9	—	3	4	6	1	SF_6
T_d	6	—	—	4	3	—	CH_4

[a]Special Point Groups:
$C_{\infty v}$—One C, any C_p, infinite number of σ_v—e.g., HCN
$D_{\infty h}$—Infinite-fold axes (C_∞), infinite number $C_2 \perp$ to C_∞, infinite number of planes through C_∞, plane $\perp C_\infty$ axis, *i*—e.g., CO_2
I_h—Six fivefold, 10 threefold, 15 twofold axes, *i*, numerous planes (σ) and rotation–reflection axes—e.g., C_{60}.

Table 1-6 Method of Classifying Molecules into Point Groups (29)

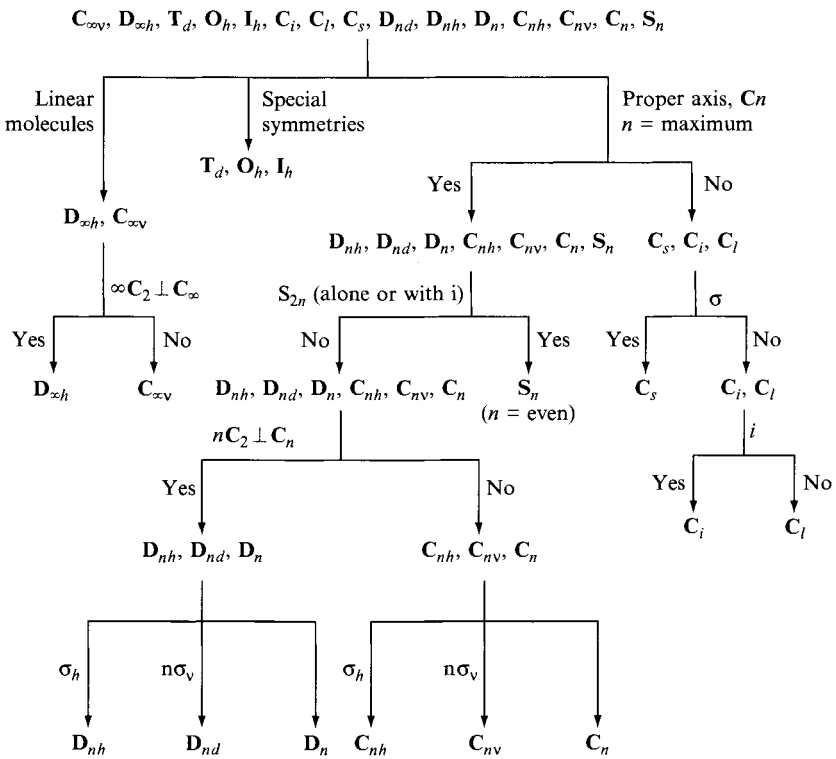

(5) If no S_n exists look for a set of n twofold axes lying perpendicular to the major C_n axis. If no such set is found, the molecule belongs to C_{nh}, C_{nv} or C_a. If a σ_h plane exists, the molecule is of C_{nh} symmetry even if other planes of symmetry are present. If no σ_h plane exists and a σ_v plane is found, the molecule is of C_{nv} symmetry. If no planes exist, it is of C_n symmetry.

(6) If in (5) nC_2 axes perpendicular to C_n axes are found, the molecule belongs to the D_{nh}, D_{nd}, or D_n point group. These can be differentiated by the presence (or absence) of symmetry planes (σ_h, σ_v, or no σ, respectively).

Several examples will be considered to illustrate the classification of molecules into point groups. Consider, for instance, the bent triatomic molecule of type $AB_2(H_2O)$ shown in Fig. 1-21. Following the rules

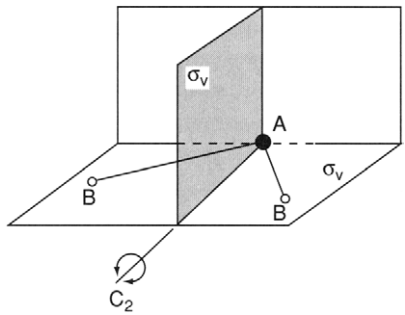

Figure 1-21 Symmetry elements for a bent AB_2 molecule. (Reproduced with permission from Ref. 30.)

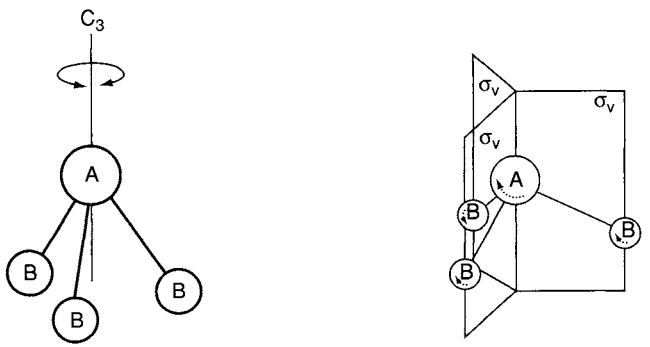

Figure 1-22 Symmetry elements for a pyramidal AB_3 molecule: (a) C_3 element; (b) σ_v elements. (Reproduced with permission from Ref. 30.)

and Table 1-6, it can be determined that the molecule is not of a special symmetry. It does have a C_2 axis of rotation but no S_4 axis. There are no $nC_2 \perp C_n$, and therefore the molecule is either C_{2h}, C_{2v}, or C_2. The molecule possesses two vertical planes of symmetry bot no σ_h plane, and therefore belongs to the C_{2v} point group.

Now consider the pyramidal molecule of type AB_3 (NH_3) shown in Fig. 1-22. This molecule also is not of a special symmetry. It has a C_3 axis of rotation but no S_6 axis. There are no nC_n axes perpendicular to the C_3 axis, and therefore the molecule belongs to the C classification. Since three vertical

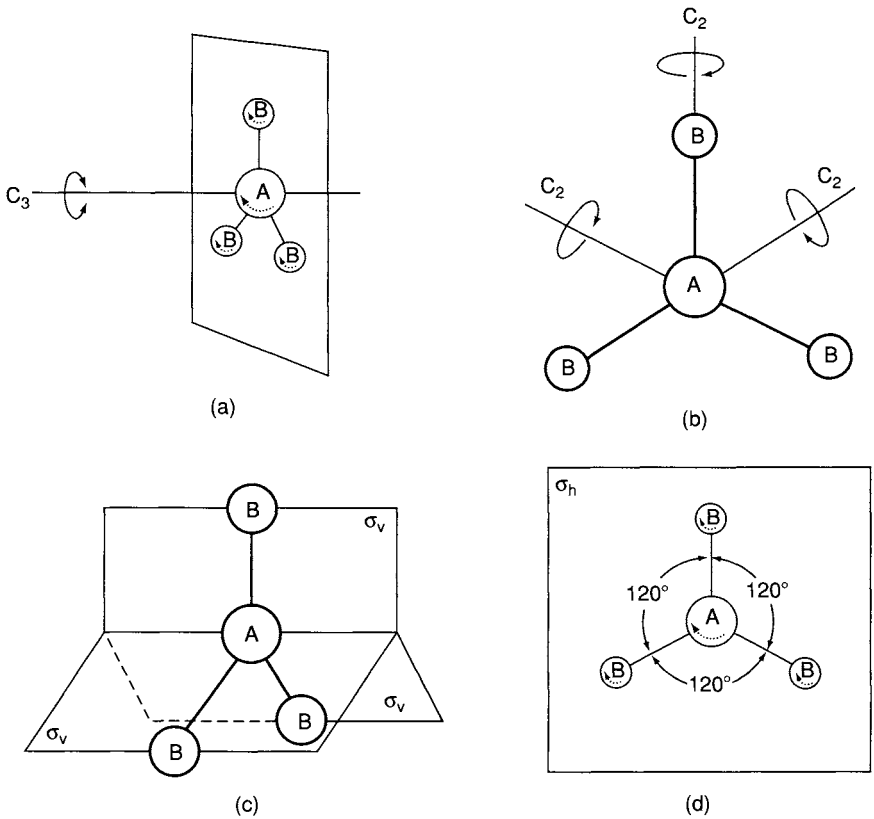

Figure 1-23 Symmetry elements for a planar AB_3 molecule (a) C_3, (b) C_2 (c) σ_v, and (d) σ_h. (Reproduced with permission from Ref. 30.)

planes of symmetry are found but no σ_h plane, the molecule can be classified into C_{3v}.

Next, consider the planar AB_3 molecule (BF_3) shown in Fig. 1-23. This molecule has no special symmetry. It has a C_3 axis of rotation without a collinear S_6 axis. It has three C_2 axes perpendicular to the C_3 axis, and therefore falls into the D classification. It has a σ_h plane of symmetry perpendicular to the C_3 axis and three σ_v planes of symmetry. However, the σ_h plane predominates and the molecule is of D_{3h} symmetry.

The next example is the hexagonal planar molecule of type A_6 or A_6B_6 (benzene) shown in Fig. 1-24. The molecule is not of a special symmetry. It has a center of symmetry and a C_6 axis of symmetry. No S_2 axis exists. Since six C_2 axes perpendicular to the C_6 axis are found, this molecule also falls into the D classification. Since it has a horizontal plane of symmetry perpendicular to the C_6 axis, the molecule belongs to the D_{6h} point group.

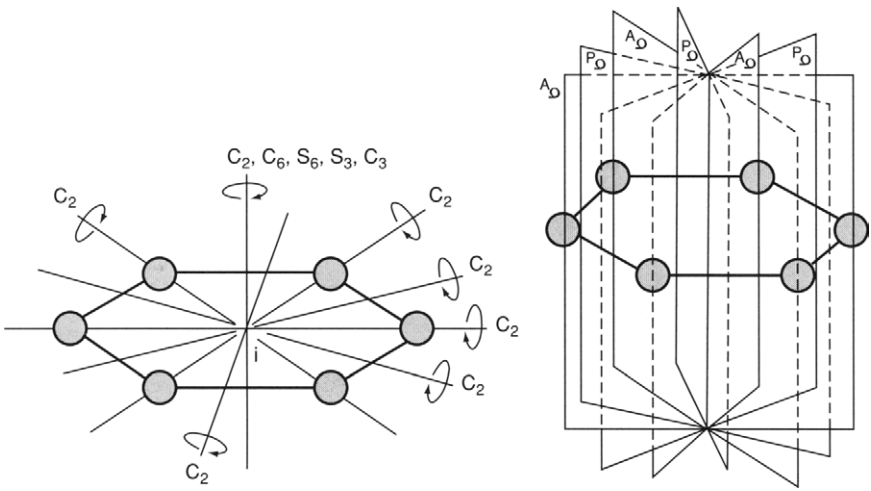

Figure 1-24 Symmetry elements for a planar hexagonal A_6B_6 molecule. (Reproduced with permission from Ref. 30.)

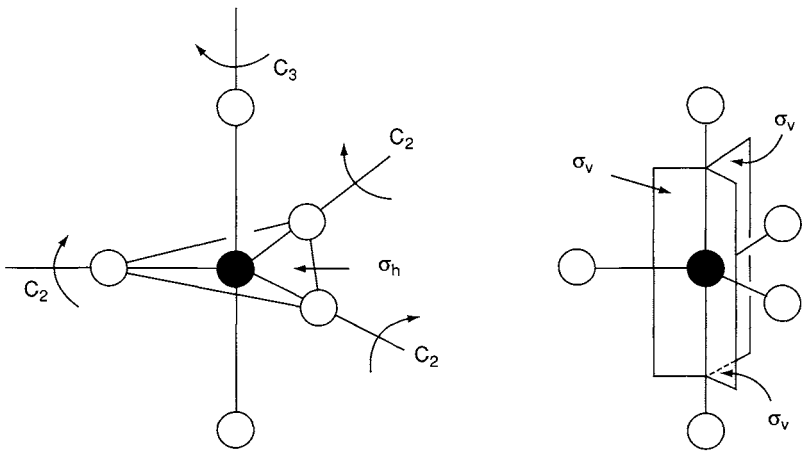

Figure 1-25 Symmetry elements for a trigonal bipyramidal AB_5 molecule.

As the last example, consider the AB_5 trigonal bipyramid (e.g., gaseous PCl_5) shown in Fig. 1-25. This molecule does not belong to a special symmetry. The axis of highest order is C_3. There is no S_6 collinear with C_3. There are three C_2 axes perpendicular to the C_3 axis, and therefore the molecule belongs to one of the D groups. Since it possesses a σ_h plane perpendicular to the C_3 axis, the proper classification is D_{3h}. Figure 1-26a, b, c shows symmetry elements for several other common point groups.

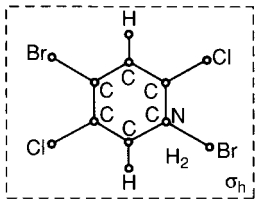

C_{2h}

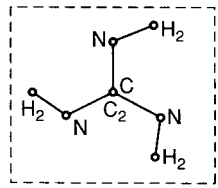

C_{3h}

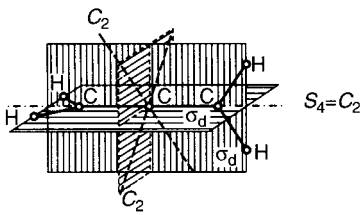

$D_{2d}(\equiv V_d)$

(a)

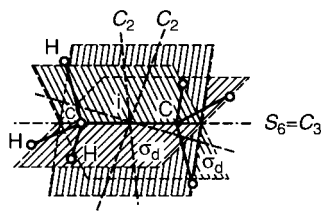

D_{3d}

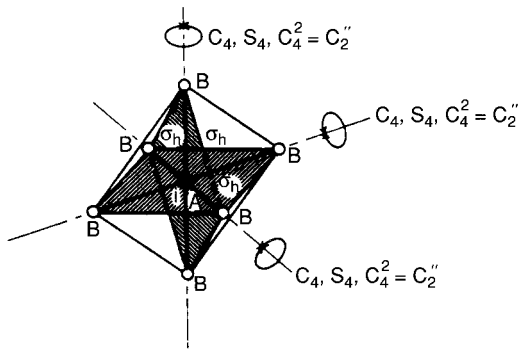

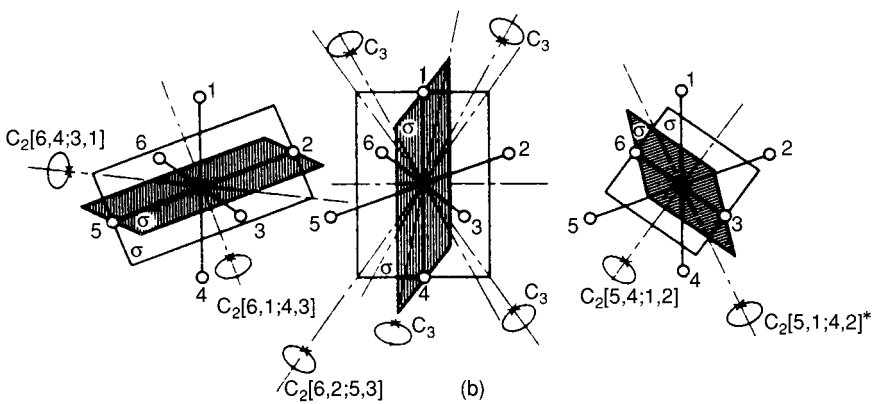

(b)

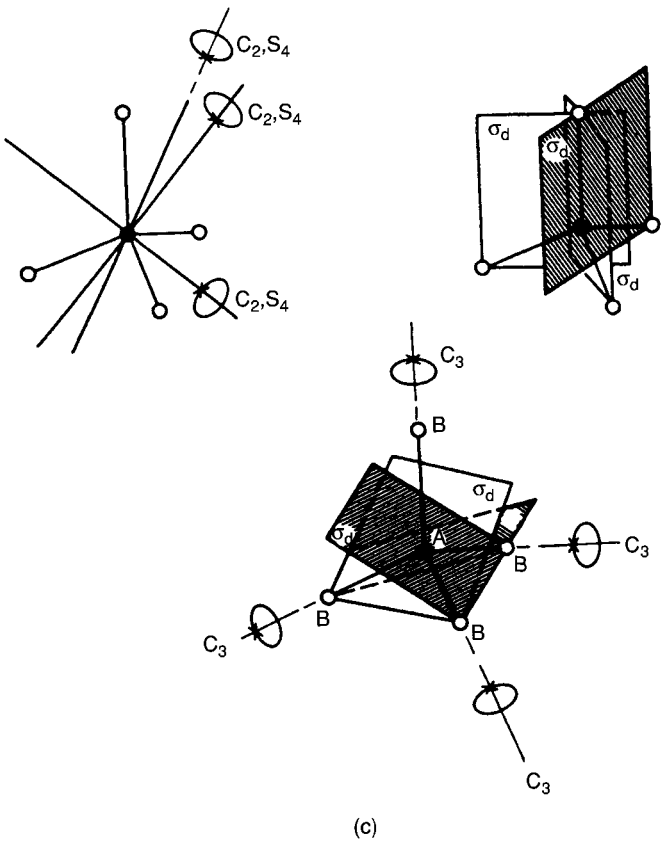

(c)

Figure 1-26 Symmetry elements for other point groups. (a) C_{2h}, C_{3h}, D_{2d}, D_{3d}; (b) O_h and (c) T_d. (Reproduced with permission from Ref. 30.)

1.12 The Character Table

Prior to interpreting the character table, it is necessary to explain the terms *reducible* and *irreducible representations*. We can illustrate these concepts using the NH_3 molecule as an example. Ammonia belongs to the point group C_{3v} and has six elements of symmetry. These are E (identity), two C_3 axes (threefold axes of rotation) and three σ_v planes (vertical planes of symmetry) as shown in Fig. 1-22. If one performs operations corresponding to these symmetry elements on the three equivalent NH bonds, the results can be expressed mathematically by using 3×3 matrices.*

*The reader should consult introductory textbooks on matrix theory.

Consider the C_3^+ (clockwise rotation by 120°) operation, shown with its changes:

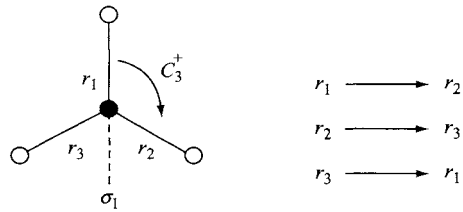

Using matrix language, this is expressed as

$$C_3^+ \begin{bmatrix} r_1 \\ r_2 \\ r_3 \end{bmatrix} = \begin{bmatrix} 0 & 1 & 0 \\ 0 & 0 & 1 \\ 1 & 0 & 0 \end{bmatrix} \begin{bmatrix} r_1 \\ r_2 \\ r_3 \end{bmatrix}. \tag{1-51}$$

The square matrix on the right-hand side is called a *representation* for the symmetry operation, C_3^+. For the σ_1 operation, we obtain

$$\sigma_1 \begin{bmatrix} r_1 \\ r_2 \\ r_3 \end{bmatrix} = \begin{bmatrix} 1 & 0 & 0 \\ 0 & 0 & 1 \\ 0 & 1 & 0 \end{bmatrix} \begin{bmatrix} r_1 \\ r_2 \\ r_3 \end{bmatrix}. \tag{1-52}$$

Similarly, for the E operation, we obtain

$$E \begin{bmatrix} r_1 \\ r_2 \\ r_3 \end{bmatrix} = \begin{bmatrix} 1 & 0 & 0 \\ 0 & 1 & 0 \\ 0 & 0 & 1 \end{bmatrix} \begin{bmatrix} r_1 \\ r_2 \\ r_3 \end{bmatrix}. \tag{1-53}$$

These representations are called *reducible representations* since they can be block-diagonalized in the form

$$\left[\begin{array}{c|cc} 1 & 0 & 0 \\ \hline 0 & A & B \\ 0 & C & D \end{array}\right] \tag{1-54}$$

via similarity transformation.* If such simplification is no longer possible, the resulting representations are called *irreducible representations*. In the present case, the irreducible representations thus obtained are

*In general, similarity transformation is expressed as $S^{-1}R(K)S$ where $R(K)$ is a reducible representation for the symmetry operation, $R(K)$, S is a matrix of the same dimension, and S^{-1} is its reciprocal (or inverse), defined by the relationship, $S^{-1}S = SS^{-1} = E$, where E is a unit matrix such as (1-53). In the present case, the S matrix is obtained by writing a U matrix (Section 1.20) for the pyramidal XY_3 molecule.

for C_3^+:

$$\begin{bmatrix} 0 & 1 & 0 \\ 0 & 0 & 1 \\ 1 & 0 & 0 \end{bmatrix} \rightarrow \left[\begin{array}{c|cc} 1 & 0 & 0 \\ \hline 0 & -\frac{1}{2} & \frac{\sqrt{3}}{2} \\ 0 & -\frac{\sqrt{3}}{2} & -\frac{1}{2} \end{array}\right], \tag{1-55}$$

for σ_1:

$$\begin{bmatrix} 1 & 0 & 0 \\ 0 & 0 & 1 \\ 0 & 1 & 0 \end{bmatrix} \rightarrow \left[\begin{array}{c|cc} 1 & 0 & 0 \\ \hline 0 & 1 & 1 \\ 0 & 0 & -1 \end{array}\right]. \tag{1-56}$$

The reducible representation for E (1-53) is already diagonalized.

The sum of the diagonal elements of a matrix is called the character (χ) of the matrix. Hereafter, we use the term character rather than the representation since there is a one-to-one correspondence between them and since mathematical manipulation with χ is simpler than with the representation. The characters of the reducible representations for the E, C_3^+ and σ_1 operations are 3, 0 and 1, respectively. The characters for C_3^- (counterclockwise rotation by 120°) is the same as that of C_3^+, and those for σ_2 and σ_3 are the same as that of σ_1. By grouping symmetry operations of the same character ("class"), we obtain

C_{3v}	E	$2C_3$	$3\sigma_v$
	3	0	1

As seen in (1-53), (1-55) and (1-56), this set of reducible representations can be resolved into a sum of characters of the irreducible representations:

A_1	1	1	1
E	2	−1	0
$A_1 + E$	3	0	1

The characters of irreducible representations are listed in the *character table* of each point group (Appendix 1). Figure 1-27 shows the character table for the point group C_{3v}. It is seen that there are three sets of characters corresponding to the A_1, A_2 and E species. In practical terms, the above result indicates that the three N—H bond stretching vibrations of the NH_3 molecule can be classified into one A_1 and one E (doubly degenerate) vibration. Thus, the character tables are important in classifying normal vibrations according to their symmetry properties (Section 1.13).

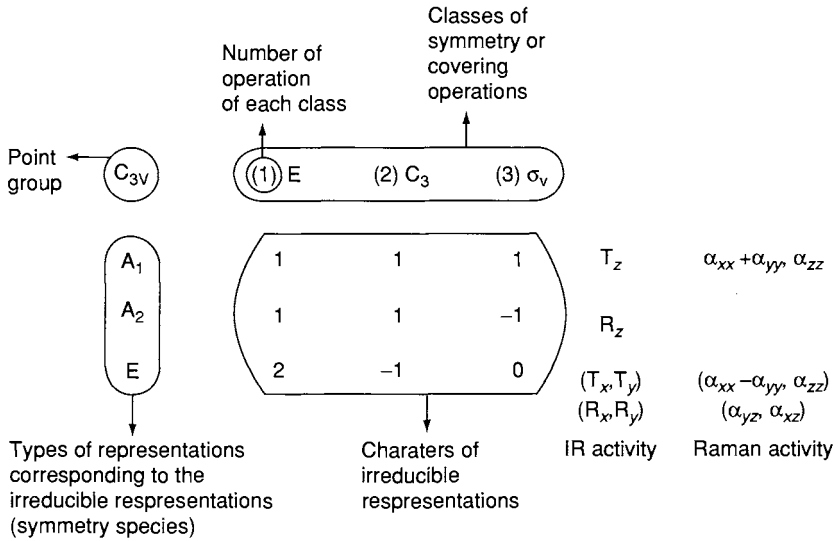

Figure 1-27 Diagrammatic interpretation of the character table for the C_{3v} point group.

The last two columns of the character table provide information about IR and Raman activities of normal vibrations. One column lists the symmetry species of translational motions along the x, y and z axes (T_x, T_y and T_z) and rotational motions around the x, y and z axes (R_x, R_y and R_z). The last column lists the symmetry species of the six components of polarizability. As will be discussed in Section 1.14, the vibration is IR-active if it belongs to a symmetry species that contains any T components and is Raman-active if it belongs to a symmetry species that contains any α components. Pairs of these components are listed in parentheses when they belong to degenerate species.

Types of Species of Irreducible Representations

(*a*) *Nonlinear Molecules*

A species is designated by the letter A if the transformation of the molecule is symmetric ($+1$) with respect to the rotation about the principal axis of symmetry. In NH_3, this axis is C_3, and, as can be seen, A_1 is totally symmetric, being labeled with positive 1's for all symmetry classes. A species that is symmetric with respect to the rotation, but is antisymmetric with respect to a rotation about the C_2 axis perpendicular to the principal axis or the vertical plane of reflection, is designated by the symbol A_2.

If a species of vibration belongs to the antisymmetric (−1) representation, it is designated by the letter *B*. If it is symmetric with respect to the rotation about the C_2 axis perpendicular to the principle axis of symmetry or to the vertical plane of reflection, it is a B_1 vibration, and if it is antisymmetric, it is a B_2 vibration. The letter *E* designates a twofold degenerate* vibration and the letter *F* denotes** a triply degenerate vibration. The character under the class of identity gives the degeneracy of the vibration, 1 for singly degenerate, 2 for doubly degenerate, and 3 for triply degenerate. For point groups containing a σ_h operation, primes (e.g., A') and double primes (e.g., A'') are used. The single prime indicates symmetry and the double prime antisymmetry with respect to σ_h. In molecules with a center of symmetry *i*, the symbols *g* and *u* are used, *g* standing for the German word *gerade* (which means even) and *u* for *ungerade* (or uneven). The symbol *g* goes with the species that transforms symmetrically with respect to *i*, and the symbol *u* goes with the species that transforms antisymmetrically with respect to *i*.

(*b*) *Linear Molecules*

Different symbols are used for linear molecules belonging to the point groups $C_{\infty v}$ and $D_{\infty h}$, namely Greek letters identical with the designations used for the electronic states of any diatomic molecules. The symbols σ or Σ are used for species symmetric with respect to the principal axis. A superscript plus sign (σ^+ or Σ^+) is used for species that are symmetric, and a superscript minus sign (σ^- or Σ^-) for species that are antisymmetric with respect to a plane of symmetry through the molecular axis. The symbols Π, Δ, and Φ are used for degenerate vibrations, with the degree of degeneracy increasing in this order. This is illustrated in Table 1-7.

Table 1-7 Character Table for the $C_{\infty v}$ Point Group

$C_{\infty v}$	E	$2C_\infty^\phi$	$2C_\infty^{2\phi}$	$2C_\infty^{3\phi}$	...	$\infty\sigma_v$
Σ^+	+1	+1	+1	+1	...	+1
Σ^-	+1	+1	+1	+1	...	−1
Π	+2	$2\cos\phi$	$2\cos 2\phi$	$2\cos 3\phi$	...	0
Δ	+2	$2\cos 2\phi$	$2\cos 2\cdot 2\phi$	$2\cos 3\cdot 2\phi$	...	0
Φ	+2	$2\cos 3\phi$	$2\cos 2\cdot 3\phi$	$2\cos 3\cdot 3\phi$	...	0
...	...	...	...	...	...	...

*The bending vibration of CO_2 is an example of a degenerate vibration. The frequency and character of the vibrations are the same, but they occur perpendicular to one another.

**Some texts use the symbol *T* for the triply degenerate vibration.

(*c*) *Molecules of Highest Symmetry*

Although it has been generally believed that molecules would never be found in icosahedral (I_h) symmetry (31, 32), we now know that such is not the case. There are at least three molecules possessing icosahedral symmetry. These are the borohydride anion (33) $B_{12}H_{12}^{2-}$; dodecahedrane, $C_{20}H_{20}$ (34), and the buckminsterfullerene or buckyball C_{60} cluster (35) (see Chapter 4, Section 4.2.7). The I_h symmetry contains fivefold to twofold axes of rotation as well as a center of symmetry. As a result, additional species of vibrations such as *G* and *H* appear in the I_h character table (36). These correspond to four-dimensional and five-dimensional representations. *G* is a four-fold and *H* is a five-fold degenerate vibration. The character table for the I_h point group is shown in Appendix 1.

1.13 Classification of Normal Vibrations by Symmetry

The $3N-6(5)$ normal vibrations of an *N*-atom molecule can be classified into symmetry species of a point group according to their symmetry properties. As an example, consider the displacements of individual atoms of the H_2O molecule (C_{2v}) using the Cartesian coordinates shown below:

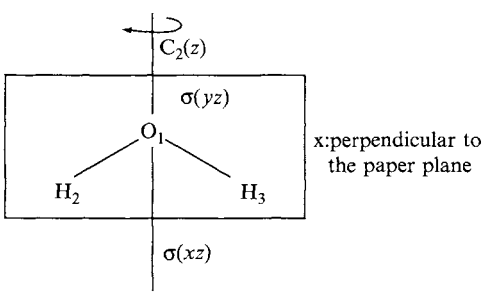

The symmetry operations to be considered are given in the table.

C_{2v}	$C_2(z)$	$\sigma(xz)$	$\sigma(yz)$
A_1	+1	+1	+1
A_2	+1	−1	−1
B_1	−1	+1	−1
B_2	−1	−1	+1

It is not necessary to consider $\sigma(yz)$ since $C_2 \times \sigma(xz) = \sigma(yz)$.

First, the symmetry species of the three displacements of the oxygen atom are readily determined as shown below:

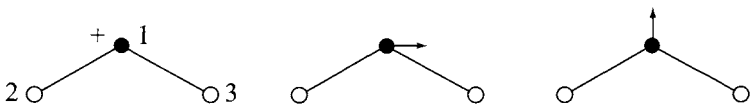

$x_1(B_1)$ $y_1(B_2)$ $z_1(A_1)$

Here the + sign denotes the out-of-plane displacement in the $+x$ direction.

Since the two hydrogen atoms are equivalent, we consider symmetry species of six linear combinations of their displacements:

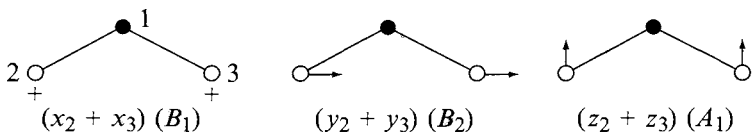

$(x_2 + x_3)\ (B_1)$ $(y_2 + y_3)\ (B_2)$ $(z_2 + z_3)\ (A_1)$

$(x_2 - x_3)\ (A_2)$ $(y_2 - y_3)\ (A_1)$ $(z_2 - z_3)\ (B_2)$

Since these nine displacements include three translational (T) and three rotational (R) motions of the whole molecule, we must substract them from our calculations. It is readily seen that T_x, T_y and T_z belong to the B_1, B_2 and A_1, whereas R_x, R_y and R_z belong to the B_2, B_1 and A_2 species, respectively. Table 1-8 summarizes these results. Thus, we find that two vibrations belong to the A_1 and one vibration belongs to the B_2 species. The approximate vibrational modes of the two A_1 type vibrations can be derived by combining z_1, $(z_2 + z_3)$ and $(y_2 - y_3)$ as follows:

Table 1-8 Number of Normal Vibrations of H_2O Molecule

	Number of Coordinates				
C_{2v}	O	H	Total	Translation and Rotation	Number of Vibrations
A_1	1	2	3	T_z	$3 - 1 = 2$
A_2	0	1	1	R_z	$1 - 1 = 0$
B_1	1	1	2	T_x, R_y	$2 - 2 = 0$
B_2	1	2	3	T_y, R_x	$3 - 2 = 1$

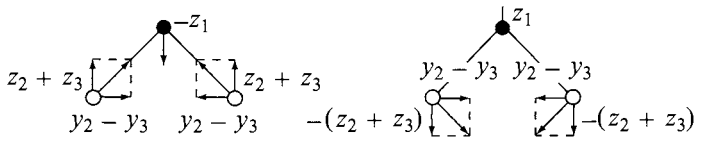

The vibrational mode of the B_2 vibration is obtained by combining $-y_1$, $(y_2 + y_3)$ and $(z_2 - z_3)$ as follows:

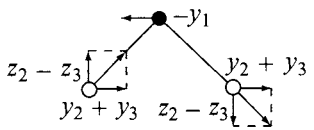

More accurate mode descriptions can be made if we consider the masses of individual atoms, bond distances, bond angles and force constants (Section 1.20). It is clear that these three vibrations correspond to the ν_1, ν_2 and ν_3, respectively, of Fig. 1-12.

More generally, the number of normal vibrations in each species can be calculated by using Herzberg's formulas (31) given in Appendix 2. In the case of the C_{2v} point group, they are expressed as:

$$
\begin{aligned}
A_1&: \quad 3m + 2m_{xz} + 2m_{yz} + m_0 - 1,\\
A_2&: \quad 3m + m_{xz} + m_{yz} - 1,\\
B_1&: \quad 3m + 2m_{xz} + m_{yz} + m_0 - 2,\\
B_2&: \quad 3m + m_{xz} + 2m_{yz} + m_0 - 2,
\end{aligned}
$$

and N (total number of atoms) is given by $4m + 2m_{xz} + 2m_{yz} + m_0$. In the foregoing, the parameters are defined as follows:

m: number of sets of nuclei not on any symmetry elements.
m_0: number of nuclei on all symmetry elements.
m_{xy}, m_{yz}, m_{xz}: number of sets of nuclei lying on the xy, yz and xz planes, respectively, but not on any other axis going through these planes.

For H_2O, $m = 0, m_0 = 1$ (oxygen atom), $m_{xy} = 0, m_{yz} = 1$ (hydrogen atom), $m_{xz} = 0$ and $N = 3$. Thus, the numbers of normal vibrations are 2, 0, 0 and 1 for the A_1, A_2, B_1 and B_2 species, respectively.

The preceding general equations can be obtained from our calculations on H_2O. As shown earlier, the displacements of the oxygen atom (m_0) are distributed into $1A_1, 1B_1$, and $1B_2$. The displacements of the two hydrogen atoms (m_{yz}) are distributed among $2A_1, 1A_2, 1B_1$ and $2B_2$. Although m_{xz} is zero for H_2O, it is not zero for other C_{2v} molecules. For example, it is 1 for CH_2Cl_2:

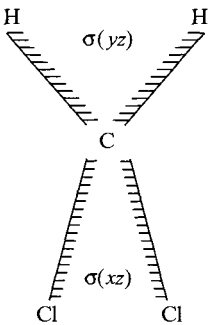

It is easily seen that m_{xz} is distributed into $2A_1, 1A_2, 2B_1$ and $1B_2$. m is zero in the case of H_2O. However, it is not zero for other molecules of C_{2v} symmetry. For example, consider an imaginary conformation of urea in which the four hydrogen atoms take the positions shown below:

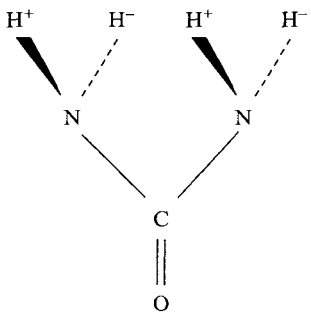

Here, H^+ and H^- are mirror images of each other with respect to the molecular plane (the whole molecule is nearly planar in the real molecule). Then, $m = 1$. The displacements of $4m$ atoms are expressed by $3 \times 4m$ coordinates, which are distributed equally into the four species ($3m$ for each). The summation of these calculations leads to the general equations given earlier.

As another example, consider the NH_3 molecule of C_{3v} symmetry. Using the table given in Appendix 2, we find that $m_0 = 1$ (nitrogen atom), $m = 0$ and $m_v = 1$ (hydrogen atom). Thus, the number of normal vibrations in the A_1, A_2 and E species are 2, 0, and 2, respectively.

Although not described earlier, classification of normal vibrations can be made by applying group theoretical treatments to individual molecules (37). The latter is useful for confirming the results obtained from Herzberg's tables.

1.14 Symmetry Selection Rules

As shown in Section 1.7, IR and Raman activities for small molecules can be determined by inspection of their normal modes. Clearly, it is difficult to apply such an approach to large and complex molecules. This problem can be solved by using the group theoretical consideration described next.

According to quantum mechanics (18, 19), the selection rule for the IR spectrum is determined by the integrals

$$\begin{aligned}
[\mu_x]_{v',v''} &= \int \psi^*_{v'}(Q_a)\mu_x\psi_{v''}(Q_a)\,dQ_a, \\
[\mu_y]_{v',v''} &= \int \psi^*_{v'}(Q_a)\mu_y\psi_{v''}(Q_a)\,dQ_a \\
[\mu_z]_{v',v''} &= \int \psi^*_{v'}(Q_a)\mu_z\psi_{v''}(Q_a)\,dQ_a.
\end{aligned} \tag{1-57}$$

Here, μ_x, μ_y and μ_z are the x, y and z components of the dipole moment at the electronic ground state, respectively. $\psi_{v'}$ and $\psi_{v''}$ are vibrational wavefunctions where v' and v'' are the vibrational quantum numbers before and after the transition, respectively. Q_a is the *normal coordinate* of the normal vibration, a. If one of these integrals is nonzero, this vibration is infrared-active. If all three integrals are zero, it is infrared-inactive.

Using (1-57) as an example, let us determine whether such an integral is zero or nonzero. For this purpose, we first expand μ_x in terms of the normal coordinate, Q_a:

$$\mu_x = (\mu_x)_0 + \left(\frac{\partial \mu_x}{\partial Q_a}\right) Q_a + \cdots$$

Then, (1-57) can be rewritten as

$$\begin{aligned}
[\mu_x]_{v',v''} = (\mu_x)_0 &\int \psi^*_{v'}(Q_a)\psi_{v''}(Q_a)\,dQ_a \\
&+ \left(\frac{\partial \mu_x}{\partial Q_a}\right) \int \psi^*_{v'}(Q_a)Q_a\psi_{v''}(Q_a)\,dQ_a + \cdots
\end{aligned} \tag{1-58}$$

The integral in the first term vanishes because of the orthogonality of $\psi_{v'}$ and $\psi_{v''}$ (except for $v' = v''$, no transition). In order for the second term to be nonzero,

$$\left(\frac{\partial \mu_x}{\partial Q_a}\right) \neq 0 \quad \text{and} \quad \int \psi_{v'}^*(Q_a) Q_a \psi_{v''}(Q_a)\, dQ_a \neq 0.$$

The latter is nonzero only when $\Delta v = \pm 1$ (harmonic oscillator, Section 1.3). In order to understand the significance of the former, we approximate the second term in (1-58) as

$$\left(\frac{\partial \mu_x}{\partial Q_a}\right) \int \psi_{v'}^*(Q_a) Q_a \psi_{v''}(Q_a) dQ_a \approx e \int \psi_{v'}(Q_a) x \psi_{v''}(Q_a)\, dQ_a. \tag{1-59}$$

Here, $\mu_x = \sum_i e_i x_i$, where e_i is the charge on the ith electron or nucleus and x_i is the x component of its position.

Consider the fundamental vibration in which the transition occurs from $v' = 0$ to $v'' = 1$. From Eq. (1-28), it is obvious that ψ_0 is invariant under any symmetry operation since it contains the Q_a^2 term. On the other hand, the symmetry of ψ_1 is the same as that of Q_a since it contains a $Q_a e^{-Q_a^2/2}$ term. In general, any integral such as

$$\int f_A f_B f_C\, d\tau$$

does not vanish if the representation of the direct product, $f_A f_B f_C$, contains the totally symmetric representation.* In the present case, ψ_0 is totally symmetric. Then the integral such as (1-59) is nonzero if the representation of the product $x\psi_1$ is totally symmetric. This is possible only when x and ψ_1 belong to the same symmetry species.

The symmetry species of $\mu_x(x)$, $\mu_y(y)$ and $\mu_z(z)$ are listed in the character tables of the respective point groups (Appendix 1).** As shown in the preceding section, the symmetry species of normal vibrations can be found by using Herzberg's tables (Appendix 2). Thus, IR activity is readily determined by the inspection of character tables; *the vibration is IR-active if the component (s) of the dipole moment belong(s) to the same symmetry species as that of the vibration.*

As an example, consider IR activity of the six normal vibrations of the NH_3 molecule, which are classified into $2A_1$ and $2E$ species of C_{3v} point group. The character table shows that μ_z belongs to the A_1 and the pair of (μ_x, μ_y) belongs to the E species. Thus, all six normal vibrations are IR-active.

The selection rule for Raman spectrum is determined by the integrals

*The proof of this theorem is given in Ref. 36.

**The symmetry property of μ_x (x-component of the dipole moment) is the same as that of T_x (translational motion along the x-axis).

$$[\alpha_{xx}]_{v',v''} = \int \psi^*_{v'}(Q_a)\alpha_{xx}\psi_{v''}(Q_a)\,dQ_a, \tag{1-60}$$

$$[\alpha_{xy}]_{v',v''} = \int \psi^*_{v'}(Q_a)\alpha_{xy}\psi_{v''}(Q_a)\,dQ_a, \tag{1-61}$$

$$\vdots \qquad\qquad \vdots$$

Here $\alpha_{xx}, \alpha_{yy}, \alpha_{zz}, \alpha_{xy}, \alpha_{yz}$ and α_{xz} are the components of the polarizability tensor discussed in Section 1.7. If one of these six integrals is nonzero, this vibration is Raman-active. If all the integrals are zero, it is Raman-inactive.

Symmetry selection rules for Raman spectrum can be derived by using a procedure similar to that for the IR spectrum. One should note, however, that the symmetry property of α_{xy}, for example, is determined by the product, $\mu_x\mu_y(xy)$ (19). The symmetry species of six components of polarizability are readily found in character tables. In point group C_{3v}, for example, $\alpha_{xx} + \alpha_{yy}$ and α_{zz} belong to the A_1 species while two pairs, $(\alpha_{xx} - \alpha_{yy}, \alpha_{xy})$ and $(\alpha_{yz}, \alpha_{xz})$, belong to the E species.* Thus, all six normal vibrations of the NH_3 molecule ($2A_1$ and $2E$) are Raman-active. More generally, *the vibration is Raman-active if the component(s) of the polarizability belong(s) to the same symmetry species as that of the vibration.*

As another example, consider an octahedral XY_6-type molecule of O_h symmetry. Using Herzberg's table, its 15 ($3 \times 7 - 6$) vibrations are classified into $A_{1g} + E_g + 2F_{1u} + F_{2g} + F_{2u}$. It is readily seen from the character table that only F_{1u} vibrations are IR-active, while A_{1g}, E_g and F_{2g} vibrations are Raman-active.

1.15 Resonance Raman Spectra

As stated in Section 1.4, resonance Raman (RR) scattering occurs when the sample is irradiated with an exciting line whose energy corresponds to that of the electronic transition of a particular chromophoric group in a molecule. Under these conditions, the intensities of Raman bands originating in this chromophore are selectively enhanced by a factor of 10^3 to 10^5. This selectivity is important not only for identifying vibrations of this particular chromophore in a complex spectrum, but also for locating its electronic transitions in an absorption spectrum.

Theoretically, the intensity of a Raman band observed at $\nu_0 - \nu_{mn}$ is given by (38):

*Instead of α_{xx} and α_{yy}, their linear combinations, $\alpha_{xx} + \alpha_{yy}$ and $\alpha_{xx} - \alpha_{yy}$ are used for mathematical convenience.

$$I_{mn} = \text{constant} \cdot I_0 \cdot (\nu_0 - \nu_{mn})^4 \sum_{p\sigma} |(\alpha_{p\sigma})_{mn}|^2. \tag{1-62}$$

Here, m and n denote the initial and final states, respectively, of the electronic ground state. Although not explicit in Eq. (1-62), e represents an electronic excited state (Fig. 1-28) involved in Raman scattering. I_0 is the intensity of the incident laser beam of frequency ν_0. The $(\nu_0 - \nu_{mn})^4$ term expresses the ν^4 rule to be discussed in Chapter 2, Section 2.6. Finally $(\alpha_{p\sigma})_{mn}$ represents the change in polarizability α caused by the $m \rightarrow e \rightarrow n$ transition, and ρ and σ are x, y and z components of the polarizability tensor (Section 1.7). This term can be rewritten as (38)

$$(\alpha_{p\sigma})_{mn} = \frac{1}{h} \sum_e \left(\frac{M_{me} M_{en}}{\nu_{em} - \nu_0 + i\Gamma_e} + \frac{M_{me} M_{en}}{\nu_{en} + \nu_0 + i\Gamma_e} \right), \tag{1-63}$$

where ν_{em} and ν_{en} are the frequencies corresponding to the energy differences between the states subscribed and h is Planck's constant. M_{me}, etc., are the electric transition moments, such as

$$M_{me} = \int \Psi_m^* \mu_\sigma \Psi_e d\tau. \tag{1-64}$$

Here, Ψ_m and Ψ_e are total wavefunctions of the m and e states, respectively, and μ_σ is the σ component of the electric dipole moment. Γ_e is the band width of the eth state, and the $i\Gamma_e$ term is called the damping constant. In normal Raman scattering, ν_0 is chosen so that $\nu_0 \ll \nu_{em}$. Namely, the energy of the incident beam is much smaller than that of an electronic transition. Under these conditions, the Raman intensity is proportional to $(\nu_0 - \nu_{mn})^4$. As ν_0 approaches ν_{em}, the denominator of the first term in the brackets of Eq. (1-63)

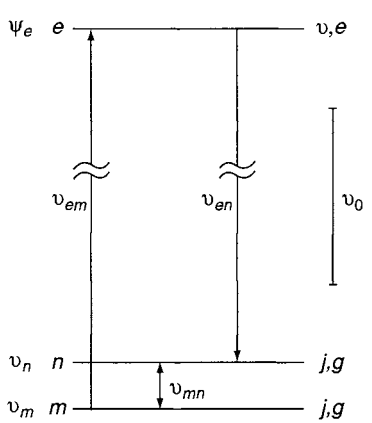

Figure 1-28 Energy level diagram for resonance Raman transition.

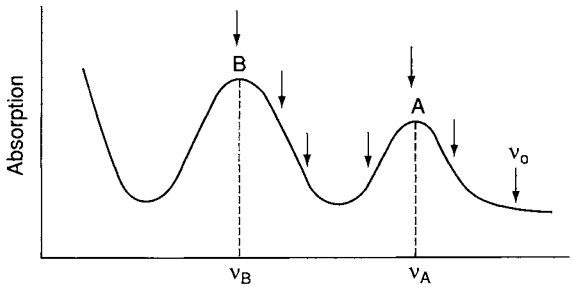

Figure 1-29 Absorption spectrum of a compound containing two chromophoric groups (A and B).

becomes very small. Hence, this term ("resonance term") becomes so large that the intensity of the Raman band at $\nu_0 - \nu_{mn}$ increases enormously. This phenomenon is called *resonance Raman (RR) scattering.*

Suppose that a compound contains two chromophoric groups that exhibit electronic bands at ν_A and ν_B as shown in Fig. 1-29. Then, vibrations of chromophore A are resonance-enhanced when ν_0 is chosen near ν_A, and those of chromophore B are resonance-enhanced when ν_0 is chosen near ν_B. For example, heme proteins such as hemoglobin and cytochromes (Chapter 6, Section 6.1) exhibit porphyrin core π–π^* transitions in the 400–600 nm region and peptide chain transitions below 250 nm. Thus, the porphyrin core and peptide chain vibrations can be selectively enhanced by choosing exciting lines, in the regions of these electronic absorptions.

More specific information can be obtained by expressing the total wavefunction as the product of the electronic and vibrational wavefunctions. (See the right-hand side labeling in Fig. 1-28). The results are (38, 39)

$$(\alpha_{p\sigma})_{mn} \cong A + B. \tag{1-65}$$

The A-term is written as

$$A \cong M_e^2 \frac{1}{h} \sum_v \frac{\langle j|v\rangle\langle v|i\rangle}{\nu_{vi} - \nu_0 + i\Gamma_v}. \tag{1-66}^*$$

Here M_e is the pure electronic transition moment for the resonant excited state e, of which v is a vibrational level of band width Γ_v, ν_{vi} is the transition frequency from the ground state vibrational level (i) to the excited vibrational level (v). The A-term becomes larger as the denominator becomes smaller (resonance condition) and as M_e becomes larger (stronger electronic absorption). The numerator contains the product of two overlap integrals of vibrational wavefunctions (*Franck-Condon overlap*) involving the i, j and v states. Because of the orthogonality of vibrational wavefunctions (Section 1.2),

*Only the resonance term is shown in (1-66) as well as in (1-67).

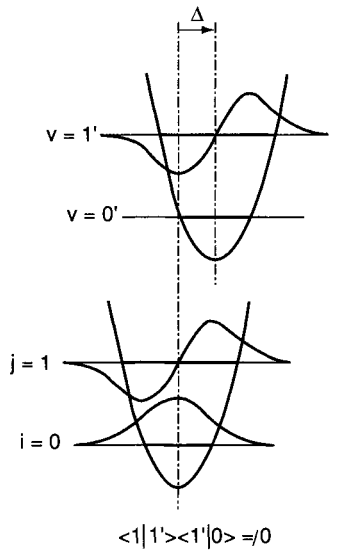

Figure 1-30 Shift of equilibrium position caused by a totally symmetric vibration.

either one of the integrals becomes zero unless the equilibrium position is shifted upon electronic excitation (Fig. 1-30). Since this occurs only for totally symmetric vibrations, the *A*-term enhancement can be seen only for totally symmetric modes.

The *A*-term resonance has been observed for a number of compounds. Figure 1-31 shows the RR spectra of TiI_4 obtained by 514.5 nm excitation (40). An overtone (nv) series up to $n = 12$ was observed in this case. (Also see Fig. 3-11 and Fig. 4-11.) The appearance of such a series can be explained if one calculates Franck–Condon overlaps under rigorous resonance conditions (41). Among the totally symmetric modes, the mode that leads to the excited state configuration is most strongly resonance-enhanced (42). For example, the NH_3 molecule is pyramidal in the ground state and planar at the excited state (216.8 nm above the ground state). Thus, the symmetric bending mode near $950\,cm^{-1}$ is enhanced 10 times more than the symmetric stretching mode near $3,300\,cm^{-1}$ when the exciting line is changed from 514.5 to 351.1 nm.

The *B*-term involves two electronic excited states (e and s) and provides a mechanism for resonance-enhancement of non-totally symmetric vibrations. The *B*-term, can be expressed as

$$B \cong M_e M'_e \frac{1}{h} \sum_v \frac{\langle j|Q|v\rangle\langle v|i\rangle + \langle j|v\rangle\langle v|Q|i\rangle}{\nu_{vi} - \nu_0 + i\Gamma_v}, \tag{1-67}$$

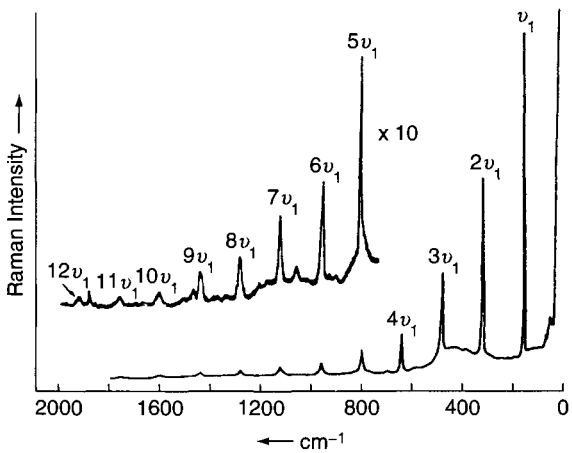

Figure 1-31 Resonance Raman spectrum of solid TiI_4 (514.5 nm excitation). $\nu_1 = 160.8\,cm^{-1}$. (Reproduced with permission from Ref. 40. Copyright 1973 American Chemical Society.)

$$M'_e = \mu_s \langle s|\partial H/\partial Q|e\rangle / \langle \nu_s - \nu_e \rangle, \tag{1-68}$$

where ν_s and μ_s are the frequency and transition dipole moment of the second excited state(s). Although the denominator in the *B*-term is the same as that of the *A*-term, its numerator contains *Q*-dependent vibrational overlap integrals as well as Franck–Condon overlap integrals. Here, Q is the normal coordinate of a particular vibration. Thus, it does not vanish even when the equilibrium position is not shifted by electronic excitation (non-totally symmetric vibration). The most important term in Eq. (1-67) is the vibronic coupling operator $\langle s|\partial H/\partial Q|e\rangle$, where H is the electronic Hamiltonian. As will be shown later, this term becomes nonzero if normal coordinates of proper symmetry are chosen. Thus, it is possible to resonance-enhance these vibrations via the *B*-term. A typical example of *B*-term resonance is found in RR spectra of heme proteins and their model compounds (43). As shown in Fig. 1-32, metalloporphyrins such as Ni(OEP) exhibit two electronic transitions; Q_0 (α) and *B* (or Soret) bands together with a vibronic sideband, Q_1 (or β) in the 600–350 nm region. According to MO calculations on the porphyrin core of D_{4h} symmetry, the $a_{1u} \rightarrow e_g^*$ and $a_{2u} \rightarrow e_g^*$ transitions have similar energies and the same excited state symmetry, since $a_{1u} \times e_g = a_{2u} \times e_g = E_u$. This results in a strong configuration interaction to produce two separate states, Q_0 and *B* (see the inset in Fig. 1-32). The transition dipole moments nearly cancel each other to produce a weak Q_0 band in the visible region, but add up to produce a strong *B* band in the UV region.

As stated earlier, the vibronic coupling operator, $\langle s|\partial H/\partial Q|e\rangle$, determines which normal vibration is resonance-enhanced via the *B*-term. This term

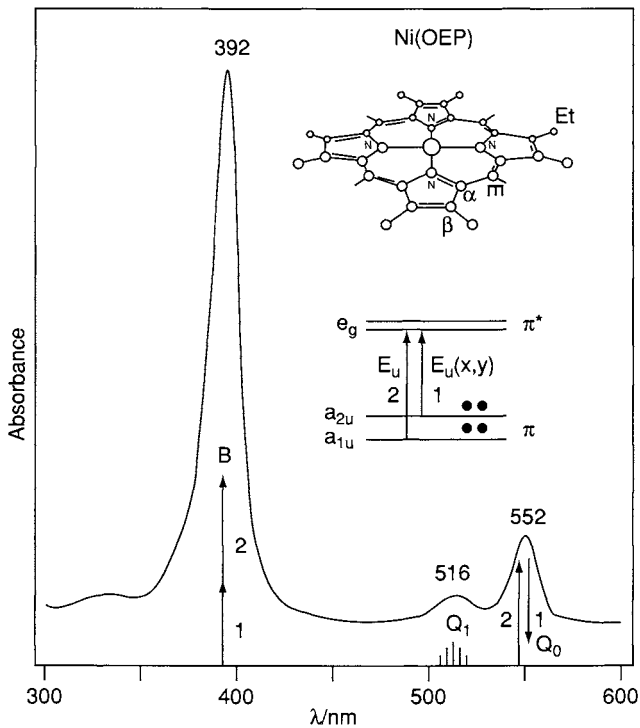

Figure 1-32 Absorption spectrum and energy level diagram of Ni (OEP). (Reproduced with permission from Ref. 43. Copyright © 1988 John Wiley & Sons, Inc.)

becomes nonzero only when the normal vibration has a proper symmetry. As discussed in Section 1.14, an integral such as

$$\int f_A f_B f_C \, d\tau \tag{1-69}$$

is nonzero if the direct product of the irreducible representations of f_A, f_B and f_C contains the totally symmetric component. Since both $e(Q_0)$ and $s(B)$ states are of E_u symmetry, only the A_{1g}, B_{1g}, B_{2g} and A_{2g} vibrations,

$$E_u \times E_u = A_{1g} + B_{1g} + B_{2g} + A_{2g}, \tag{1-70}$$

can be resonance-enhanced via the B-term.* Figure 1-33 shows the RR spectra of Ni(OEP) obtained by B, Q_1 and Q_0 excitation (44). The former is

*The general method for resolving direct products into symmetry species is found in textbooks of group theory[14–18]. Appendix 3 summarizes the general rules for obtaining the symmetry species of direct products.

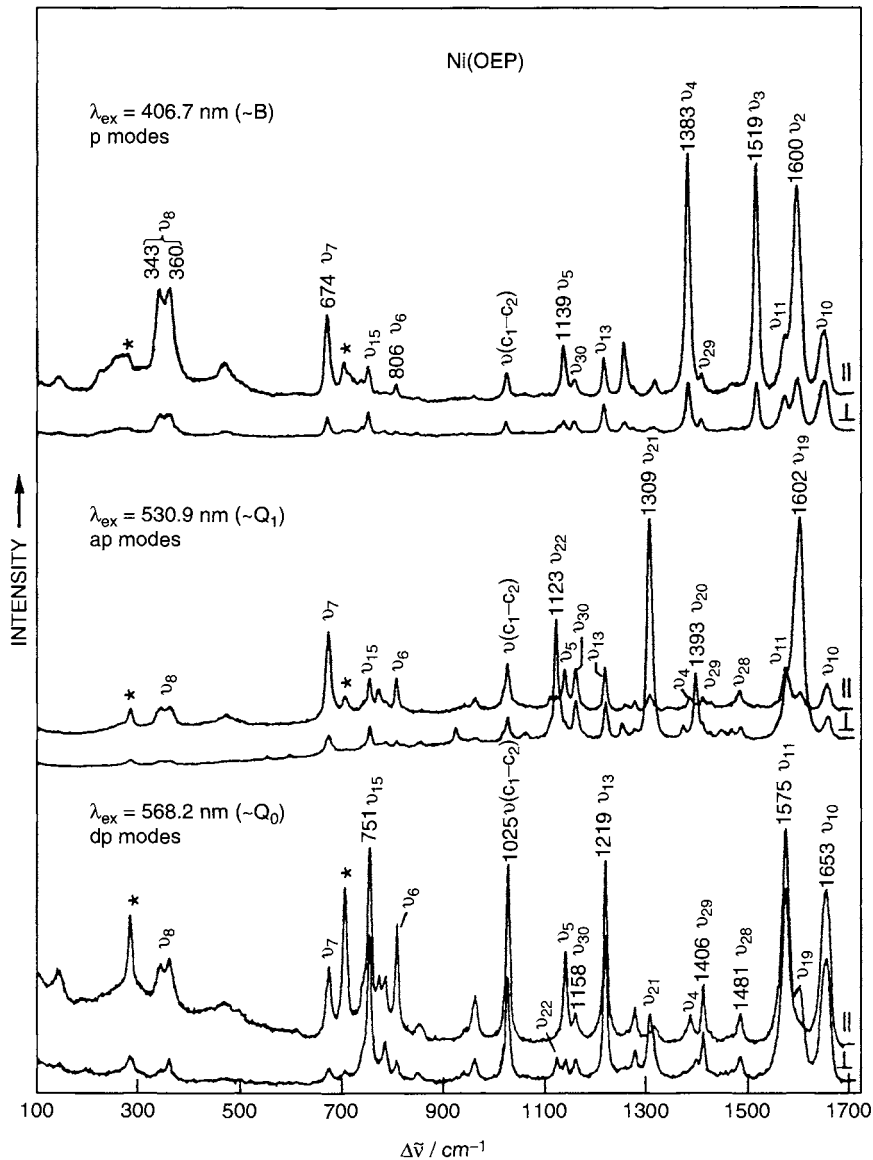

Figure 1-33 Resonance Raman spectra of Ni (OEP) obtained by three different excitations. (Reproduced with permission from Ref. 44. Copyright 1990 American Chemical Society.)

dominated by totally symmetric vibrations, whereas the latter two are dominated by B_{1g}, B_{2g} and A_{2g} vibrations since A_{1g} modes are not effective in mixing the B and Q_0 states because of the high symmetry of the porphyrin core. Distinction of these modes can be made by measuring the depolarization ratios (Section 1.9), which should be $\frac{3}{4}$ (depolarized) for B_{1g} and B_{2g}, and $\frac{3}{4} \sim \infty$ (inverse polarization) for A_{2g} vibrations. It should be noted that the RR spectrum obtained by Soret (B) excitation is dominated by A_{1g} vibrations, since resonance enhancement occurs through the A-term discussed earlier.

1.16 Space Group Symmetry

1.16.1 Symmetry Elements for a Molecule in the Condensed State

If one takes into account symmetry elements combined with translations, one obtains operations or elements that can be used to define the symmetry of space. Here, a translation is defined as the superposition of atoms or molecules from one site onto the same atoms or molecules in another site without the use of a rotation. The symmetry element called the *screw axis* involves an operation combining a translation with a rotation. The symmetry element called the glide plane involves an operation combining a reflection with a translation. These operations can be used to describe the symmetry of homogeneous spatial materials such as crystals and polymers, as well as space itself if one takes the identity element to be the set of all translations. This condition implies that these translations in a crystal are those that describe the lattice in contrast to those that are fractional translations associated with some rotation (screw motions and glides). A crystal may be considered to be made up of a large number of blocks of the same size and shape. One such block is defined as a unit cell. The unit cell must be capable of repetition in space without leaving any gap. The unit cell may be a primitive or nonprimitive unit cell. The distinction between these will be made later in this section.

The screw axis and the glide plane are further defined as follows:

Screw axis (n_p)
Rotation followed by a translation;
n = order of axis;
p/n = fraction of the unit cell over which translation occurs;
$n = 2, 3, 4$ or 6;
$p = 1, 2, 3, \ldots, n-1$.

For example, 2_1 = twofold screw axis, translation one-half the distance of the unit cell; and 3_1 = threefold screw axis, translation one-third the distance of the unit cell.

Figure 1-34 shows the operation of a twofold screw axis, in which the translation is $\frac{1}{2}$ of the unit cell (fractional translation).

Glide Plane

Reflection followed by a translation.

Figure 1-35 shows the operation of a glide plane.

The new symmetry elements that are added to the point symmetry elements are the screw axis and glide plane. As a result, 230 different combinations of symmetry elements become possible in what are called space groups. For a development of space groups see Burns and Glazer (45). Table 1-9 shows the distribution of the space groups among the seven crystal systems. Some of the space groups are never found in actual crystals, and about one-half of the known crystals belong to the 13 space groups of the monoclinic system. Figure 1-36 shows the lattices of the seven major crystal systems (one triclinic, four orthorhombic, two monoclinic, two tetragonal, three cubic, one hexagonal, one trigonal).

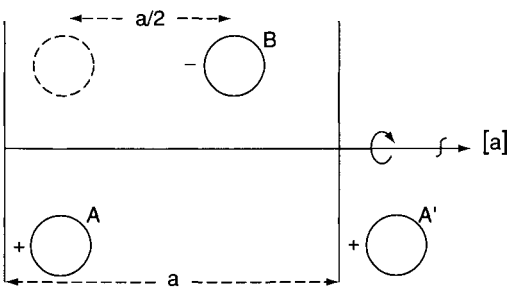

Figure 1-34 The operation of a twofold screw axis. (Reproduced with permission from Ref. 46.)

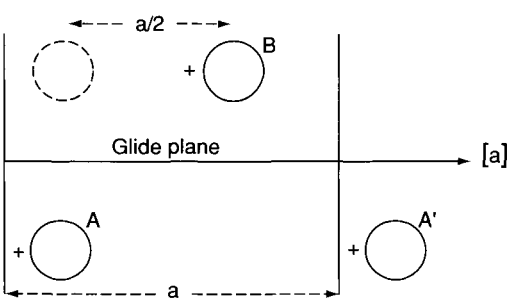

Figure 1-35 The operation of a glide plane. (Reproduced with permission from Ref. 46.)

Table 1-9 Distribution of Space Groups among the Seven Crystal Systems

Crystal System	Number of Space Groups
Triclinic	2
Monoclinic	13
Orthorhombic	59
Trigonal	25
Hexagonal	27
Tetragonal	68
Cubic	36

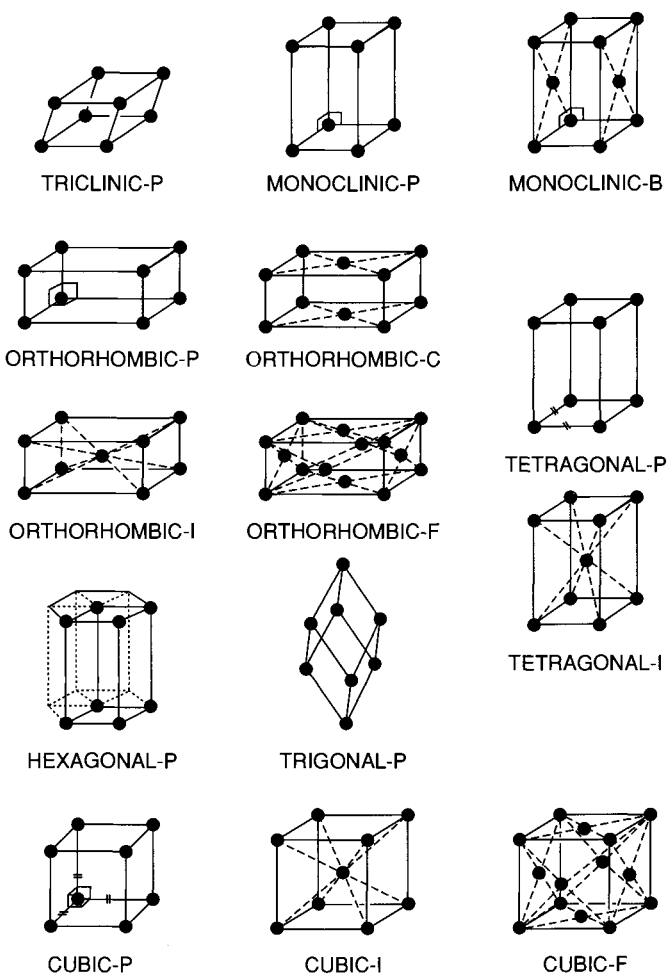

Figure 1-36 The seven crystal systems corresponding to 14 Bravais lattices. (Reproduced with permission from Ref. 45.)

1.16.2 Space Group

Just as the point group collects all of the point symmetry elements, the space group is seen collecting all of the space symmetry elements in crystals involving translation. For the space group selection rules, it is necessary to work on crystals for which space groups are known from X-ray studies, or where sufficient information is available to make a choice of structure. Alternatively, the structure may be assumed, and the space group selection rules can serve as a test of this assumption. In deriving space group selection rules, one must deal with a primitive unit cell. A primitive unit cell is the smallest unit in a crystal which, by a series of translations, would build up the whole crystal.

The Hermann–Mauguin notation is generally used by crystallographers to describe the space group. Tables exist to convert this notation to the Schoenflies notation. The first symbol is a capital letter and indicates whether the lattice is primitive. The next symbol refers to the principal axis, whether it is rotation, inversion, or screw, e.g.,

$P2_1$ = primitive lattice with a two-fold axis of rotation, translation one-half the distance of the unit cell
$C2$ = nonprimitive centered lattice with a twofold axis of rotation.

A mirror plane is symbolized as m, and a glide plane by c, e.g.,

$P2_1/m$ m = mirror plane perpendicular to principal axis;
$C2/c$ c = glide plane perpendicular to principal axis.

Table 1-10 shows the space group symbolism used.

Table 1-10 Space Group Symbolism

First symbol refers to the Bravais lattice
P = primitive lattice
C = centered lattice
F = face-centered lattice
I = body-centered lattice
R = rhombohedral (unit cell can be primitive or nonprimitive; see notes to Table 1-11)
Principal axis of ration given number n = order
e.g., 2 = twofold axis of rotation
For screw axis p/n = fraction of primitive lattice over which translation parallel to screw axis occurs.
e.g., $P2_1$ = primitive lattice with a twofold axis of rotation, translation; one-half unit cell
Mirror plane = m
Glide planes = symbols a, b, c along (a), (b), (c) axes
symbol $n = (b + c)/2$ or $(a + b)/2$
symbol $d = (a + b)/4$ or $(b + c)/4$ or $(a + c)/4$
e.g., $P2_1/m$; m = mirror plane perpendicular to principal axis
$C2/c$; c = glide plane axis perpendicular to principal axis

As previously mentioned, the primitive unit cell is the smallest unit of a crystal that reproduces itself by translations. Figure 1-37 illustrates the difference between a primitive and a centered or nonprimitive cell. The primitive cell can be defined by the lines a and c. Alternatively, we could have defined it by the lines a' and c'. Choosing the cell defined by the lines a'' and c'' gives us a nonprimitive cell or centered cell, which has twice the volume and two repeat units. Table 1-11 illustrates the symbolism used for the various types of lattices and records the number of repeat units in the cell for a primitive and a nonprimitive lattice. The spectroscopist is concerned with the primitive (Bravais) unit cell in dealing with lattice vibrations. For factor group selection rules, it is necessary to convert the number of molecules per crystallographic unit cell Z to Z', discussed later, which is the number of molecules per primitive cell. For example,

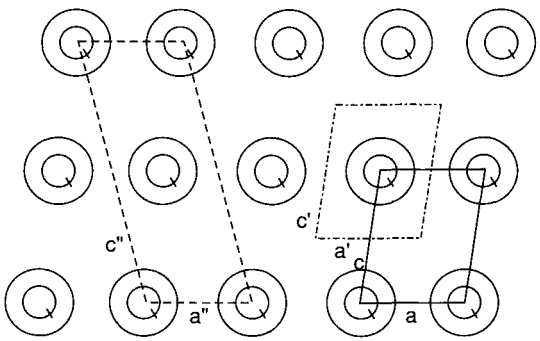

Figure 1-37 Differentiation between primitive and centered unit cells. (Reproduced with permission from Ref. 46.)

Table 1-11 Primitive and Centered Lattices

Type	Symbol	Number of Repeat Units in Cell
Primitive	P	1
Rhombohedral[a]	R	3 or 1[b]
Body-centered	I	2
Side-centered	A, B, or C	2
Face-centered	F	4

[a]Also called trigonal.

[b]There are cases in which the number of repeat units in the crystallographic cell may be three or one. For the cases where it is three, Z will be divisible by three. For example, for TiS, $D_{3d}^5 - R\bar{3}m$ (No. 166), $Z = 9$, and therefore $Z' = 9/3 = 3$. However, for Cr_2O_3, $D_{3d}^6 - R\bar{3}c$ (No. 167), $Z = 2$, and $Z' = 2/1 = 2$. Thus, in the latter crystal the cell can be considered to be primitive.

$$Z' = \text{number of molecules in the primitive cell}$$
$$= \frac{Z(\text{number of molecules in crystallographic cell})}{\text{repeat units in cell}}.$$

If $Z = 4$ for an F-type lattice, then

$$Z' = 4/4 = 1.$$

In the site symmetry compilation for the 230 space groups given in Appendix 4, the data are for a primitive cell and can be used directly.

1.16.3 Factor Group

It is necessary to define a factor group and to describe how it relates to a space group. In a crystal, one primitive cell or unit cell can be carried into another primitive cell or unit cell by a translation. The number of translations of unit cells then would seem to be infinite since a crystal is composed of many such units. If, however, one considers only one translation and consequently only two unit cells, and defines the translation that takes a point in one unit cell to an equivalent point in the other unit cell as the identity, one can define a finite group, which is called a *factor group* of the space group.

The factor groups are isomorphic (one-to-one correspondence) with the 32 point groups and, consequently, the character table of the factor group can be obtained from the corresponding isomorphic point group.

1.16.4 Site Group

It also becomes necessary to define a site group. A unit cell of a crystal is composed of points (molecules or ions) located at particular positions in the cell. It turns out, however, that the points can only be located at certain positions in the lattice that are called sites, that is, they can only be located on one of the symmetry elements of the factor group and thus remain invariant under that operation independent of translation. The point has fewer symmetry elements than the parent factor group and belongs to what is called a "site group," which is a subgroup of the factor group. [A subgroup (S) contains a set of symmetry elements that are also part of a parent group (G).] In general, factor groups can have a variety of different sites possible, that is, many subgroups can be formed from the factor group. Also, a number of distinct sites in the Bravais unit cell with the same site group are possible.

1.17 Normal Vibrations in a Crystal

In order to discuss the selection rules for crystalline lattices it is necessary to consider elementary theory of solid vibrations. The treatment essentially follows that of Mitra (47). A crystal can be regarded as a mechanical system of nN particles, where n is the number of particles (atoms) per unit cell and N is the number of primitive cells contained in the crystal. Since N is very large, a crystal has a huge number of vibrations. However, the observed spectrum is relatively simple because, as shown later, only where equivalent atoms in primitive unit cells are moving in phase as they are observed in the IR or Raman spectrum. In order to describe the vibrational spectrum of such a solid, a frequency distribution or a distribution relationship is necessary. The development that follows is for a simple one-dimensional crystalline diatomic linear lattice. See also Turrell (48).

Consider a simple one-dimensional infinite chain, consisting of alternating masses M and m separated by a distance a with a force constant f:

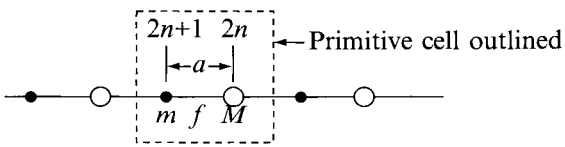

The two particles are located at the even- and odd-numbered lattice points $2n$ and $2n+1$, respectively. The displacements u_{2n} and u_{2n+1} of the even and odd particles are given by the equations of motion

$$\begin{aligned} M\ddot{u}_{2n} &= f(u_{2n+1} + u_{2n-1} - 2u_{2n}), \\ m\ddot{u}_{2n+1} &= f(u_{2n+2} + u_{2n} - 2u_{2n+1}). \end{aligned} \tag{1-71}$$

Assuming the following solutions for u_{2n} and u_{2n+1}:

$$u_{2n} = y_1 \exp i(2\pi\nu t + 2nka), \tag{1-72}$$

$$u_{2n+1} = y_2 \exp i[2\pi\nu t + (2n+1)ka], \tag{1-73}$$

and substituting the values of u_{2n} and u_{2n+1} in Eq. (1-71) one obtains two equations for the amplitudes y_1 and y_2. Here k is the wave vector and corresponds to the phase differences for each successive cell. A solution for these equations exists, and the secular determinant is illustrated as follows:

$$\begin{vmatrix} 2f - 4\pi^2\nu^2 M & -2f\cos ka \\ -2f\cos ka & 2f - 4\pi^2\nu^2 m \end{vmatrix} = 0. \tag{1-74}$$

A dispersion formula results, based on frequency dependency on masses, force constant and distance between the two masses, such as

$$\nu^2 = \frac{1}{4\pi^2}\left[\frac{f}{\mu} \pm \left(\frac{f^2}{\mu^2} - \frac{4f^2 \sin^2 ka}{Mm}\right)^{\frac{1}{2}}\right], \tag{1-75}$$

where μ is the reduced mass. The finite length of the lattice restricts the values of k in the range $-\pi/2a \leq k \leq \pi/2a$. The region between these limits of k is called the first Brillouin zone. There are two solutions for ν, since in Eq. (1-75) ν depends on the positive or negative signs and these correspond to the optical and acoustical branches, respectively. The two roots are

$$\begin{aligned} \nu &= 1/2\pi(2f/\mu)^{1/2} && \text{(optical branch)}, \\ \nu &= 1/2\pi[2f(M+m)]^{1/2}ka && \text{(acoustic branch)}. \end{aligned} \tag{1-76}$$

The positive roots of Eq. (1:75) are plotted in the positive half of the Brillouin zone as shown in Fig. 1-38a. It may be observed that the upper curve, which is called the optical branch, represents frequencies occurring in the optical

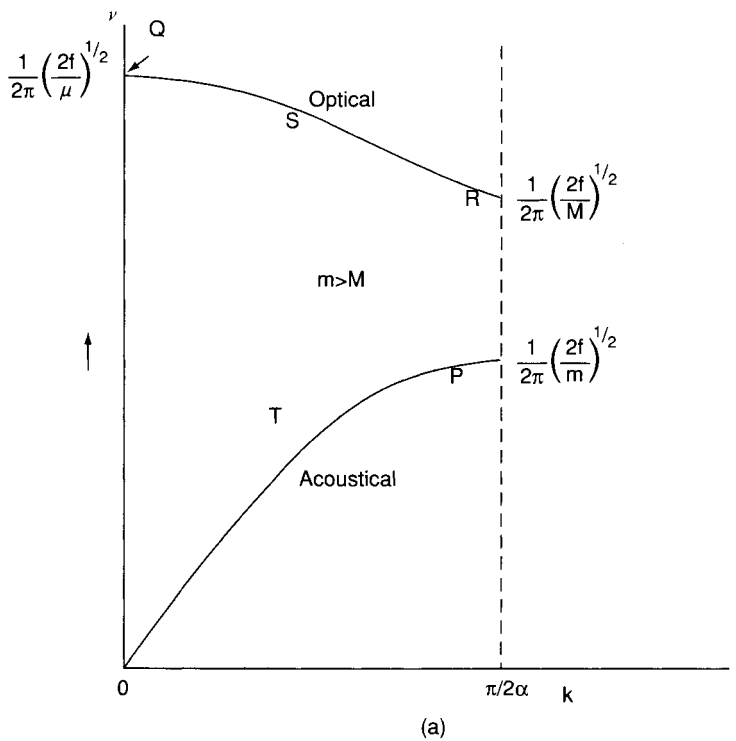

(a)

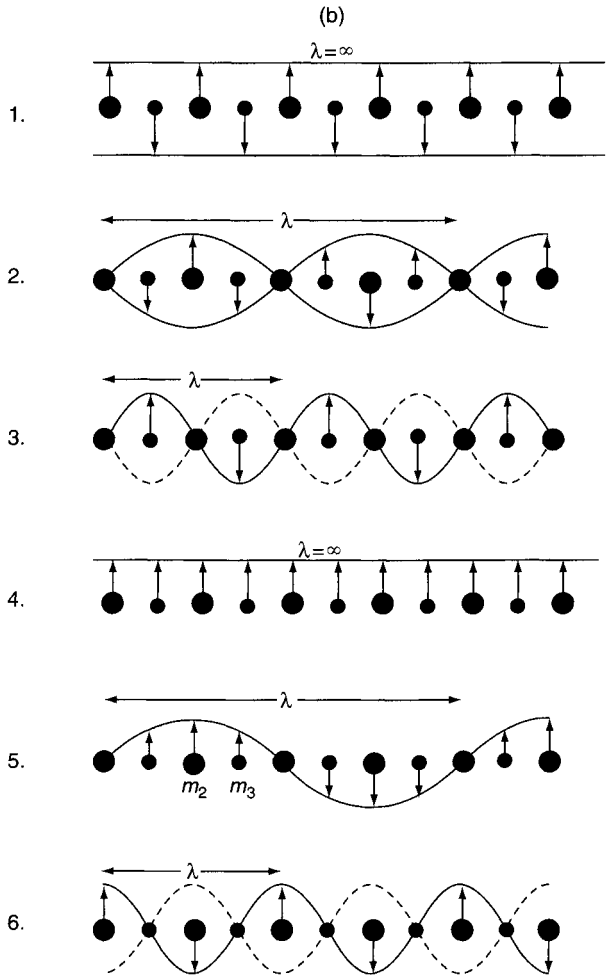

Figure 1-38 (a) Dispersion relation for the optical and acoustic branches in solids. (b) Wave motion in an infinite diatomic lattice. (Reproduced with permission from Ref. 49.)

spectral region (infrared or Raman). The low curve passes through $v = 0$ and is termed the acoustical branch (so-called because the frequencies occur in the sonic or ultrasonic region). Various wave motions are associated with both the optical and acoustical branches illustrated in Fig. 1-38b. Figure 1-38b-1 illustrates the wave motion of the optical branch at $k = 0$ and at point Q in Fig. 1-38a. Here the two atoms vibrate rigidly against each other. Figure 1-38b-2 shows the wave motion at point S on the optical branch. Figure 1-38b-3 demonstrates the wave motion at point R on the optical branch, where the light atoms are moving back and forth against

each other with the heavy atoms being fixed. In Fig. 1-38b-4 at point O ($k = 0$) of the acoustic branch, the wave motion involves a translation at the entire lattice. Figure 1-38b-5 shows the wave motion at point T on the acoustic branch. Figure 1-38b-6 shows the wave motion at point P of the acoustical branch, where only the heavy atoms vibrate back and forth against each other and the light atoms are stationary.

The optical spectral region consists of internal vibrations (discussed in Section 1.13) and lattice vibrations (external). The fundamental modes of vibration that show infrared and/or Raman activities are located in the center Brillouin zone where $k = 0$, and for a diatomic linear lattice, are the long-wave limit. The lattice (external) modes are weak in energy and are found at lower frequencies (far infrared region). These modes are further classified as translations and rotations (or librations), and occur in ionic or molecular crystals. Acoustical and optical modes are often termed "phonon" modes because they involve wave motions in a crystal lattice chain (as demonstrated in Fig. 1-38b) that are quantized in energy.

If the primitive cell contains σ molecules, each of which contains ρ atoms, then the number of acoustic modes is 3, and that of optical modes is $(3\sigma\rho - 3)$. The latter is classified into $(3\rho - 6)\sigma$ internal modes and $(6\sigma - 3)$ lattice modes. Analysis of these optical modes will be carried out in the following section.

Further discussion of solid vibrations of three-dimensional lattices is beyond the scope of this text. The reader may refer to Turrell (48) or other solid state texts (49).

1.18 Selection Rules for Solids (Factor Group)

By simply extending the methods used for the point group selection rules, one can obtain selection rules for molecules involving rotation–translation and reflection–translation. Two approaches are available. The older method is the Bhagavantum–Ventkatarayudu (BV) method (50), and necessitates the availability of the structure of the material being studied. The other method is that of Halford–Hornig (HH) (51–53) and considers only the local symmetry of a solid and the number of molecules in the unit cell and is simpler to work with. This method is also called the correlation method and depends on the proper selection of the site symmetry in the unit cell.

1.18.1 Unambiguous Choice of Site Symmetry in the Unit Cell

For cases where an unambiguous choice of site symmetry cannot be made, the use of Wyckoff's tables of crystallographic data (54) can prove helpful. Wyckoff's tables consist of the site correlations for some space groups. In instances where there is some doubt as to which site correlates (Appendix 5)

with an axis of rotation, e.g., $[C_2(x), C_2(y), C_2(z)]$, or with a plane of symmetry $[\sigma(xy), \sigma(yz), \sigma(zx)]$, the proper site can be chosen. For example, consider orthorhombic $PuBr_3$, which has a D_{2h}^{17} (*Cmcm*) space group and a crystallographic unit cell with $Z = 4$. For a *C*-type lattice there are two repeat units in the cell, and therefore

$$Z' = \text{number of molecules in the cell}$$
$$= \frac{Z(\text{number of molecules in crystallographic cell})}{\text{repeat units in cell}} = \frac{4}{2} = 2.$$

From Appendix 4, we can observe that for D_{2h}^{17} (space group 63) the following site symmetries are possible: $2C_{2h}(2)$; $C_{2v}(2)$; $C_i(4)$; $C_2(4)$; $2C_s(4)$; $C_1(8)$. With the number of molecules in the unit cell equal to two, we must place two Pu^{3+} ions on a set of particular sites and six Br^- on other sets of sites. We observe that two site symmetries are available for the two Pu^{3+} ions—either C_{2h} or C_{2v}, each having two equivalent sites per set to place the metal ions. An unambiguous choice cannot be made with the data available. For the six Br^- ions, no site symmetry has six equivalent sites available. Thus, we must conclude that the six Br^- ions must be nonequivalent, and some are on one site and others on another site. At this point one must consult the Wyckoff tables (see Appendix 5) on published crystallographic data, and when this is done, we find the notation tabulated here.

Ion	Site Position
$2Pu^{3+}$	*c*
$2Br^-$	*c*
$4Br^-$	*f*

We can deduce the Wyckoff nomenclature of the site positions from the site symmetries by listing the site positions in alphabetical order, as shown in the next table.

Site in Appendix 4	Alphabetical Order	Wykoff's Alphabetical Ordering of Site Position	Ion Site
$2C_{2h}(2)$	$C_{2h}(2)$	*a*	
	$C_{2h}(2)$	*b*	
$C_{2v}(2)$	$C_{2v}(2)$	*c*	$2Pu^{3+}(c)$
			$2Br^-(c)$
$C_i(4)$	$C_i(4)$	*d*	
$C_2(4)$	$C_2(4)$	*e*	
$2C_s(4)$	$C_s(4)$	*f*	$4Br^-(f)$
	$C_s(4)$	*g*	
$C_1(8)$	$C_1(8)$	*h*	

We can place the two Pu^{3+} ions on a *c* site (C_{2v}), two Br^- ions on a *c* site (C_{2v}), and four Br^- must be on an *f* site (C_s). If we examine the correlation tables in Appendix 6, we observe that three correlations are possible for a D_{2h} space group with a site symmetry of C_{2v}. Similarly, three correlations are possible for the site symmetry C_s. Each correlation is based on a different rotational axis or reflection plane being involved. For example:

	$C_2(z)$	$C_2(y)$	$C_2(x)$	$\sigma(xy)$	$\sigma(zx)$	$\sigma(yz)$
D_{2h}	C_{2v}	C_{2v}	C_{2v}	C_s	C_s	C_s
Site Correlation		*c*	*a*, *b*, *e*,	*g*		*f*

One must decide which site group to use. Appendix 5 can be used to determine the proper site. For each space group, the correlation to go with each site is included. Knowing the site symmetry as given by the Wyckoff tables, one can determine which site correlation to use. For this example, the *c*-site position for a C_{2v} site is correlated with C_{2v} involving a C_2 rotation around the *y* axis, and the *f*-site position for a C_s site is correlated with C_s, involving a reflection plane in the *yz* plane. In this manner an unambiguous choice of the site symmetry for the Pu^{3+} and Br^- ions is made. This method of obtaining the proper site symmetry is possible whenever the Wyckoff tables contain the molecule of interest. If the information is not available in the Wyckoff tables, then one must resort to a study of the actual crystallographic structure of the crystalline material, if it is available.

Although only two equivalent sites per set are available for C_{2v} symmetry, it is possible to place the two Pu^{3+} and two Br^- ions in a C_{2v} site, since the number of such sites is infinite. When the site symmetry is C_p, C_{pv}, or C_s and $p = 1, 2, 3$, etc., the number of sites is infinite. This point should be kept in mind when using Appendix 5. Figure 1-39 demonstrates the packing diagram of $PuBr_3$.

1.18.2 Examples of the Halford-Hornig Site Group Method

In this section, we shall attempt to illustrate the HH method using several examples.

To derive factor group (space group) selection rules, it is necessary to utilize X-ray data for a molecule from a literature source or from Wyckoff's (54) *Crystal Structures*. The factor group and site symmetries of the ion, molecule, or atoms must be available, as well as the number of molecules per unit cell reduced to a primitive unit cell.

(*a*) *$LaCl_3$ Solid*

Let us consider the $LaCl_3$ crystal. The unit cell of $LaCl_3$ is seen in Fig. 1-40. The data available from Wyckoff indicate a space group #176, C_{6h}^2–$P6_3/m$.

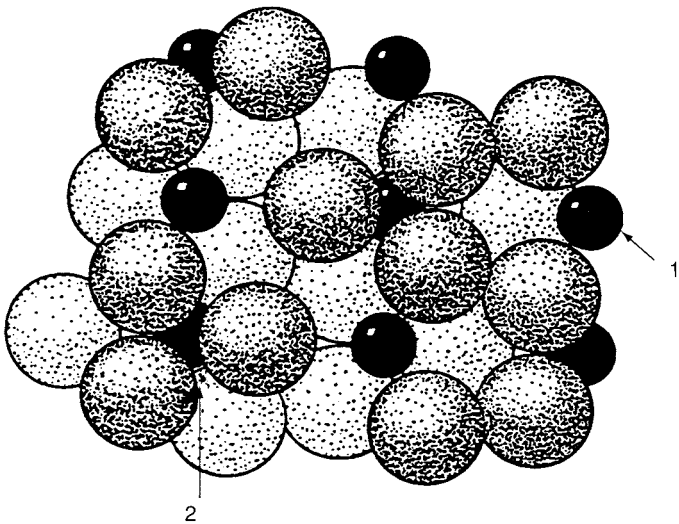

Figure 1-39 Packing diagram for $PuBr_3$. 1 and 2 indicate Br atom sites. (Reproduced with permission from Ref. 55. Copyright © 1972 John Wiley & Sons, Inc.)

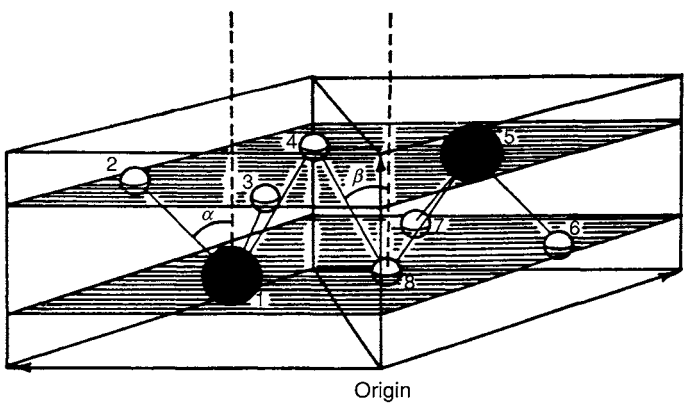

Figure 1-40 Unit cell for $LaCl_3$. The large circles represent lanthanum ions while the small circles represent chlorine ions.

The unit cell is $2(Z')$. The two La atoms sit on a C_{3h} site, and the six chlorine atoms are on a C_s site (see Appendix 4). Since the Hermann–Mauguin nomenclature cites that the unit cell is primitive ($Pb6_3/m$) we need not reduce it. For the two La atoms there are six degrees of freedom $(3n, Z') = 3 \times 1 \times 2 = 6$. The six Cl atoms possess 18 degrees of freedom $(3n, Z') = 3 \times 3 \times 2 = 18$. Since all vibrational modes can be considered external modes, we need only correlate the site group to factor group. For the

Table 1-12 Correlation Table for La^{3+} in $LaCl_3$

Degrees of Freedom (DOF)		Site Group	Factor Group	Modes	
T	R	C_{3h}	C_{6h}^2	T	R
0	0	A'	$A_x\ (R_z)$	0	0
			B_u	0	0
4	0	$(T_x, T_y)E'$	E_{2g}	1	0
			$E_{1u}\ (T_x, T_y)$	1	0
2	0	$(T_z)A''$	$A_u\ (T_g)$	1	0
			B_g	1	0
0	0	E''	E_{2u}	0	0
			$E_{1g}\ (R_x, R_y)$	0	0

La atoms we can initiate a correlation chart using the correlation tables (Appendix 6) (55). See Table 1-12. For a derivation of the correlation tables, see Ref. 45.

The six degrees of freedom (DOF) for the La atoms are placed where the site group indicates translation vectors. For example, the E' species in the C_{3h} site has T_x, T_y (two vectors). Therefore, the two La atoms with four DOF are placed with E' species. Likewise, the remaining two DOF are placed with A'' species. We need not consider site rotations since there can be no site rotations for single atoms. Examining the correlation tables (see Appendix 6), we can assign the four E' species to one E_{2g} and one E_{1u} in the C_{6h}^2 factor group, since "doubly degenerate" counts for two. Likewise, we can assign the two A'' species in C_{3h} sites to A_u and B_g in the factor group C_{6h}^2. Thus, two La atoms have E_{2g}, E_{1u}, B_g, and A_u as the active modes totaling the six DOF.

Similarly, one can calculate the correlation chart for the six Cl atoms as illustrated in Table 1-13. For the six Cl atoms, activity is demonstrated for $2A_g, 2B_u, 2E_{2g}, 2E_{1u}, A_u, B_g, E_{2u}$ and E_{1g} totaling 18 DOF. Summarizing the modes for $LaCl_3$ we obtain

$$\text{For 2 La:}\quad \Gamma_{T'} = E_{2g} + E_{1u} + A_u + B_g,$$

$$\text{For 6 Cl:}\quad \Gamma_{T'} = 2A_g + 2E_{2g} + E_{1g} + B_g + 2B_u + 2E_{1u} + E_{2u} + A_u,$$

where T' equals the total lattice or external modes of vibration. Including the three acoustic modes ($A_u + E_{1u}$), the total of 24 modes for $LaCl_3$ is distributed as follows:

$$\Gamma n_i = 3E_{2g} + E_{1g} + 2B_g + 2A_g + 3E_{1u} + 2B_u + E_{2u} + 2A_u.$$

Table 1-13 Correlation Table For Cl^- in $LaCl_3$

Degrees of Freedom (DOF)		Site Group	Factor Group	Modes	
T	R	C_s	C_{6h}^2	T	R
12	0	$(T_x, T_y)A'$	A_g (R_z)	2	0
			B_u	2	0
			E_{2g}	2	0
			E_{lu} (T_x, T_y)	2	0
6	0	$(T_z)A''$	A_u (T_z)	1	0
			B_g	1	0
			E_{2u}	1	0
			E_{lg} (R_x, R_y)	1	0

For a C_{6h}^2 factor group, the vibrations B_g, B_u and E_{2u} are inactive. Subtracting off the inactive modes, the three acoustic, total modes are

$$\underset{R}{3E_{2g}} + \underset{R}{E_{1g}} + \underset{R}{2A_g} + \underset{IR}{2E_{1u}} + \underset{IR}{A_u}.$$

The $3E_{2g}$, E_{1g} and $2A_g$ modes would be Raman-active, and the $2E_{1u} + A_u$ modes would be IR-active. The summary for $LaCl_3$ is

R	IR	C	P
10	5	0	1

At $k = 0$, acoustic modes have zero frequency and are not observed in the Raman or IR experiments. They may be observed by performing slow neutron scattering experiments.

As shown in the following section, one can apply the same procedures for an organic molecule such as cyclopropane, C_3H_6. For such molecules one correlates for the molecular point group → site group → factor group to obtain the internal modes, and the site group → factor group for the external modes. This would be the procedure if one is dealing with covalent organic compounds with internal modes of vibrations as well as external modes.

(*b*) *Solid Cyclopropane, C_3H_6*

Cyclopropane belongs to the C_{2v}^7–$Pmn2_1$ space group (No. 31) with $Z' = 2$. Figure 1-41 shows the structure of cyclopropane. The molecular point group is D_{3h}. The site group C_s is a subgroup of both the C_{2v}^7, and D_{3h} groups. The proper choice of C_s is obtained from Appendix 5 and is found to be $C_s(\sigma_{yz})$. A total of $3n \cdot Z' = 3 \cdot 9 \cdot 2 = 54$ modes are expected, of which $(3n - 6)Z' = 42$ are internal modes. There are, therefore, $54 - 42 = 12$ external modes. For

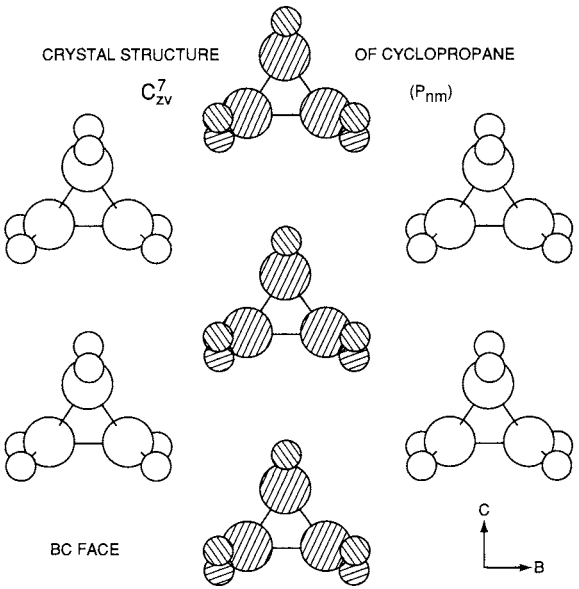

Figure 1-41 Proposed crystal structure of cyclopropane. The shaded molecules are not in the same plane as the unshaded ones and are inclined oppositely. (Reproduced with permission from Ref. 47.)

organic molecules such as cyclopropane, it is necessary to correlate the molecular point group to the site group and factor group to obtain the internal modes. For cyclopropane the correlation follows:

$$\begin{array}{ccc} \text{Point Group} \rightarrow & \text{Site Group} \rightarrow & \text{Factor Group.} \\ D_{3h} & C_s(\sigma_{yz}) & C_{2v}^7 \end{array}$$

The external modes are determined as for the $LaCl_3$ case by correlating the site group → factor group.

Internal modes for C_3H_6:

$$\Gamma_{n_r} = 12A_1 + 9A_2 + 9B_1 + 12B_2$$

External modes for C_3H_6:

$$\begin{aligned} \Gamma_{T+T'} &= A_2 + B_1 + 2A_1 + 2B_2 && \text{Total translations + acoustics} \\ \Gamma_T &= A_1 + B_1 + B_2 && \text{Translations} \\ \Gamma_{T'} &= A_2 + A_1 + B_2 && \text{Acoustics} \\ \Gamma_{R'} &= A_1 + 2B_1 + 2A_2 + B_2 && \text{Rotations} \end{aligned}$$

Summary for C_3H_6:
A total of $3nZ' = 3 \cdot 9 \cdot 2 = 54$ modes are expected:

$$\begin{aligned}
\Gamma_{n_i} &= 12A_1 + 9A_2 + 9B_1 + 12B_2 && \text{Internal modes}\\
\Gamma_T &= A_1 + B_1 + B_2 && \text{Translations}\\
\Gamma'_T &= A_1 + A_2 + B_2 && \text{Acoustics}\\
\Gamma'_R &= A_1 + 2A_2 + 2B_1 + B_2 && \text{Rotations}\\
\Gamma_n &= 15A_1 + 12A_2 + 12B_1 + 15B_2 && \text{Total}\\
&\text{Activity} \quad (\text{IR,R}) \quad (\text{R}) \quad (\text{IR,R}) \quad (\text{IR,R})
\end{aligned}$$

Of these, 39 are infrared-active and 51 are Raman-active, and $A_1 + B_1 + B_2$ are acoustic modes and are not observed.

Correlation tables for cyclopropane internal and external modes are tabulated in Tables 1-14 and 1-15.

We have illustrated the methods to obtain solid state selection rules. It should be mentioned that tables for factor group or point group analyses have been prepared by Adams and Newton (56, 57) where one can read the number and type of species allowed directly from the table. Although useful, the approach neglects the procedures as how to obtain results in the tables. For further examples of the correlation method, see Refs. 58–61, and the Correlation Theory Bibliography.

In general, a vibrational band in the free state splits into several bands as a result of solid intermolecular interactions in the unit cell. The number of split components can be predicted by the factor group analysis discussed earlier. Such splitting is termed factor group splitting or Davydov splitting, and the magnitude of this splitting is determined by the strength of the intermolecular interaction and the number of molecules in the unit cell interacting. In molecular crystals this splitting is in the range of 0–10 cm^{-1}.

Table 1-14 Correlation Table for Cyclopropane Internal Modes

Molecular Point Group D_{3h}^*	Site Group $C_3(\sigma_{yz})$	Factor Group C_{2v}^7
$3A_1'$		
$1A_1''$		
$(R_z)1A_2'$	$12A'$	$12A_1(T_z)$
$(T_z)2A_2''$		$9A_2$
$(T_x, T_y)4E'$	$9A''$	$9B_1(T_x)$
$(R_x, R_y)3E''$		$12B_2(T_y)$

*Number of species for molecular point group determined from Appendix2.

Table 1-15 Correlation Table for Cyclopropane External Modes

Degrees of Freedom (DOF)		Site Group	Factor Group	Modes	
T	R	$C_s(\sigma_{yz})$	C_{2v}^7	T	R
4	2	$(T_x, T_y)(R_z)A'$	A_1 (T_z)	2	1
			A_2 (R_z)	1	2
2	4	$(T_z)(R_x, R_y)A''$	B_1 $(T_x)(R_y)$	1	2
			B_2 $(T_y)(R_x)$	2	1

1.19 Polarized Raman Spectra of Single Crystals

Porto et al. (61) illustrated the importance of polarized Raman spectra in obtaining the symmetry properties of normal vibrations, and their assignments. If one examines the character table for the D_{3d} point group (see Appendix 1), one may observe that the A_{1g} and E_g vibrations are Raman-active. The A_{1g} modes become Raman-active if any of the polarizability components $\alpha_{xx}, \alpha_{yy}, \alpha_{zz}$ change during irradiation. Let us consider a single crystal of calcite, which exists in a D_{3d}^6 space group ($Z = 2$), and having $1A_{1g}$ and $4E_g$ vibrations (a total of nine) as determined by factor group analysis. If we irradiate this crystal in the y direction (see Fig. 1-42) and observe the Raman scattering in the x direction and polarized scattering in the z direction ($y(zz)x$

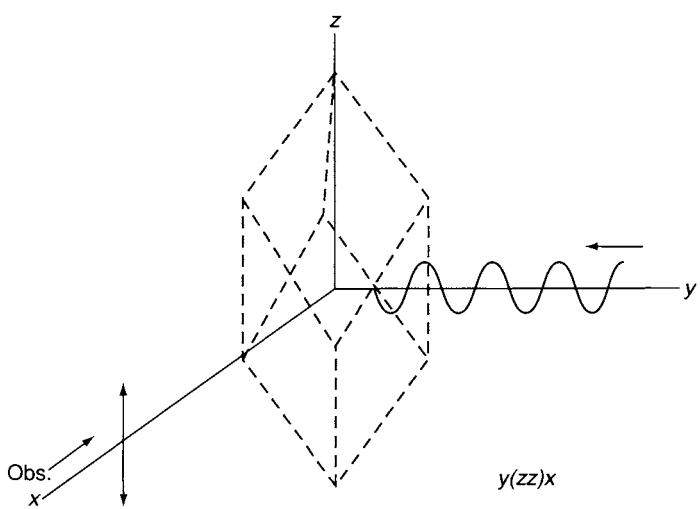

Figure 1-42 Schematic representation of experimental conditions used for the measurement of depolarization ratios of calcite crystal. (Reproduced with permission from Ref. 29. Copyright © 1986, John Wiley & Sons, Inc.)

in the Damen–Porto nomenclature); we should observe only the A_{1g} species. We can understand how this occurs by simplifying Eq. (1-46) and obtaining

$$P_z = \alpha_{zz} E_z,$$

since $E_x = E_y = 0$ and $P_x = P_y = 0$. The polarizability component α_{zz} belongs to the A_{1g} species, and only A_{1g} modes should be observed under the conditions of $y(zz)x$. Figure 1-43a illustrates the Raman spectrum obtained at $y(zz)x$ radiation (61). Only the 1,088 cm^{-1} vibration appears, and this belongs to the A_{1g} species. Under the radiation conditions $z(xx)y$, both A_{1g} and E_g species should appear. Figure 1-43b shows four of five vibrations appearing (the 1,434 cm^{-1} band is not shown). The 1,088 cm^{-1} band is the A_{1g} mode, while the others are the E_g modes. The assignments for calcite are therefore made using the polarized Raman technique. These assignments may be confirmed by irradiating the calcite crystal under the $y(xy)x$ and $x(zx)y$ conditions (Fig. 1-43c,d), where only the E_g modes appear.

This example illustrates the usefulness of the polarized Raman technique. For a further discussion on the analysis of calcite, see Nakamoto (37), Nakagawa and Walter (62) and Mitra (47) for data on gypsum.

1.20 Normal Coordinate Analysis

As shown in Section 1.3, force constants of diatomic molecules can be calculated by using Eq. (1-20). In the case of polyatomic molecules, force constants can be calculated via normal coordinate analysis (NCA), which is much more involved than simple application of Eq. (1-20). Its complete description requires complex and lengthy mathematical treatments that are beyond the scope of this book. Here, we give only the outline of NCA using the H_2O molecule as an example. For complete description of NCA, the reader should consult references (63–65) and general reference books cited at the end of this chapter.

1.20.1 Internal Coordinates

The kinetic and potential energies of a polyatomic molecule can be expressed in terms of Cartesian coordinates ($\Delta x, \Delta y, \Delta z$) or internal coordinates such as increments of bond length (Δr) and bond angles ($\Delta\alpha$). In the former case, $3N$ coordinates are required for an N-atom molecule. Figure 1-44 shows the nine Cartesian coordinates of the H_2O molecule. Since the number of normal vibrations is 3 ($3 \times 3 - 6$), this set of Cartesian coordinates includes six extra coordinates. On the other hand, only three coordinates ($\Delta r_1, \Delta r_2$ and $\Delta\alpha$) shown in Fig. 1-44 are necessary to express the energies in terms of internal

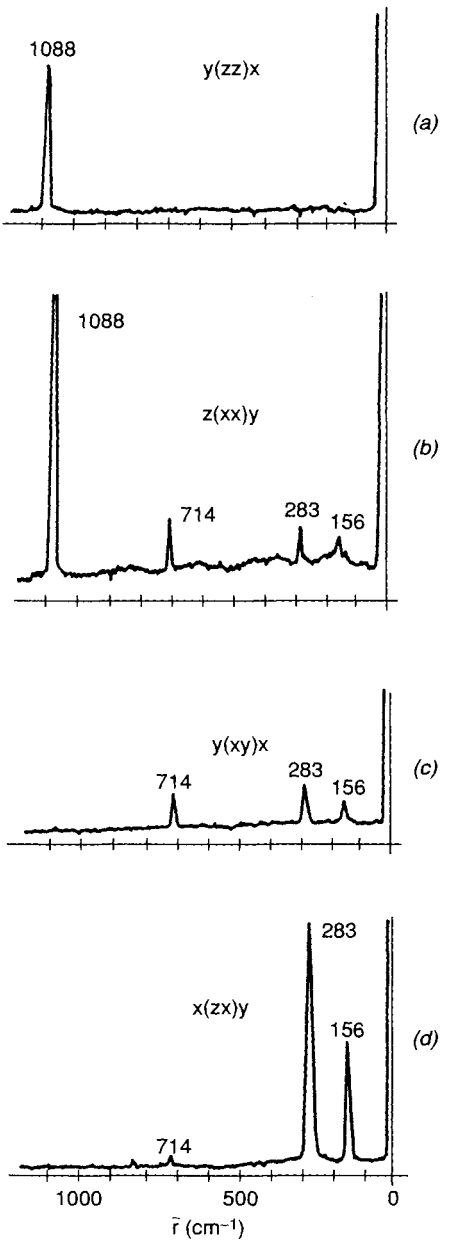

Figure 1-43 Polarized Raman spectra of calcite. (Reproduced with permission from Ref. 61.)

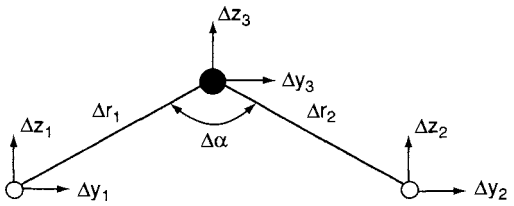

Figure 1-44 The nine Cartesian and three internal coordinates for H_2O. The three x coordinates are not shown since they are in the direction perpendicular to the paper plane.

coordinates. Furthermore, the latter has the advantage that the force constants obtained have clearer physical meaning than those obtained by using Cartesian coordinates since they represent force constants for particular bond stretching and angle bending. Thus, internal coordinates are commonly used for NCA. If it is necessary to use more than $3N-6(5)$ internal coordinates, such a set includes extra (redundant) coordinates that can be eliminated during the process of calculation. Using the general formulas developed by Decius (65), one can calculate the types and numbers of internal coordinates for a given molecule, as follows.

The number of bond stretching coordinates is given by

$$n_r = b, \tag{1-77}$$

where b is the number of bonds disregarding type, which for H_2O is two. The number of angle bending coordinates is given by

$$n_\alpha = 4b - 3a + a_1, \tag{1-78}$$

where a is the number of atoms in the molecule, and a_1 is the number of bonds meeting at the central atom. For H_2O, n_α is equal to one.

1.20.2 Symmetry Coordinates

If a molecule contains equivalent coordinates due to its symmetry properties, it is possible to simplify the calculation (*vide infra*) by using symmetry coordinates rather than internal coordinates. In the case of H_2O, they are

$$R_1 \sim (\Delta r_1 + \Delta r_2) \tag{1-79}$$

$$R_2 \sim \Delta\alpha, \tag{1-80}$$

$$R_3 \sim (\Delta r_1 - \Delta r_2). \tag{1-81}$$

R_1 and R_2 correspond to the two A_1, whereas R_3 corresponds to the B_2 vibration (see Fig. 1-12). Selection of symmetry coordinates can be facilitated

by use of the method of Nielsen and Berryman (66). However, the preceding symmetry coordinates must be normalized so that

$$\sum_k (U_{jk})^2 = 1, \tag{1-82}$$

where U_{jk} is the coefficient of the kth internal coordinate in the jth symmetry coordinate. For R_1, $(U_{11})^2 + (U_{12})^2 = 1$. This gives $U_{11} = U_{12} = 1/\sqrt{2}$. Thus,

$$R_1 = \left(1/\sqrt{2}\right)(\Delta r_1 + \Delta r_2).$$

Similarly

$$\begin{aligned} R_3 &= \left(1/\sqrt{2}\right)(\Delta r_1 - \Delta r_2), \\ R &= \Delta\alpha. \end{aligned} \tag{1-83}$$

Next, a set of symmetry coordinates must satisfy the orthogonality condition:

$$\sum_k (U_{jk})(U_{ik}) = 0. \tag{1-84}$$

For R_1 and R_2, $(1/\sqrt{2})(0) + (1/\sqrt{2})(0) + (0)(1) = 0.$
For R_1 and R_3, $(1/\sqrt{2})(1/\sqrt{2}) + (1/\sqrt{2})(-1/\sqrt{2}) + (0)(0) = 0.$
For R_2 and R_3, $(0)(1/\sqrt{2}) + (0)(-1/\sqrt{2}) + (1)(0) = 0.$

Thus, R_1, R_2 and R_3 shown in Eqs. (1-83) are orthogonal to each other.

It is necessary to determine if the preceding symmetry coordinates transform according to the character table of the point group C_{2v} (Appendix 1). By applying each symmetry operation, we find that R_1 and R_2 transform as A_1 species, while R_3 transforms as B_2 species. For example,

$$\begin{aligned} &E(R_1) = 1, \quad C_2(R_1) = 1, \quad \sigma_v(xz)(R_1) = 1 \quad \text{and} \quad \sigma_v(yz)(R_1) = 1; \\ &E(R_3) = 1, \quad C_2(R_3) = -1, \quad \sigma_v(xz)(R_3) = -1 \quad \text{and} \quad \sigma_v(yz)(R_3) = 1. \end{aligned}$$

Using matrix notation, the relationship between the internal and symmetry coordinates is written as

$$\begin{bmatrix} R_1(A_1) \\ R_2(A_1) \\ R_3(B_2) \end{bmatrix} = \begin{bmatrix} \frac{1}{\sqrt{2}} & \frac{1}{\sqrt{2}} & 0 \\ 0 & 0 & 1 \\ \frac{1}{\sqrt{2}} & \frac{-1}{\sqrt{2}} & 0 \end{bmatrix} \begin{bmatrix} \Delta r_1 \\ \Delta r_2 \\ \Delta\alpha \end{bmatrix}, \tag{1-85}$$

where the first matrix on the right is called the U-matrix.

1.20.3 Potential Energy–*F*-Matrix

The next step is to express the potential energy in terms of the *F*-matrix, which consists of a set of force constants. In the case of H_2O, it is written as

$$2V = f_{11}(\Delta r_1)^2 + f_{11}(\Delta r_2)^2 + f_{33}r^2(\Delta\alpha)^2 + 2f_{12}(\Delta r_1)(\Delta r_2) + 2f_{13}r(\Delta r_1)(\Delta\alpha) + 2f_{13}r(\Delta r_2)(\Delta\alpha) \tag{1-86}$$

Here, f_{11}, f_{12}, f_{13} and f_{33} are the stretching, stretching-stretching interaction, stretching–bending interaction, and bending force constants, respectively, and r (equilibrium distance) is multiplied to make f_{13} and f_{33} dimensionally similar to the others. Using matrix expression, Eq. (1-86) is written as

$$2V = [\Delta r_1 \ \Delta r_2 \ \Delta\alpha] \begin{bmatrix} f_{11} & f_{12} & rf_{13} \\ f_{12} & f_{11} & rf_{13} \\ rf_{13} & rf_{13} & r^2f_{33} \end{bmatrix} \begin{bmatrix} \Delta r_1 \\ \Delta r_2 \\ \Delta\alpha \end{bmatrix}. \tag{1-87}$$

Using matrix notation, the general form of Eq. (1-87) is written as

$$2V = \tilde{\mathbf{R}}\mathbf{F}\mathbf{R}, \tag{1-88}^*$$

where **F** is the force constant matrix (**F**-matrix), and **R** and its transpose $\tilde{\mathbf{R}}$ are column and row matrices, respectively, which consist of internal coordinates. To take advantage of symmetry properties of the molecule, one must transform the F-matrix into F_s via

$$\mathbf{F}_s = \mathbf{U}\mathbf{F}\tilde{\mathbf{U}}. \tag{1-89}$$

In the case of H_2O, F_s becomes:

$$\mathbf{F_S} = \left[\begin{array}{cc:c} f_{11} + f_{12} & r\sqrt{2}f_{13} & 0 \\ r\sqrt{2}f_{13} & r^2f_{33} & 0 \\ \hdashline 0 & 0 & f_{11} - f_{12} \end{array}\right] \tag{1-90}$$

Thus, the original 3×3 matrix is resolved into one 2×2 matrix (A_1 species) and one 1×1 matrix (B_2 species). In large molecules, such coordinate transformation greatly simplifies the calculation.

In the preceding, the potential energy was expressed in terms of the four force constants (stretching, stretching-stretching interaction, stretching-bending interaction, and bending). This type of potential field is called the *generalized valence force* (GVF) *field* and is most commonly used for normal coordinate calculations. In large molecules, however, the GVF field requires too many force constants, which are difficult to determine with limited experimental data. To overcome this difficulty, several other force fields have been

*Hereafter, the bold-face letters indicate matrices.

developed, and some of these are given in reference books cited at the end of this chapter.

1.20.4 Kinetic Energy—G-Matrix

The kinetic energy is not easily expressed in terms of internal (symmetry) coordinates. Wilson (63) has shown that

$$2T = \tilde{\dot{\mathbf{R}}}\mathbf{G}^{-1}\dot{\mathbf{R}}, \tag{1-91}$$

where $\dot{\mathbf{R}}$ is the time derivative of $\mathbf{R}$, $\tilde{\dot{\mathbf{R}}}$ is its transpose, and $\mathbf{G}^{-1}$ is the reciprocal of the G-matrix. G-matrix elements can be calculated by using Decius table (65). In the case of H_2O, it becomes

$$\mathbf{G} = \begin{bmatrix} \mu_3 + \mu_1 & \mu_3 \cos\alpha & -\dfrac{\mu_3}{r}\sin\alpha \\ \mu_3 \cos\alpha & \mu_3 + \mu_1 & -\dfrac{\mu_3}{r}\sin\alpha \\ -\dfrac{\mu_3}{r}\sin\alpha & -\dfrac{\mu_3}{r}\sin\alpha & \dfrac{2\mu_1}{r^2} + \dfrac{2\mu_3}{r^2}(1 - \cos\alpha) \end{bmatrix}. \tag{1-92}$$

Here, μ_1 and μ_3 are the reciprocal masses of the H and O atoms, respectively, and α is the bond angle. Again, it is possible to diagonize the G-matrix via coordinate transformation:

$$\mathbf{G}_s = \mathbf{U}\mathbf{G}\tilde{\mathbf{U}}$$

where $\mathbf{G}_s$ is the G-matrix that is expressed in terms of symmetry coordinates. In the case of H_2O, it becomes

$$\mathbf{G_s} = \left[\begin{array}{cc:c} \mu_3(1 + \cos\alpha) + \mu_1 & -\dfrac{\sqrt{2}}{r}\mu_3 \sin\alpha & 0 \\ -\dfrac{\sqrt{2}}{r}\mu_3 \sin\alpha & \dfrac{2\mu_1}{r^2} + \dfrac{2\mu_3}{r^2}(1 - \cos\alpha) & 0 \\ \hdashline 0 & 0 & \mu_3(1 - \cos\alpha) + \mu_1 \end{array}\right]. \tag{1-93}$$

1.20.5 Solution of Secular Equation

As stated in Section 1.6, normal vibrations are completely independent of each other. This means that the potential and kinetic energies in terms of normal coordinates (Q) must be written without cross terms. Namely,

$$2T = \tilde{\dot{\mathbf{Q}}}\dot{\mathbf{Q}},$$
$$2V = \tilde{\mathbf{Q}}\Lambda\mathbf{Q},$$

where $\mathbf{\Lambda}$ is a diagonal matrix containing λ ($= 4\pi^2 c^2 \tilde{\nu}^2$) terms as diagonal elements (19). On the other hand, the energy expressions in terms of internal (symmetry) coordinates contain cross terms such as $(\Delta r)(\Delta\alpha)$:

$$2T = \tilde{\dot{\mathbf{R}}}\mathbf{G}^{-1}\dot{\mathbf{R}}, \tag{1-91}$$

$$2V = \hat{\mathbf{R}}\mathbf{F}\mathbf{R}. \tag{1-88}$$

To eliminate these cross terms, it is necessary to solve the secular equation of the form $|\mathbf{GF} - \mathbf{E}\lambda| = 0$ (63) where E is a unit matrix containing ones as the diagonal elements.* In the case of H_2O, this equation for the A_1 block becomes

$$|\mathbf{GF} - \mathbf{E}\lambda| = \begin{vmatrix} G_{11}F_{11} + G_{12}F_{21} - \lambda & G_{11}F_{12} + G_{12}F_{22} \\ G_{21}F_{11} + G_{22}F_{21} & G_{21}F_{12} + G_{22}F_{22} - \lambda \end{vmatrix} = 0, \tag{1-94}$$

or

$$\lambda^2 - (G_{11}F_{11} + G_{22}F_{22} + 2G_{12}F_{12})\lambda + (G_{11}G_{22} - G_{12}^2)(F_{11}F_{22} - F_{12}^2) = 0. \tag{1-95}$$

For the B_2 vibration,

$$\lambda = F_{33}G_{33}.$$

1.20.6 Calculation of Force Constants

In general, normal coordinate analysis is carried out on a molecule for which the atomic masses, bond distances and overall structures are known. Thus, the G-matrix can be readily calculated using known molecular parameters. Since the force constants are not known *a priori*, it is customary to assume a set of force constants that have been obtained for similar molecules, and to calculate vibrational frequencies by solving the secular equation $|\mathbf{GF} - \mathbf{E}\lambda| = 0$. Then, these force constants are refined until a set of calculated frequencies gives reasonably good agreement with those observed.

For the A_1 vibrations of H_2O, the G-matrix elements are calculated by using the following parameters:

$$\mu_1 = \mu_H = \frac{1}{1.008} = 0.99206,$$

$$\mu_3 = \mu_o = \frac{1}{15.995} = 0.06252,$$

$$r = 0.96(\text{Å}),\ \alpha = 105°,$$

*All the off-diagonal elements are zero in a diagonal as well as in a unit matrix.

$$\sin\alpha = \sin 105^\circ = 0.96593,$$
$$\cos\alpha = \cos 105^\circ = -0.25882.$$

If we assume a set of force constants,

$$f_{11} = 8.4280, \quad f_{12} = -0.1050,$$
$$f_{13} = 0.2625, \quad f_{33} = 0.7680,$$

we obtain a secular equation,

$$\lambda^2 - 10.22389\lambda + 13.86234 = 0.$$

The solution of this equation gives

$$\lambda_1 = 8.61475, \quad \lambda_2 = 1.60914.$$

These values are converted into $\tilde{\nu}$ through the $\lambda = 4\pi^2 c^2 \tilde{\nu}^2$ relationship. The results are

$$\tilde{\nu}_1 = 3{,}824\ \text{cm}^{-1}, \quad \tilde{\nu}_2 = 1{,}653\ \text{cm}^{-1}.$$

For the B_2 vibration, we obtain

$$\lambda_3 = G_{33}F_{33} = [\mu_1 + \mu_3(1 - \cos\alpha)](f_{11} - f_{12})$$
$$= 9.13681,$$
$$\tilde{\nu}_3 = 3{,}938\ \text{cm}^{-1}.$$

The calculated frequencies just obtained are in good agreement with the observed values, $\tilde{\nu}_1 = 3{,}825\,\text{cm}^{-1}$, $\nu_2 = 1{,}654\,\text{cm}^{-1}$ and $\tilde{\nu}_3 = 3{,}936\,\text{cm}^{-1}$, all corrected for anharmonicity (66). Thus, the set of force constants assumed initially is a good representation of the potential energy of the H_2O molecule. For large molecules, use of computer programs such as those developed by Schachtschneider (67) greatly facilitate the calculation.

1.21 Band Assignments and Isotope Shifts

Inspection of IR and Raman spectra of a large number of compounds shows that a common group exhibits its group vibrations in the same region regardless of the rest of the molecule. These "group frequencies" are known for a number of inorganic (37) and organic compounds (68,69). Figures 1-45 and 1-46 show group frequencies and corresponding normal modes for the CH_3 and CH_2 groups, respectively. Notations such as ν (stretching) and δ (bending) will be used throughout this book. Band assignments of other small molecules are tabulated by Shimanouchi (70). Using group frequency tables, it is possible to assign the observed spectra and to identify the atomic groups responsible for each group vibrations.

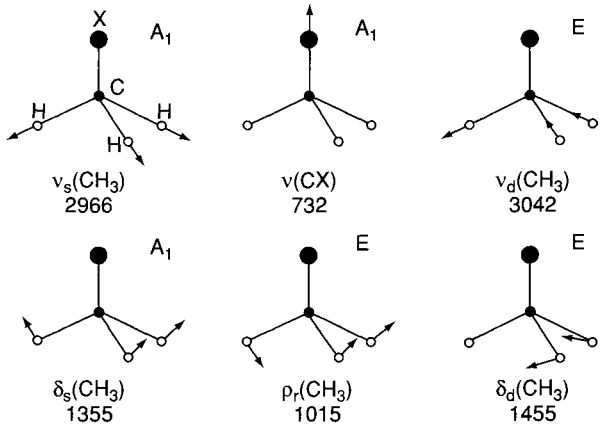

Figure 1-45 Normal vibrations of CH_3X-type molecule (frequencies are given for X = Cl): ν_s, symmetric stretching; ν_d, degenerate stretching; δ_s, symmetric bending; δ_d, degenerate bending; ρ_r rocking.

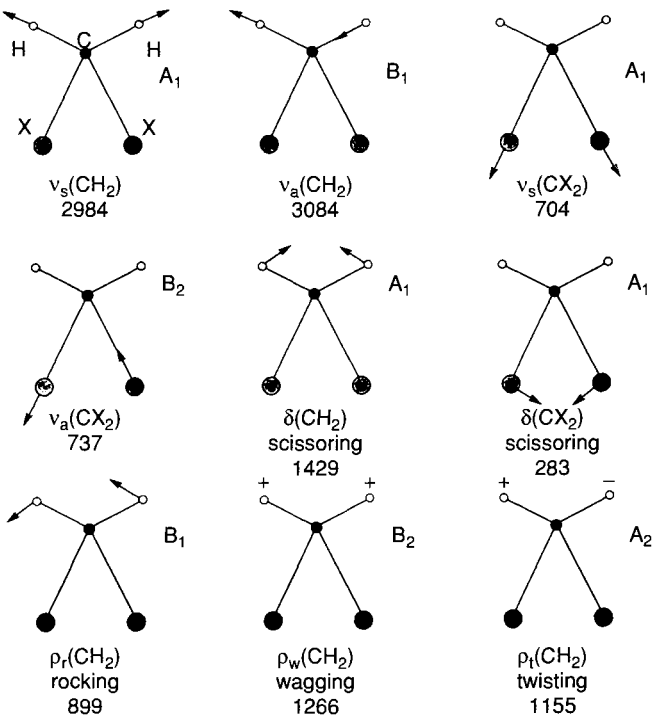

Figure 1-46 Normal vibrations of CH_2X_2 -type molecule (frequencies are given for X = Cl): ν_s, symmetric stretching; ν_a, antisymmetric stretching; δ, symmetric bending (scissoring); ρ_r, rocking; ρ_w, wagging; ρ_t, twisting.

However, the concept of group frequencies is applicable only when the vibrations of a particular group are isolated from those of the rest of the molecule. If atoms of similar masses are connected by bonds of similar strength, the amplitudes of oscillation are similar for all atoms. For example, this situation occurs in a system like

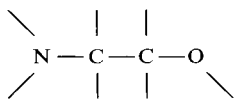

In such a case, it is not possible to describe normal modes in terms of one local mode such as ν(C—C), ν(C—N) or ν(C—O). Instead, they are described as a mixing of these local modes ("vibrational coupling"). As will be shown in Chapter 4, Section 4.1.2, examples of such vibrational couplings are seen in metalloporphyrins and peptides.

In Section 1.6, we have shown the relationship between Cartesian and normal coordinates (Eq. (1-44)). Similar relationships exist between internal (symmetry) and normal coordinates:

$$\begin{aligned} R_1 &= l_{11}Q_1 + l_{12}Q_2 + \cdots + l_{1N}Q_N, \\ R_2 &= l_{21}Q_1 + l_{22}Q_2 + \cdots + l_{2N}Q_N, \\ &\vdots \qquad\qquad \vdots \\ R_i &= l_{i1}Q_1 + l_{i2}Q_2 + \ldots + l_{iN}Q_N. \end{aligned}$$

Thus, the mixing ratio of individual coordinates in a given normal vibration (e.g., Q_1) is determined by the ratio

$$l_{11} : l_{21} : \cdots : l_{i1}.$$

If one of these values (e.g., l_{11}) is large relative to others, this normal vibration is assigned to the local mode, R_1. If both l_{11} and l_{21} are large relative to others, it is assigned to a coupled vibration between R_1 and R_2. The l_{iN} values are obtained once vibrational frequencies are calculated by the procedures described in the preceding section (37). Such calculations show that the $\nu_1(Q_1)$ at 3,825 cm^{-1} and $\nu_2(Q_2)$ at 1,653 cm^{-1} are almost pure ν(O—H) and δ(HOH), respectively.

Experimentally, band assignments are facilitated by the observation of isotope shifts. As shown in Table 1-3, the vibrational frequency of H_2 (4,160 cm^{-1}) is markedly downshifted (2,994 cm^{-1} when H is replaced by D. The magnitude of this isotope shift is predicted by Eq. (1-40):

$$\frac{\tilde{\nu}_{H_2}}{\tilde{\nu}_{D_2}} = \sqrt{\frac{\mu_{D2}}{\mu_{H2}}} \cong \sqrt{2} = 1.414.$$

Obviously, this large shift originates in the mass effect; the mass of D is twice that of H. Such isotope shifts are seen in many isotopic pairs such as $^{6}Li/^{7}Li$, $^{10}B/^{11}B$, $^{12}C/^{13}C$, $^{14}N/^{15}N$, $^{16}O/^{18}O$, $^{32}S/^{34}S$ and $^{35}Cl/^{37}Cl$. As will be shown in Section 4.1.3, heavy metal isotopes ($^{58}Ni/^{62}Ni$ and $^{54}Fe/^{56}Fe$, etc.) are indispensable in assigning metal-ligand vibrations of coordination compounds (71).

References

1. F. P. Kerschbaum, *Z. Instrumentenk* **34**, 43 (1914).
2. B. Veskatesachar and L. Sibaiya, *Indian J. Phys.* **5**, 747 (1930).
3. J. H. Hibben, "The Raman Effect and Its Chemical Application" Reinhold Publishing Corp., New York, 1939.
4. F. H. Spedding and R. F. Stamm, *J. Chem. Phys.* **10**, 176 (1942).
5. D. H. Rank and J. S. McCartney, *J. Opt. Soc. Am.* **38**, 279 (1948).
6. H. L. Welsh, M. F. Crawford, T. R. Thomas, and G. R. Love, *Can. J. Phys.* **30**, 577 (1952).
7. N. S. Ham and A. Walsh, *Spectrochim. Acta* **12**, 88 (1958).
8. H. Stammreich, *Spectrochim. Acta* **8**, 41 (1956).
9. H. Stammreich, *Phys. Rev.* **78**, 79 (1950).
10. H. Stammreich, R. Forneris, and K. Sone, *J. Chem. Phys.* **23**, 1972 (1955).
11. H. Stammreich, R. Forneris, and Y. Tavares, *J. Chem. Phys.* **25**, 580, 1277 and 1278 (1956).
12. H. Stammreich, *Experientia* **6**, 224 (1950).
13. T. R. Gilson and P. J. Hendra, "Laser Raman Spectroscopy," pp. 1–266. Wiley-Interscience, London, 1970.
14. D. H. Rank and R. V. Wiegand, *J. Opt. Soc. Am.* **32**, 190 (1942).
15. R. F. Stamm and C. F. Salzman, *J. Opt. Soc. Am.* **43**, 126 (1953).
16. J. R. Ferraro, *in* "Raman Spectroscopy, Theory and Practice" (H. A. Szymanski, ed.), pp. 44–81. Plenum Press, New York, 1967.
17. J. R. Ferraro, R. Jarnutowski, and D. C. Lankin, *Spectroscopy* **7**, 30 (1992).
18. G. W. King, "Spectroscopy and Molecular Structure." Holt, Rinehart and Winston, New York, 1964.
19. H. Eyring, J. Walter, and G. E. Kimball, "Quantum Chemistry." John Wiley, 1944.
20. C. F. Shaw, III, *J. Chem. Educ.* **58**, 343 (1981).
21. C. D. Allemand, *Appl. Spectrosc.* **24**, 348 (1970).
22. F. G. Dijkman and J. H. Van der Maas, *Appl. Spectroc.* **30**, 545 (1976).
23. G. Fini and P. Mirone, *Appl. Spectrosc.* **29**, 230 (1975).
24. J. R. Scherer and G. F. Bailey, *Appl. Spectrosc.* **24**, 259 (1970).
25. T. G. Spiro and T. C. Strekas, *Proc. Nat. Acad. Sci.* **69**, 2622 (1972).
26. D. A. Long, "Raman Spectroscopy." McGraw-Hill, New York, 1977.
27. P. J. Hendra, "Raman instrumentation and sampling," *in* "Laboratory Methods in Infrared Spectroscopy" (R. G. Miller, ed.), p. 249. Heyden, London, 1971.
28. D. P. Strommen and K. Nakamoto, *Appl. Spectrosc.* **37**, 436 (1983).
29. M. Zeldin, *J. Chem. Educ.* **43**, 17 (1966).
30. J. R. Ferraro and J. S. Ziomek, "Introductory Group Theory and Its Application to Molecular Structure" (2nd Ed.). Plenum Press, New York, 1975.
31. G. Herzberg, "Molecular Spectra and Molecular Structure. II. Infrared and Raman Spectra of Polyatomic Molecules." D. Van Nostrand, New York, 1945.